THE UNIVERSITY OF MICHIGAN

COLLEGE OF ENGINEERING
Department of Atmospheric and Oceanic Science

Technical Report

ON THE SIMULATION OF THE AXISYMMETRIC CIRCULATION OF THE ATMOSPHERE

Humberto A. Fuenzalida

Aksel A. Wiin-Nielsen
Project Director

DRDA Project 002630

supported by:

NATIONAL SCIENCE FOUNDATION
GRANT NO. GA-16166
WASHINGTON, D.C.

administered through:

DIVISION OF RESEARCH DEVELOPMENT AND ADMINISTRATION ANN ARBOR

August 1973

TABLE OF CONTENTS

		Page
LIST OF TABLES		v
LIST OF FIGURES		vi
LIST OF APPENDICES		ix
LIST OF SYMBOLS		x
ABSTRACT		xv
CHAPTER		
I.	INTRODUCTION	1
	1.1 Motivation of the Study	1
	1.2 Brief Review of Most Recent Previous Work	3
	1.3 A Scope and Outline of the Study	5
II.	THE MODEL	8
	2.1 Basic Equations	8
	2.1.1 Quasi-geostrophic Equations	8
	2.1.2 Two-level Approximations	15
	2.1.3 Zonally Averaged Equations	18
	2.1.4 Subgrid Parameterizations	21
	2.1.5 Additional Diagnostic Relations	
	2.2 Boundary Contitions	25
	2.2.1 Boundary Conditions at the Poles	26
	2.2.2 Boundary Conditions at the Equator	32
	2.3 Energetics of the Model	36
	2.3.1 Momentum Transport	36
	2.3.2 Heat Transport	42
	2.3.3 Energy Balance	42
III.	DIABATIC HEATING	49
	3.1 Introduction	49
	3.2 Heat Balance for an Atmospheric Column	50
	3.3 Surface Heat Balance	53
	3.4 Vertical Transfer Processes and the Water Balance	55
	3.5 Computation of the Heating Function	58
	3.6 Tuning of the Heating Model	60
	3.6.1 Numerical Procedure	61
	3.6.2 Determination of Parameters	62
	3.6.3 Characteristics of the Tuned Heating Function	68
	3.6.4 Diabatic Heating in the Simulation	78

TABLE OF CONTENTS (continued)

		Page
IV.	LINEAR SIMULATIONS	83
	4.1 Northern Hemisphere Simulation	85
	4.1.1 Temperature Field	85
	4.1.2 Zonal Motion	88
	4.1.3 Meridional Circulation	90
	4.1.4 Transport of Heat and Momentum	92
	4.1.5 Energetics	92
	4.2 Southern Hemisphere Simulation	100
	4.2.1 Temperature Field	100
	4.2.2 Zonal Motion	103
	4.2.3 Meridional Circulations	105
	4.2.4 Transport of Heat and Momentum	105
	4.2.5 Energetics	105
V.	SENSITIVITY STUDY	111
	5.1 Streamfunction Constant	111
	5.2 Static Stability	114
	5.3 Boundary Layer Friction	
	5.4 Internal Friction	117
	5.5 Eddy Coefficients	118
	5.5.1 Heat Eddy Exchange Coefficient	120
	5.5.2 Potential Vorticity Eddy Exchange Coefficients	124
	5.6 An Improved Case	127
VI.	EDDY EXCHANGE PROCESSES	133
	6.1 Nature of the Eddy Exchange	
	6.1.1 Exchange Properties of Eddies	136
	6.1.2 Generation of Eddies: Baroclinic Instability	140
	6.2 Recent Models of the Heat Transport	143
	6.3 A Parameterization for Momentum Transport	145
	6.4 Results of a Nonlinear Simulation	148
VII.	CONCLUSIONS	160
APPENDIX I		165
APPENDIX II		173
APPENDIX III		176
APPENDIX IV		182
REFERENCES		184

LIST OF TABLES

Table		Page
3.6.1	Boundary layer vertical transfer of water vapor and sensible heat	63
3.6.2	Latent heat release normalization factor : m	65
3.6.3	Radiation parameters after tuning	69
3.6.4	Energy balance after tuning	71
5.0.1	List of sensitivity experiments	112
5.5.1	Eddy exchange coefficients from Sela & Wiin-Nielsen (1971)	119

LIST OF FIGURES

Figure		Page
3.2.1	Energy fluxes related to the diabatic heating of the atmosphere	52
3.3.1	Energy fluxes related to the surface layer	52
3.6.1	Energy balance of the earth-atmosphere system	72
3.6.2	Heat transport by the ocean-atmosphere system and by the oceans	73
3.6.3	Heat released by the oceans	75
3.6.4	Mean annual heating function	76
3.6.5	Atmospheric heat budget and its components	77
3.6.6	Seasonal distribution of the atmospheric diabatic heating	79
3.6.7	Diabatic heating of an atmospheric column	80
3.6.8	Comparison of mean annual heating obtained in the simulation and the tuning	81
4.0.1	Flow chart of computation of linear simulations	84
4.1.1	Thermal field at 50 cb for the Northern Hemisphere in the linear simulation	86
4.1.2	Thermal field at 100 cb for the Northern Hemisphere in the linear simulation	86
4.1.3	Meridional temperature profile for January and July at 50 cb , Northern Hemisphere linear simulation	87
4.1.4	Meridional temperature profile for January and July at 100 cb, Northern Hemisphere linear simulation	87
4.1.5	Zonal flow at 25 cb for the Northern Hemisphere in the linear simulation	89
4.1.6	Zonal flow at 75 cb for the Northern Hemisphere in the linear simulation	89
4.1.7	Vertical velocity at 50 cb for the Northern Hemisphere in the linear simulation	91
4.1.8	Heat transport by the atmosphere for the Northern Hemisphere in the linear simulation	91

LIST OF FIGURES (continued)

Figure		Page
4.1.9	Angular momentum transport for the Northern Hemisphere January in the linear simulation	93
4.1.10	Simulated variations of zonal available potential energy and zonal kinetic energy for the Northern Hemisphere in the linear simulation	95
4.1.11	Simulated variations of the generation of zonal available potential energy and dissipation of zonal kinetic energy for the Northern Hemisphere in the linear simulation	95
4.1.12	Simulated variations of energy conversions for the Northern Hemisphere in the linear simulation	98
4.1.13	Simulated energy box diagram in a typical year for the Northern Hemisphere in the linear simulation	98
4.2.1	Same as Figure 4.1.1 but for Southern Hemisphere	101
4.2.2	Same as Figure 4.1.2 but for Southern Hemisphere	101
4.2.3	Same as Figure 4.1.3 but for Southern Hemisphere	102
4.2.4	Same as Figure 4.1.4 but for Southern Hemisphere	102
4.2.5	Same as Figure 4.1.5 but for Southern Hemisphere	104
4.2.6	Same as Figure 4.1.6 but for Southern Hemisphere	104
4.2.7	Same as Figure 4.1.7 but for Southern Hemisphere	106
4.2.8	Same as Figure 4.1.8 but for Southern Hemisphere	107
4.2.9	Same as Figure 4.1.9 but for Southern Hemisphere and showing corrected values for January and July	107
4.2.10	Same as Figure 4.1.10 but for Southern Hemisphere	109
4.2.11	Same as Figure 4.1.11 but for Southern Hemisphere	109
4.2.12	Same as Figure 4.1.12 but for Southern Hemisphere	110
4.2.13	Same as Figure 4.1.13 but for Southern Hemisphere	110
5.5.1	Profiles of K_2 in experiments #7, #8 and #9	122

LIST OF FIGURES (continued)

Figure		Page
5.5.2	Temperature profile for January at 50 cb in experiments #10, #11 and #12	122
5.6.1	Same as Figure 4.1.5 for an improved case	129
5.6.2	Same as Figure 4.1.6 for an improved case	129
5.6.3	Same as Figure 4.1.7 for an improved case	130
5.6.4	Same as Figure 4.1.8 for an improved case	130
5.6.5	Same as Figure 4.1.13 for an improved case	132
6.4.1	Seasonal variations of eddy coefficients in the nonlinear simulation of the Northern Hemisphere	149
6.4.2	Same as Figure 4.1.1 for nonlinear simulation	151
6.4.3	Same as Figure 4.1.2 for nonlinear simulation	151
6.4.4	Same as Figure 4.1.3 for nonlinear simulation	152
6.4.5	Same as Figure 4.1.4 for nonlinear simulation	152
6.4.6	Same as Figure 4.1.5 for nonlinear simulation	153
6.4.7	Same as Figure 4.1.6 for nonlinear simulation	153
6.4.8	Same as Figure 4.1.7 for nonlinear simulation	155
6.4.9	Same as Figure 4.1.8 for nonlinear simulation	156
6.4.10	Same as Figure 4.2.9 for nonlinear simulation	156
6.4.11	Same as Figure 4.1.10 for nonlinear simulation	158
6.4.12	Same as Figure 4.1.11 for nonlinear simulation	158
6.4.13	Same as Figure 4.1.12 for nonlinear simulation	159
6.4.14	Same as Figure 4.1.13 for nonlinear simulation	159

LIST OF SYMBOLS

A	internal friction factor, defined on page 22
A_Z	zonal available potential energy
a	radius of the earth
b	turbulent transfer of sensible heat across the boundary layer
C(M, N)	conversion of energy from form M to form N
c	complex phase velocity ($= c_r + i\, c_i$)
c_p	specific heat at constant pressure for dry air
c_d	drag coefficient
E	evaporation
f	Coriolis parameter ($= 2\Omega \sin\varphi$)
f_o	standard value of Coriolis parameter
f(, t)	shape factor defined on page 182
$\mathfrak{F}_i$	horizontal friction stress vector at level i
$\mathfrak{F}_{i,x}$	horizontal friction stress x component at level i
G	generation of available potential energy or a quasi-conservative quantity
g	acceleration of gravity
H	diabatic heating
$H_a^{(i)}$	downward flux of energy by process i related to the diabatic heating of an atmospheric column
$H_s^{(i)}$	downward flux of energy by process i across the surface
HT	poleward heat transport by the atmosphere
$(HT)_2$	poleward heat transport by the atmosphere at level 2
H_*	scale height
I	integral defined in page 56

LIST OF APPENDICES

	Page
APPENDIX I : FINITE DIFFERENCES EQUATIONS	165
APPENDIX II : SPLINE INTERPOLATION	173
APPENDIX III : INSTABILITY OF A TWO-LEVEL MODEL	176
APPENDIX IV : TIME DEPENDENT COEFFICIENTS	182

j_i	fraction of a latitude circle covered with i^{th} kind of surface
K	kinetic energy
K_i	eddy exchange coefficient at level i
k	coefficient defined on page 56
k_*	constant used in expression (3.4.2)
$\hat{k}$	vertical unit vector
L	typical horizontal scale or latent heat for water
M	total angular momentum transport
M_i	angular momentum transport at level i
n	parameter of beta distribution
$P_n(x)$	Legendre polynomial of order n
p	independent variable pressure
Q_i	potential vorticity at level i
q	constant defined on page 16
R	gas constant for dry air
Ro	Rossby number defined on page 11
Ri	Richardson number defined on page 12
R_o	incoming solar radiation at the top of the atmosphere
r	rainfall or parameter of beta distribution defined on page 182
r_a	atmospheric albedo
r_s	surface albedo
T_i	temperature at level i
T_D	oceanic subsurface temperature
t	independent variable time
U	typical wind speed or velocity of a basic flow

u	zonal velocity
$\mathbb{V}$	wind vector
V	component of $\mathbb{V}$
v	meridional velocity
x	zonal coordinate or independent variable (= $\sin\varphi$)
y	meridional coordinate or dependent variable
z	height of an isobaric surface
α	specific volume of the dry air
β	Rossby parameter or beta probability density function
Γ	atmospheric absorption to longwave radiation or spectral density function
γ	ratio of specific heats for dry air
δ	aspect ratio or factor defined on page 45
ϵ	ratio of 100 cb temperature to sea surface temperature
ε	boundary layer friction constant defined on page 21 or dimensionless number defined on page 12
ζ	relative vorticity
η	meridional displacement of a parcel
θ	potential temperature
κ	typical magnitude of the static stability of the atmosphere (= $\partial \ln \theta / \partial z$)
λ	independent variable longitude or constant defined on page 16
λ_n	n^{th} eigenvalue
μ	mesoscale dynamic viscosity
ν	mesoscale kinematic viscosity (= μ / ρ)

ν_1	atmospheric downward emissivity
ν_2	atmospheric upward emissivity
ρ	density of dry air
σ	velocity potential or Stefan-Boltzmann constant
$\bar{\sigma}$	static stability
τ	time scale
Φ	perturbation streamfunction
ϕ	amplitude of Φ or geopotential of an isobaric surface
φ	independent variable latitude
χ	atmospheric opacity to solar radiation
ψ	streamfunction
Ω	angular velocity of the earth
ω	vertical velocity in the isobaric system
$\varkappa$	$(= R/c_p)$
$( )_\sigma$	irrotational component
$( )_\psi$	solenoidal component
$( )_\lambda$	zonal component
$( )_\varphi$	meridional component
$( )_r$	radial component
$( )_s$	standard or surface value
$( )_o$	constant value
$( )_p$	isobaric component or particular solution
$( )_H$	horizontal component
$( )_0$	variable at 0 cb level

$( )_1$	variable at 25 cb level
$( )_2$	variable at 50 cb level
$( )_3$	variable at 75 cb level
$( )_4$	variable at 100 cb level
$( )_Z$	zonal mean
$( )_E$	eddy component, deviation from zonal mean
$( )'$	isobaric deviation
$\overline{( )}$	time mean or horizontal mean
$( )^*$	complex conjugate
$( )^T$	transpose matrix

ABSTRACT

ON THE SIMULATION OF THE AXISYMMETRIC CIRCULATION OF THE ATMOSPHERE

by

Humberto Adrian Fuenzalida

Chairman: Aksel C. Wiin-Nielsen

The governing equations of a two-layer quasi-geostrophic model are cast in terms of potential vorticities and zonally averaged. Using suitable boundary conditions at the pole and equator they are integrated in time for three years. The thermal forcing is provided by an ad hoc diabatic heating function which includes radiative fluxes, latent heat released by condensation, turbulent transport in the boundary layer and thermal interaction with the oceans. The poleward eddy fluxes of sensible heat and angular momentum are parameterized first by means of diagnostically determined exchange coefficients for heat and potential vorticity, which depend on latitude and pressure, but do not vary in time. The integration results include the temperature field at 100 and 50 cb, the zonal flow at 75 and 25 cb, and the vertical motion at 50 cb, all of which are evaluated every third day. The kinetic and available potential energies and their conversions, generation and dissipation are also evaluated with the same frequency. Starting from isothermal and motionless conditions the model reaches a quasi-steady state after a few months. Separate integrations are performed for each hemisphere using the same set of eddy coefficients determined from Northern Hemisphere data by Wiin-Nielsen and Sela (1971). By comparison with empirical data the outcome of the simulation shows that substantial improvement is obtained with respect to previous results

(Sela and Wiin-Nielsen, 1971) by virtue of a more realistic thermal forcing. A sensitivity analysis of the model reveals that some results can be modified by a change of the value of the streamfunction constant and the boundary layer friction and that assuming an exchange coefficient independent of latitude and pressure leads to unrealistic results.

An analysis of the mixing process for quasi-conservative properties together with results by Green(1970), Bretherton(1966), and Pedlosky(1964), and the hypothesis that unstable waves are the responsible agents for the eddy transport, leads to a parameterization of the eddy fluxes such that they depend on the mean gradient of potential vorticity and vary with time. This is a generalization of a result by Stone(1972). An integration of the model using this parameterization provides results which are in better agreement with observations than those obtained in the former simulations.

CHAPTER I

INTRODUCTION

1.1 MOTIVATION OF THE STUDY

Today there exists a complete hierarchy of atmospheric models. In terms of spatial dimensionality they range from the Global Average Models (GAM), which due to a very detailed vertical specification allow a description of photochemical and radiative processes, to the so-called General Circulation Models (GCM) which cover the globe with typically ten levels of a 300-km mesh size grid. Between the one-dimensional GAM and the three-dimensional GCM stand the Models in the Meridional Plane (MPM) with a two-dimensional grid and a moderate cost of operation. They were not created as an economic compromise, but rather are the natural outcome of the symmetry imparted to the atmospheric motions by the rotation of the earth and the thermal forcing imposed by the sun.

Atmospheric motions can be decomposed in a zonal (longitudinal) mean and deviations from it. In extratropical latitudes and for motions in the meridional plane, the temporal mean of the deviations over, say a month, is orders of magnitude smaller than the instantaneous values revealing a turbulent behavior. This turbulent motion is able to diffuse any entity, in particular those with Lagrangian variations smaller than local changes, i.e., a quantity which is conservative to some extent.

Due to the nonlinearity of the governing equations the isolated study of the zonal component of the atmospheric dependent variables is not possible. The zonally averaged equations of

momentum and energy will contain mean products of the variables, whose behavior cannot be predicted by the system formed by these equations only. Thus, starting with a complete set of relations, we end up with more unknowns than equations. This closure problem is the basic difficulty faced in the formulation of the MPM. It is not present in the GAM because the nonlinear terms, which represents interaction within the fluid, vanish when integrated over a closed surface. Neither is it present in the GCM which deals explicitly with the zonal deviations.

The MPM have not enjoyed much popularity among scientists dedicated to climate study probably because the parameterizations of heat and momentum transports have never been done properly. In the present state of climatic simulation they could be extremely helpful since the GCM have a prohibitive cost in experiments comprising several years and the GAM are unable to consider interactions between low and high latitudes.

Lately, the interest in the MPM has been revived by the immediate need of answers to questions related to the impact of present and future technology on the environment. Such answers are to be obtained through climate simulations covering several decades if the interactions between the oceans and the atmosphere are to be included. Even with the next generation of computers this is a prohibitive task for GCM, (SMIC , 1971). Therefore, it is not a mere academic exercise to attempt new formulations of the eddy transfers in a MPM. On the contrary their applications are presently needed.

From a less applied point of view, the ability to simulate the zonal part of the atmospheric phenomena provides a frame within which the deviations or eddies must evolve and possesses a substantial intrinsic interest since the zonal motion constitutes a large fraction of the total atmospheric energy content.

1.2 BRIEF REVIEW OF MOST RECENT PREVIOUS WORK

The kind of turbulent motion we are attempting to parameterize differs in several important aspects from the most commonly studied turbulence. First of all it is highly anisotropic. Typical eddies range from 10,000 to 3,000 km in horizontal dimensions while their vertical extent hardly exceeds 10 km. This configuration forces the particles trajectory to be quasihorizontal. Secondly, the turbulence is nonhomogeneous. Mechanisms that generate this turbulent motion (baroclinic instability, large scale orography and heat sources) are active over most of the wave number range so that eddy motions generate mean values (and other statistics) with important variations in latitude and longitude. Finally, because of the seasonal variations of the acting mechanisms the process in nonstationary. Therefore, the extension of results of turbulence theory to our case is not permissible unless specifically justified.

This parameterization problem is an old one. Lately the heat transport has been modelled successfully (Stone, 1972b), but the momentum transport is still waiting for a solution. This may be due to the fact that momentum as opposed to temperature is not a quasiconservative quantity (Green, 1970).

Following the completion of a diagnostic study of the annual variations of the atmospheric energy cycle, Wiin-Nielsen (1967), this author attempted to simulate the part related to the zonal flow using a simple dynamic model forced by a Newtonian heating function Wiin-Nielsen, 1969, 1970). In these investigations the heat transport was parameterized through an austauch coefficient and the momentum transport was neglected in a first order approximation.

Taking Green's (1970) suggestion, that exchange coefficients should be considered in relation to conservative quantities only, Wiin-Nielsen and Sela (1971) evaluated annual diagnostic coefficients for the exchange of quasigeostrophic potential vorticity at several levels and every $2\frac{1}{2}$ degrees of latitude. Casting the two-level quasigeostrophic model in terms of potential vorticities Sela and Wiin-Nielsen (1971) made another attempt to simulate the axisymmetric component of the general circulation. The heat transport was parameterized by an eddy coefficient dependent on latitude and the thermal forcing was Newtonian. The results of this investigation gave the impression that much could be improved by a more realistic specification of the heating function. In particular, the release of latent heat by condensation and the exchange of sensible heat with the underlying surface of the earth were considered to be the most important mechanisms ignored in the simulation.

The eddy exchange coefficients evaluated by Wiin-Nielsen and Sela (loc. cit.) constitute a first step to prove the usefulness of parameterizations of conservative quantities and are able to generate good simulations of the annual energy cycle, but even if such evaluations were developed to the extent of providing a time dependence for the coefficients these diagnostic values are closely linked to the present

climatic conditions and are of little use in predicting climatic evolutions under conditions significantly different from the current ones.

One has to realize that parameterizations,because of their very nature are approximations to the actual mechanisms. They can never attain complete fidelity and their success depends on the fraction of the variance of the process that can be accounted for in terms of dependent variables. Ideally a parameterization must depend to a large extent on the internal variables of the model and include coefficients or functions with a much smaller variability than that of the process to be modelled.

Both Green (1970) and Stone (1972b) have designed parameterizations for the heat transport using an eddy exchange coefficient proportional to the meridional gradient of temperature. The proportionality factor depends on quantities which have a more restricted variation than the heat flux itself. We will attempt a time dependent formulation which can be considered an extension of their results and because it introduces a feedback mechanism it is more useful in the study of climatic variations.

1.3 A SCOPE AND OUTLINE OF THE STUDY

This study endeavours first to show that a crude dynamic model can account for most of the energy cycle and reproduce its annual variations to a larger extent than that obtained by Sela and Wiin-Nielsen (1971). At the same time these results provide more evidence to support the parameterizations in terms of quasi-conservative quantities. A second related goal is an improvement in the modelling of the momentum transport.

To attain the first goal the model used by Sela and Wiin-Nielsen (loc. cit.) was critically reviewed, its boundary conditions were studied from an analytical point of view and the energetics formulated without referring to balance considerations. All this is done in Chapter 2.

Chapter 3 contains the description of the thermal forcing which now includes latent heat release and exchange of sensible heat with the oceans. This formulation also allows the evaluation of surface temperatures. The heating function is tuned to satisfy the present seasonal variations and its behavior in the simulations is quite satisfactory.

Results from the simulations of both hemispheres separately are reported in Chapter 4. These results are directly comparable with those of Sela and Wiin-Nielsen (loc. cit.) since values of constants and the eddy exchange coefficients are the same. The only difference is a larger time step and grid size. The validation method used to judge the performance of the model is a comparison with observed values. At this point we hope to have shown that substantial improvement was obtained by the use of a more realistic thermal forcing. The main deficiencies of the model are due to its quasi-geostrophic character and the time independent value assigned to the eddy exchange coefficients. It is felt that the advantage of parameterizing the transport of a quasi-conservative quantity such as potential vorticity rather than momentum, which has a very active source in the Coriolis force, is confirmed by this result.

Chapter 5 contains the outcome of sensitivity studies. Various constants of the model are modified to find to what extent the results depend on their particular values. A numerical study is made of the most relevant features of the latitudinal dependence of the three eddy exchange coefficients included in the model to extimate their importance and identify features that depend on them. One result that follows from this study is the inadequacy of a constant austauch coefficient modelling for the transport under consideration. Finally, the results of an improved case are shown.

In Chapter 6 an analysis is made of the different mechanisms that can perform the heat and momentum transport. Under the assumption that the main agents responsible for these fluxes are the waves generated by the baroclinic instability of the zonal flow some results obtained by Green (loc. cit.) and Stone (loc. cit.) are generalized in the light of investigations by Bretherton (1966b) and Pedlosky (1964a) to produce a time dependent formulation for the exchange coefficients.

Finally, Chapter 7 summarizes the conclusions of the work and contains some ideas as to how to make improvements in further attempts.

CHAPTER II

THE MODEL

2.1 BASIC EQUATIONS

This study will be done by using the standard two-level quasi-geostrophic model introduced by Phillips (1956). In the next pages we will summarize the most important simplifications introduced in its formulation and indicate the limitations they convey.

2.1.1 Quasi-geostrophic Equations

The dynamic model to be used is based on the quasi-geostrophic equation of vorticity.

$$\left(\frac{\partial}{\partial t} + \mathbf{V}_\psi \cdot \nabla\right)(\zeta + f) = -f_0 \nabla \cdot \mathbf{V}_\sigma - g \frac{\partial}{\partial p} \hat{k} \cdot \nabla \times \mathbf{F} \qquad (2.1.1)$$

where the independent variables are time, t, and the space coordinates λ, φ, p, longitude, latitude and pressure, respectively. Hence the local derivative $\frac{\partial}{\partial t}$ and the two-dimensional operator

$$\mathbf{V} \cdot \nabla \equiv \frac{V_\lambda}{a \cos\varphi} \frac{\partial}{\partial \lambda} + \frac{V_\varphi}{a} \frac{\partial}{\partial \varphi} \qquad (2.1.2)$$

are evaluated isobarically. The horizontal velocity has been decomposed in a solenoidal part $\mathbf{V}_\psi = \hat{k} \times \nabla \Psi$, where $\hat{k}$ is the vertically upward unit vector and Ψ a streamfunction, and an irrotational component $\mathbf{V}_\sigma = \nabla \sigma$, where σ is a velocity potential. The vertical component of the relative vorticity is given by the horizontal part of the Laplacian of the streamfunction.

$$\zeta \equiv \frac{1}{a\cos\varphi}\left[\frac{\partial V_\varphi}{\partial\lambda} - \frac{\partial}{\partial\varphi}\left(V_\lambda\cos\varphi\right)\right]$$

$$\equiv \frac{1}{a^2\cos\varphi}\left[\frac{\partial}{\partial\lambda}\left(\frac{1}{\cos\varphi}\frac{\partial\psi}{\partial\lambda}\right) + \frac{\partial}{\partial\varphi}\left(\cos\varphi\frac{\partial\psi}{\partial\varphi}\right)\right] \qquad (2.1.3)$$

As customary f represents the Coriolis parameter, $2\Omega\sin\varphi$, where Ω is the angular velocity of the earth. The subscript zero denotes a constant value. The divergence operator is given by

$$\nabla\cdot\mathbb{V} \equiv \frac{1}{a\cos\varphi}\left[\frac{\partial V_\lambda}{\partial\lambda} + \frac{\partial}{\partial\varphi}\left(V_\varphi\cos\varphi\right)\right] \qquad (2.1.4)$$

By the same token the vertical component of the rotational operator is

$$\hat{k}\cdot\nabla\times\mathbb{V} \equiv \frac{1}{a\cos\varphi}\frac{\partial V_\varphi}{\partial\lambda} - \frac{1}{a\cos\varphi}\frac{\partial}{\partial\varphi}\left(V_\lambda\cos\varphi\right)$$

where the vector $\mathbb{V}$ has components $(V_\lambda, V_\varphi, V_r)$ along unit vectors oriented west to east, south to north and upwards respectively.

The last term in (2.1.1) accounts for the frictional force due to the vertical variation of the horizontal stress $\mathbb{F}$. Here g represents the acceleration of gravity.

The irrotational part of the wind will be eliminated using the equation of continuity

$$\nabla\cdot\mathbb{V}_\sigma + \frac{\partial\omega}{\partial p} = 0 \qquad (2.1.5)$$

where ω is the individual variation of pressure, the vertical "velocity" of the coordinate system x, y, p.

A third relation to be used is the first principle of the thermodynamics in its quasi-geostrophic form

$$\left(\frac{\partial}{\partial t} + \mathbf{V}_\psi \cdot \nabla\right)\frac{\partial \phi}{\partial p} - \omega\alpha\left(\frac{\partial \ln\theta}{\partial p}\right)_s = -\frac{R}{C_p}\frac{H}{p} \qquad (2.1.6)$$

Here the subscript s denotes a standard value independent of the horizontal coordinates and time. The potential temperature is related to the temperature T , density ρ and pressure by

$$\theta = T p^{-\varkappa} \cdot \text{const} = \text{const} \cdot p^{1/\delta} \rho^{-1} \qquad (2.1.7)$$

where $\varkappa = \frac{R}{C_p}$, R is the dry air gas constant and C_p the specific heat of the dry air at constant pressure. Finally z is a dependent variable which denotes the height of an isobaric surface and H the diabatic heating rate.

In the quasi-geostrophic formulation the balance equation, which completes the basic set, is reduced to $\psi = f_o \phi$, where $\phi = gz$.

In the process of obtaining this set of relations starting from the complete equations (vorticity, divergence, continuity and the first principle of thermodynamics) scale, filtering and constraint-preserving simplifications that limit the applicability of the equations have been introduced. A brief description of them, based on the discussion of Charney (1960) and Charney and Stern (1962), follows.

The first filtering approximation we will be concerned with is the hydrostatic assumption which filters out vertically travelling sound waves. The scaling condition equivalent to the replacement of the vertical equation of motion by the hydrostatic relation is $\delta = \frac{D}{L} \ll 1$ where D and L are vertical and horizontal distances across which the dependent variables vary in their typical order of magnitude.

δ is sometimes called the aspect ratio. This approximation upsets the conservations of angular momentum and energy under adiabatic and reversible conditions. In order to restore them the kinetic energy has to be redefined excluding the vertical motion, Coriolis and metric terms including the vertical velocity must be deleted from the horizontal equations of motion, and the radial spherical coordinate must be replaced by the radius of the earth ("shallowness" approximation). The hydrostatic approximation is satisfied with a high degree of accuracy in the atmospheric large scale systems and permits the introduction of the isobaric quasi-Lagrangian coordinate system x, y, p.

The next filtering approximations are the geostrophic conditions. These are stated as a small Rossby number, $R_o \equiv \frac{U}{2\Omega L} < O(1)$, where U is a typical value for the horizontal velocity, and by setting a lower bound to the value of the typical time scale, τ, (time required for a dependent variable to change by its characteristic magnitude) in terms of the advective time: $\tau \geq O(LU^{-1})$.

Although the Rossby number just defined does not show it explicitly this approximation fails in the vicinity of the equator. The small Rossby number allows a perturbation expansion which has as zero order approximation the geostrophic relation, and as first order approximation the quasi-geostrophic equations.

The replacement of the divergence equation by the geostrophic relation filters out gravity waves and to maintain the energy constraint it is necessary to redefine the kinetic energy as that due to the solenoidal part of the wind only.

The third scale consideration relates to the importance of the conversion of available potential into kinetic energy. The term

that determinates the conversion in the vorticity equation is the divergence term whose order of magnitude is then assumed to be one or more, e. g.

$$\varepsilon \equiv \frac{4\Omega^2 L^2}{g\kappa D} \equiv \left(\frac{L}{L_R}\right)^2 \geq O(1)$$

where κ is the typical magnitude of the static stability, $\partial \ln \theta / \partial z$, and L_R is the Rossby radius of deformation. Since $\varepsilon Ro^2 Ri = 1$ this condition is sometimes stated as requiring a large value of the Richardson number $R_i = \frac{g\kappa D}{U^2}$.

The next set of relations are chosen as to guarantee horizontal pressure deviations much smaller than the magnitude of the variable itself. These are $\kappa\varepsilon \ll 1$, $D/H_* \leq O(1)$. Since $\varepsilon \geq O(1)$ the first relation implies a very small value for the static stability. In fact observations show ε to be order one, and Eady (1949) concluded that this corresponds to the most efficient systems in converting potential to kinetic energy. In this case $\kappa < O(1)$ is enough. The second relation selects systems whose vertical extension D is similar or smaller than the scale height H_*.

The smallness of the horizontal baric deviations carries with it a similar bound on the density, specific volume and more important, on the static stability, which then can be replaced by a standard value within the accuracy in use (first order in R). However, such a substitution breaks the link between total potential and kinetic energy and no stabilization results from the energy conversion, Lorenz (1960). This assumption does not seem of great importance in climate simulation according to some recent results by Stone (1973).

The relation $D/H_* \lesssim O(1)$ together with the hydrostatic and geostrophic approximations imply an irrotational part of the wind, V_σ, of order εR_o while the solenoidal part, V_ψ, is order one. By the same token the relations used to transform derivatives from a quasi-Lagragian system of reference (x, y, ξ), isobaric or isentropic, to the fixed (x, y, z) system are of the form

$$\left(\frac{\partial}{\partial s}\right)_\xi = \left(\frac{\partial}{\partial s}\right)_z - \varepsilon R_o \left(\frac{\partial \xi}{\partial s}\right)_z \left(\frac{\partial}{\partial z}\right)$$

where s stands for time or any horizontal space variable, and all variables are dimensionless.

Finally, we use a simplification of the governing equations which can be justified through a scale analysis when the beta-plane geometry is being used. This simplification is related to the space variations of the Coriolis parameter in the divergence term of the vorticity equation and in the linear balance equation. The spherical geometry makes invalid the scale argument normally used. But, the simplicity introduced by this approximation is most desirable since it makes the streamfunction proportional to the geopotential. Because this approximation gives good results in the beta-plane geometry and the great simplification it provides we will use it. Once this decision has been taken it is necessary to replace the Coriolis parameter by a constant value in the terms affected by the previous simplification. Such substitution has to be done to avoid fictitious sources of vorticity. However, this is obtained at expense of a discontinuity in the Coriolis parameter at the equator and henceforth on the geostrophic winds.

The sole simplification of the governing equations by an order of magnitude criterion can lead to serious inconsistencies when

they are integrated over long times. One way to keep some control on this aspect is to modify the equations without altering energy invariants that the original complete set of equations satisfy. Although in some of the filtering approximations care was taken to maintain the energy invariants, at least with good approximation, it is necessary to check the final equations and the energetic processes derived from them. We will do this in 2.3.3.

Equation (2.1.1) and (2.1.5) allow the elimination of $\nabla \cdot \mathbf{V}_\sigma$ giving

$$\left(\frac{\partial}{\partial t} + \mathbf{V}_\psi \cdot \nabla\right)\left(\zeta + f\right) = f_0 \frac{\partial \omega}{\partial p} - g \frac{\partial}{\partial p} \hat{k} \cdot \nabla \times \mathbf{F}_H \qquad (2.1.8)$$

where the last term represents the friction term that includes internal and boundary layer effects, $\mathbf{F}_H$ is the horizontal stress vector. Substituting $\Phi = gz$ and $\bar{\sigma} = -\alpha \frac{\partial \ln \theta}{\partial p}$, a standard value depending only on p, and including the heating term we can write

$$\left(\frac{\partial}{\partial t} + \mathbf{V}_\psi \cdot \nabla\right) \frac{\partial \phi}{\partial p} + \bar{\sigma}\omega = -\frac{H}{p} \frac{R}{C_p} \qquad (2.1.9)$$

Equations (2.1.8) and (2.1.9) constitute the basic relations which are used in the two-level quasi-geostrophic model, beside $\phi = f_0 \psi$. Eliminating the geopotential and substituting the streamfunction where necessary we obtain

$$\left(\frac{\partial}{\partial t} + \hat{k} \times \nabla\psi \cdot \nabla\right)\left(\nabla^2 \psi + f\right) = f_0 \frac{\partial \omega}{\partial p} - g \frac{\partial}{\partial p} \hat{k} \cdot \nabla \times \mathbf{F}_H \qquad (2.1.10)$$

$$\left(\frac{\partial}{\partial t} + \hat{k} \times \nabla\psi \cdot \nabla\right) \frac{\partial \psi}{\partial p} + \frac{\bar{\sigma}}{f_0}\omega = -\frac{R}{f_0 C_p} \frac{H}{p} \qquad (2.1.11)$$

These equations determine the solenoidal field of horizontal motion through Ψ and the vertical circulation by ω, when the stress $\mathcal{F}$ has been expressed as a function of them and the diabatic heating H is prescribed.

In frictionless adiabatic conditions these equations (by elimination of ω) define an invariant under horizontal nondivergent motion

$$\left(\frac{\partial}{\partial t} + \mathbf{V}_\psi \cdot \nabla\right)\left(f + \zeta + \frac{\partial}{\partial p}\frac{f_o^2}{\bar{\sigma}}\frac{\partial \Psi}{\partial p}\right) = 0 \qquad (2.1.12)$$

this is the pseudo-potential vorticity of Charney (1971), which replaces Ertel's potential vorticity in quasi-geostrophic motion (Charney and Stern, 1962).

2.1.2 Two-level Approximations

In the two-level model the vertical resolution is kept to a minimum: two levels for ψ and one for ω. Using the classical notation we will denote the levels 0, 25, 50, 75 and 100 cb by 0, 1, 2, 3, 4 respectively.

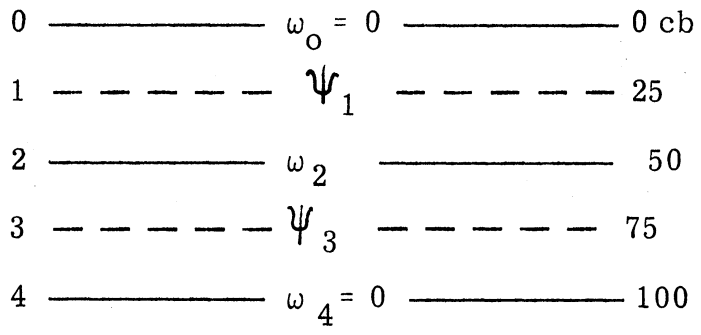

the boundary conditions are then applied to ω : $\omega = 0$ at levels 0 and 4. Orography effects are not considered in this study.

Equation (2. 1. 10) applied to levels 1 and 3 gives

$$\frac{\partial \zeta_1}{\partial t} + \mathbb{V}_1 \cdot \nabla \left(f + \zeta_1 \right) = \frac{2 f_0}{p_s} \omega_2 - \frac{2 g}{p_s} \hat{k} \cdot \nabla \times \left(\mathbb{F}_2 - \mathbb{F}_0 \right) \qquad (2.1.13)$$

$$\frac{\partial \zeta_3}{\partial t} + \mathbb{V}_3 \cdot \nabla \left(f + \zeta_3 \right) = - \frac{2 f_0}{p_s} \omega_2 - \frac{2 g}{p_s} \hat{k} \cdot \nabla \times \left(\mathbb{F}_4 - \mathbb{F}_2 \right) \qquad (2.1.14)$$

where $p_s = 100$ cb and $\mathbb{V}_1, \mathbb{V}_3$ are understood to be solenoidal velocities. Equation (2. 1. 11) applied to level 2 gives

$$\frac{\partial}{\partial t} \left(\Psi_3 - \Psi_1 \right) + \mathbb{V}_2 \cdot \nabla \left(\Psi_3 - \Psi_1 \right) + \frac{\bar{\sigma} p_s}{2 f_0} \omega_2 = - \frac{R}{f_0 C_p} H_2 \qquad (2.1.15)$$

To close the system we set

$$\mathbb{V}_2 = \frac{1}{2} \left(\mathbb{V}_1 + \mathbb{V}_3 \right)$$

Substituting ω_2 from (2. 1. 15) into (2. 1. 13) we obtain

$$\left(\frac{\partial}{\partial t} + \mathbb{V}_1 \cdot \nabla \right) \left[f + \zeta_1 - \frac{4 f_0^2}{\bar{\sigma} p_s^2} \left(\Psi_3 - \Psi_1 \right) \right] =$$

$$- \frac{4 R f_0}{\bar{\sigma} p_s^2 C_p} H - \frac{2 g}{p_s} \hat{k} \cdot \nabla \times \left(\mathbb{F}_2 - \mathbb{F}_0 \right)$$

We define a thermal wind by $\mathbb{V}_T = \frac{1}{2} \left(\mathbb{V}_1 - \mathbb{V}_3 \right)$ and a corresponding streamfunction $\Psi_T = \frac{1}{2} \left(\Psi_1 - \Psi_3 \right)$. Then replacing

$$q_1^2 = \frac{8 f_0^2}{\bar{\sigma} p_s^2} \qquad \lambda^2 = \frac{4 R f_0}{\bar{\sigma} C_p p_s^2}$$

we can write

$$\left(\frac{\partial}{\partial t} + \mathbb{V}_1 \cdot \nabla \right) \left(f + \zeta_1 - q_1^2 \Psi_T \right) = - \lambda^2 H_2 - \frac{2 g}{p_s} \hat{k} \cdot \nabla \times \left(\mathbb{F}_2 - \mathbb{F}_0 \right) \qquad (2.1.16)$$

In a similar way we get

$$\left(\frac{\partial}{\partial t}+\mathbb{V}_3\cdot\nabla\right)\left(f+\zeta_3+q_1^2\Psi_T\right)=-\lambda^2 H_2-\frac{2g}{p_s}\hat{k}\cdot\nabla\times\left(\mathbb{F}_4-\mathbb{F}_2\right) \tag{2.1.17}$$

These two equations define the potential vorticities at levels 1 and 3. These quantities are going to be of central importance in the eddy flux parameterization.

Note that the left hand side of these equations can be expressed in terms of Ψ_1 , and Ψ_3 only, since

$$\zeta_1=\nabla^2\Psi_1 \qquad \mathbb{V}_1=\hat{k}\times\nabla\Psi_1$$

$$\Psi_T=\tfrac{1}{2}\left(\Psi_1-\Psi_3\right)$$

$$\zeta_3=\nabla^2\Psi_3 \qquad \mathbb{V}_3=\hat{k}\times\nabla\Psi_3$$

Defining the potential vorticities

$$Q_1=f+\nabla^2\Psi_1-q_1^2\Psi_T \tag{2.1.18}$$

$$Q_3=f+\nabla^2\Psi_3+q_1^2\Psi_T \tag{2.1.19}$$

we can formulate a diagnostic identity as follows

$$\nabla^2\Psi_T-q_1^2\Psi_T=\tfrac{1}{2}\left(Q_1-Q_3\right) \tag{2.1.20}$$

and write our prognostic equations in the form:

$$\frac{\partial Q_1}{\partial t}=-\nabla\cdot\left(\mathbb{V}_1 Q_1\right)-\lambda^2 H-\frac{2g}{p_s}\hat{k}\cdot\nabla\times\left(\mathbb{F}_2-\mathbb{F}_0\right) \tag{2.1.21}$$

$$\frac{\partial Q_3}{\partial t}=-\nabla\cdot\left(\mathbb{V}_3 Q_3\right)+\lambda^2 H-\frac{2g}{p_s}\hat{k}\cdot\nabla\times\left(\mathbb{F}_4-\mathbb{F}_2\right) \tag{2.1.22}$$

The thermal streamfunction relates to the temperature at level 2 by the relation $\phi = F_o \Psi$, which gives

$$F_o \Psi_T = \phi_T = \frac{1}{2}\left(\phi_1 - \phi_3\right)$$

Using the hydrostatic relation applied at level 2 we obtain

$$F_o \Psi_T = \frac{1}{2}\alpha_2 \frac{p_s}{2} = \frac{1}{2}\frac{RT_2}{p_2}\frac{p_s}{2}$$

where T_2 is the mean temperature between 25 and 75 cb.

Therefore

$$2F_o \Psi_T = RT_2 \qquad (2.1.23)$$

2.1.3 Zonally Averaged Equations

In order to study the axisymmetric circulation we average the governing equations with respect to longitude. Let us define the operator

$$\left(\ \right)_z = \frac{1}{2\pi}\int_0^{2\pi} \left(\ \right) d\lambda$$

and apply it to equations (2.1.20) to (2.1.23). Then

$$\frac{\partial Q_{1z}}{\partial t} = -\frac{1}{a\cos\varphi}\frac{\partial}{\partial\varphi}\left[\cos\varphi\left(v_1 Q_1\right)_z\right] - \lambda^2 H_{2z}$$

$$+\frac{2g}{p_s}\frac{1}{a\cos\varphi}\frac{\partial}{\partial\varphi}\left[\cos\varphi\left(\mathcal{F}_{2x} - \mathcal{F}_{ox}\right)_z\right] \qquad (2.1.24)$$

$$\frac{\partial Q_{3z}}{\partial t} = -\frac{1}{a\cos\varphi}\frac{\partial}{\partial\varphi}\left[\cos\varphi\left(v_3 Q_3\right)_z\right] + \lambda^2 H_{2z}$$

$$+\frac{2g}{p_s}\frac{1}{a\cos\varphi}\frac{\partial}{\partial\varphi}\left[\cos\varphi\left(F_{4x}-F_{2x}\right)_z\right] \qquad (2.1.25)$$

$$\frac{1}{a\cos\varphi}\frac{\partial}{\partial\varphi}\cos\varphi\,\frac{\partial\psi_{Tz}}{\partial\varphi} - q^2\psi_{Tz} = \frac{1}{2}\left(Q_{1z}-Q_{3z}\right) \qquad (2.1.26)$$

$$2 f_o \psi_{Tz} = R T_{2z} \qquad (2.1.27)$$

The advective terms in (2.1.24) and (2.1.25) can be decomposed as:

$$\left(v_i Q_i\right)_z = \left[\left(v_{iz}+v_{iE}\right)\left(Q_{iz}+Q_{iE}\right)\right]_z \qquad i=1,3$$

$$= v_{iz} Q_{iz} + \left(v_{iE} Q_{iE}\right)_z = \left(v_{iE} Q_{iE}\right)_z$$

since in a quasigeostrophic model $v_{iz} = 0$. The subscript E denotes deviations from the zonal mean.

Considering simple parameterizations of the internal and boundary layer friction described below and an exchange coefficient law for the eddy transport of potential vorticity, whose validity will be analyzed later

$$\left(v_{iE} Q_{iE}\right)_z = -K_1(\varphi)\frac{\partial Q_{iz}}{a\partial\varphi} \qquad (2.1.28)$$

$$\left(v_{3E} Q_{3E}\right)_z = -K_3(\varphi)\,\frac{\partial Q_{3z}}{a\,\partial\varphi} \tag{2.1.29}$$

the prognostic equations become

$$\frac{\partial Q_{1z}}{\partial t} = \frac{1}{a^2\cos\varphi}\,\frac{\partial}{\partial\varphi}\left(K_1\cos\varphi\,\frac{\partial Q_{1z}}{\partial\varphi}\right) - \lambda^2 H_{2z} - A\left(\zeta_{1z} - \zeta_{3z}\right) \tag{2.1.30}$$

$$\frac{\partial Q_{3z}}{\partial t} = \frac{1}{a^2\cos\varphi}\,\frac{\partial}{\partial\varphi}\left(K_3\cos\varphi\,\frac{\partial Q_{3z}}{\partial\varphi}\right) + \lambda^2 H_{2z}$$

$$+ A\left(\zeta_{1z} - \zeta_{3z}\right) - \frac{\varepsilon}{2}\left(3\zeta_{3z} - \zeta_{1z}\right) \tag{2.1.31}$$

These equations allow the computation of future potential vorticities Q_{1z} and Q_{3z} if we know the current values of the heating H_{2z} and the vorticities ζ_{1z}, ζ_{3z}, Q_{1z}, Q_{3z}. With the new values of Q_{1z} and Q_{3z} equation (2.1.26) permits the evaluation of the new ψ_{Tz}. Then (2.1.27) gives the temperature T_{2z} and the identities

$$\nabla^2\psi_{Tz} = \zeta_{Tz} = \frac{1}{2}\left(\zeta_{1z} - \zeta_{3z}\right)$$

$$\frac{1}{2}\left(Q_{1z} + Q_{3z}\right) - f = \frac{1}{2}\left(\zeta_{1z} + \zeta_{3z}\right) \tag{2.1.32}$$

give the new vlaues of ζ_{1z} and ζ_{3z}. Finally if we have H_{2z} as a function of T_{2z}, for all time and location, a new time integration is possible and this process can be repeated indefinitely.

Knowing the vorticities we can compute the zonal flow by integration. The vertical motion can be calculated from the thermodynamic relation (2.1.15) or the omega equation of the system. Meridional flow, if necessary, can be obtained by the continuity equation (2.1.5). The temperatures at the 100 cb level will also be obtained through the heating function H_{zz}.

2.1.4 Subgrid Parameterizations

The only subgrid processes that will be included, outside of those considered in the heating function, are the boundary layer friction and the internal dissipation due to vertical shear.

Boundary layer friction enter the vorticity equations (2.1.24) and (2.1.25) in terms of the form

$$F_i = \frac{2g}{p_s} \frac{1}{a\cos\varphi} \frac{\partial}{\partial\varphi}\left[\cos\varphi \left(\mathcal{F}_{i+1,x} - \mathcal{F}_{i-1,x}\right)_z\right] \qquad i = 1,3$$

It will be assumed that $\mathcal{F}_0 = 0$ and that $\mathcal{F}_4$ is entirely due to the vertical flux of momentum in the Prandtl layer. A simple formulation for this process is $\mathcal{F}_4 = C_d \rho_4 V_4 \mathbb{V}_4$ which with an additional linearization, that consists of using V_4 and ρ_4 as constants, gives

$$\frac{2g}{p_s} \frac{1}{a\cos\varphi} \frac{\partial}{\partial\varphi}\left(\cos\varphi\, \mathcal{F}_{4x}\right) = -\frac{2g}{p_s} C_d \rho_4 V_4 \zeta_{4z}$$

The drag coefficient C_d can attain values between 10^{-3} and 10^{-2} depending on the roughness of the underlying surface (Cressman, 1960). Then define

$$\varepsilon = \frac{2g C_d \rho_4}{p_s} V_4$$

a constant for a given value of C_d. In the experiments a value $\varepsilon = 3 \times 10^{-6}\ \text{sec}^{-1}$ was chosen corresponding to $C_d = 2.5$ for $V_4 = 5\,\text{msec}^{-1}$. The unknown value of vorticity at 100 cb will be estimated by linear extrapolation as $\zeta_4 = \frac{1}{2}(3\zeta_3 - \zeta_1) = \zeta_2 - 2\zeta_T$. Then

$$\frac{2g}{p_s}\frac{1}{a\cos\varphi}\frac{\partial}{\partial\varphi}\left(\mathcal{F}_{4x}\cos\varphi\right) = -\frac{\varepsilon}{2}\left(3\zeta_3 - \zeta_1\right)$$

Outside the surface layer we will use $\mathcal{F} = \mu\frac{\partial V}{\partial z}$ so that

$$\mathcal{F}_{2x} = \mu\left.\frac{\partial u}{\partial z}\right|_2 = -\rho_2^2 \nu g \left.\frac{\partial u}{\partial p}\right|_2$$

In finite difference form

$$\mathcal{F}_{2x} = \frac{g\nu p_s}{R^2 T_2^2}\,u_T$$

Considering $A \equiv \frac{g^2\nu}{R^2T_2^2}$ as a constant we obtain

$$\frac{2g}{p_s}\frac{1}{a\cos\varphi}\frac{\partial}{\partial\varphi}\left(\mathcal{F}_{2x}\cos\varphi\right)_z = -2A\zeta_{Tz} = -A\left(\zeta_{1z} - \zeta_{3z}\right)$$

Therefore, the dissipation term in (2. 1. 24) becomes

$$\frac{2g}{p_s}\frac{1}{a\cos\varphi}\frac{\partial}{\partial\varphi}\left[\cos\varphi\left(\mathcal{F}_{2x} - \mathcal{F}_{0x}\right)_z\right] = -A\left(\zeta_{1z} - \zeta_{3z}\right)$$

while the corresponding term in (2. 1. 25) is

$$\frac{2g}{p_s}\frac{1}{a\cos\varphi}\frac{\partial}{\partial\varphi}\left[\cos\varphi\left(\mathcal{F}_{4x} - \mathcal{F}_{2x}\right)_z\right] = A\left(\zeta_{1z} - \zeta_{3z}\right) - \frac{\varepsilon}{2}\left(3\zeta_{3z} - \zeta_{1z}\right)$$

2.1.5 Additional Diagnostic Relations

Equations (2.1.30), (2.1.31), (2.1.26) and (2.1.27) together with identities (2.1.18) and (2.1.19) provide a way to evaluate the vorticities ζ_1 , ζ_3 , the thermal streamfunction ψ_T and the temperature at a midtropospheric level, T_2 , once a procedure to obtain the diabatic heating is designed. This problem will be postponed until Chapter 3, where it will be shown how to obtain also the temperature at 100 cb or a near surface level.

Presently we will be concerned with the determination of the zonal flow and the meridional circulations.

Zonal velocities at levels 1 and 3 will be computed by integration from the meridional distribution of relative vorticities. This procedure is more accurate and economic than the use of streamfunctions.

By definition

$$\zeta_{iz} = -\frac{1}{a\cos\varphi}\frac{\partial}{\partial\varphi}\left(u_{iz}\cos\varphi\right) \qquad i=1,2,3$$

An integration from equator to pole gives

$$u_{iz}\left(\varphi=0\right) = a\int_0^{\pi/2} \zeta_{iz}\cos\varphi'\,d\varphi'$$

Then integrating from equator to any latitude circle one obtains

$$u_{iz}\left(\varphi\right) = \frac{a}{\cos\varphi}\int_{\varphi}^{\pi/2} \zeta_{iz}\cos\varphi'\,d\varphi' \qquad (2.1.33)$$

This relation can be used also for U_T since it depends on vorticity only.

The vertical motion can be calculated from the thermodynamic equation in the geostrophic formulation (2.1.15). In terms of the thermal streamfunction this equation can be written as

$$\frac{\partial}{\partial t}\psi_T + \nabla\cdot\left(\nabla_2\psi_T\right) - \frac{\bar{\sigma}\, p_s}{4 f_0}\omega_2 = \frac{R}{2 f_0 C_p} H_2 \qquad (2.1.34)$$

Taking the zonal average we obtain

$$\frac{\partial}{\partial t}\psi_{TZ} + \frac{1}{a\cos\varphi}\frac{\partial}{\partial\varphi}\left[\left(v_2\psi_T\right)_Z\cos\varphi\right] - \frac{\bar{\sigma}\, p_s}{4 f_0}\omega_{2Z} = \frac{R}{2 f_0 C_p} H_{2Z} \qquad (2.1.35)$$

Since in a quasi-geostrophic theory $v_{2Z} = 0$

$$\left(v_2\psi_T\right)_Z = \left(v_{2E}\psi_{TE}\right)_Z = -K_2(\varphi)\frac{\partial\psi_{TZ}}{a\partial\varphi} \qquad (2.1.36)$$

The last equality needs some comments. In Chapter 6 we will try to justify a diffusive parametrization for quasi-conservative properties. The thermal streamfunction does not fit into this category in the same sense as potential vorticities, i.e., considering only the advection by the solenoidal part of the horizontal wind. Equation (2.1.34) shows that ψ_T is conserved under adiabatic conditions when the contribution of the vertical motion is also taken into account. However, Clapp (1970) has provided observational evidence that a parameterization through an eddy coefficient is adequate for the horizontal heat transfer by transient eddies. We will use it realizing that some inconsistency in our approach is introduced. Equation (2.1.35) allows the evaluation

of ω_{2z} if the eddy coefficient $K_2(\varphi)$ is available:

$$\omega_{2z}=\frac{4f_o}{\bar{\sigma}p_s}\left[\frac{\partial}{\partial t}\psi_{Tz}-\frac{1}{a^2\cos\varphi}\frac{\partial}{\partial\varphi}\left(K_2\cos\varphi\frac{\partial\psi_{Tz}}{\partial\varphi}\right)-\frac{R}{2f_oC_p}H_{2z}\right] \quad (2.1.37)$$

Once the vertical motion is known the meridional velocity is provided by the equation of continuity integrated with respect to latitude:

$$v_{1z}=-v_{3z}=\frac{2a}{p_s\cos\varphi}\int_{\varphi}^{\pi/2}\omega_{2z}\cos\varphi'\,d\varphi' \quad (2.1.38)$$

2.2 BOUNDARY CONDITIONS

It is our purpose to integrate equations (2.1.30) and (2.1.31) in time and relation (2.1.26) in space over each hemisphere. To accomplish such a task we need boundary conditions at both poles and equator and an initial condition which as we shall see bears little importance to the outcome of the experiments. For the time being we will be concerned with the boundary conditions only. The three equations present regular singularities at the poles that owe their existence to the coordinate system. From a physical point of view the solutions sought have to be finite everywhere in the domain $|\varphi|\leq\frac{\pi}{2}$. Furthermore, the parabolic character of the predictive equations for potential vorticity indicates that a kind of insulating conditions

$$\frac{\partial}{\partial\varphi}Q_{iz}=0 \qquad i=1,3 \quad (2.2.1)$$

are appropriate at any finite boundary. Likewise, to preclude any flux of heat across boundaries one should select

$$\frac{\partial}{\partial \varphi}\Psi_{Tz} = 0 \qquad (2.2.2)$$

However, the same insulating conditions could be obtained by imposing zero eddy diffusion coefficients at the boundaries:

$$K_1 = K_2 = K_3 = 0$$

and using some other form of boundary condition. Furthermore, at the poles a limiting process is necessary since the area vanishes there. To decide upon the most appropriate boundary condition we will now consider a more detailed analysis.

For the axisymmetric flow the poles are natural (although singular) boundaries, on the contrary the equator has to be chosen a boundary because of limitations of the governing equations and data availability. This is an essential distinction which introduces profound differences in the search for suitable boundary conditions.

2.2.1 Boundary Conditions at the Poles

Equation (2.1.26) is to be integrated over the domain $0 \leq \varphi \leq \frac{\pi}{2}$. Having in mind that the thermal streamfunction Ψ_{Tz} is proportional to the mean temperature between 25 and 75 cb, any boundary condition in terms of Ψ_{Tz} only would be too restrictive. Hence more suitable forms will express conditions on the first derivative at both ends of the interval.

At this point it seems appropriate to consider the balance of terms in equation (2.1.26) since our main concern is global and seasonal variations , a suitable scaling magnitude for spatial derivatives is the radius of the earth a. Then the Laplacian is of order a^{-2} a quantity which compared with q^2 is about 160 times smaller.

Hence in (2. 1. 26) the second term on the left hand side balance almost completely the right hand side. To a good approximation we have:

$$\psi_{TZ} \approx -\frac{1}{2q^2}\left(Q_{1Z} - Q_{3Z}\right) \qquad (2.\,2.\,4)$$

which is the inner solution. Unless boundary conditions are chosen in such a way that they are compatible with this inner solution thermal boundary layers are bound to appear. Observational data does not support the existence of such layers and care must be exercised when choosing the boundary conditions for ψ_{TZ}, Q_{1Z} and Q_{3Z}

Returning to the complete differential equation (2. 1. 26) if we use a new independent variable $x = \sin\varphi$ it can be written as

$$\left(1-x^2\right)y'' - 2xy' - a^2q^2y(x) = F(x) \qquad (2.\,2.\,5)$$

where $y(x) \equiv \psi_{TZ}(\varphi)$ and $F(x) = \frac{a^2}{2}\left(Q_{1Z} - Q_{3Z}\right)$

The homogeneous equation

$$\left(1-x^2\right)y'' - 2xy' - a^2q^2y(x) = 0 \qquad (2.\,2.\,6)$$

has eigenvalues $\lambda_n = a^2q^2 + n(n+1) \qquad n = 0, 2, 4, \ldots$

with Legendre polynomials $P_n(x)$ as eigenfunctions. This choice of n implies an even $y(x)$ which keeps some global invariants on the hemisphere, as will be shown further on. The equation then can be solved by a Fourier analysis technique

$$y(x) = -\sum_{\substack{n=0 \\ \text{even}}}^{\infty} \frac{c_n}{\lambda_n} P_n(x)$$

where

$$F(x) = \sum_{\substack{n=0 \\ \text{even}}}^{\infty} c_n P_n(x)$$

This procedure suggest that at x=1 no other condition than finiteness is strictly required once the regular solution has been chosen.

In the Fourier technique the choice of the regularly behaved solution at $x = \pm 1$ is made when the second solution of the Legendre equation is left aside. The problem is now how to perform this selection in a finite difference formulation.

The differential equation (2. 2. 6) has two linearly independent solutions. A power series technique around x=1 gives a first solution

$$y_1 = 1 + \frac{a^2 q^2}{2}\left[1 - x\right] + \cdots$$

while the second is

$$y_2 = y_1 \mathrm{Ln}\left[1-x\right] + \sum_{n=0}^{\infty} b_n \left[1 - x\right]^n$$

Hence a boundary condition of the form

$$\frac{y'_{x=1}}{y_{x=1}} = -\frac{a^2 q^2}{2}$$

would select the finite solution of the homogeneous equation. We still have to consider the contributions from the forcing function F (x).

The particular solution of (2. 2. 5) can be expressed in terms of a Green's function $G(x, x')$ as

$$y_p(x) = \int_0^1 G(x,x')\, F(x')\, dx'$$

and since

$$G(x,x') = -\sum_{\substack{n=0 \\ \text{even}}}^{\infty} \frac{P_n(x)\, P_n(x')}{a^2 q^2 + n(n+1)}$$

it is seen that $G(x,x')$ and its derivative are finite at $x = \pm 1$. Hence $y_p'(x=\pm 1)$ is finite when $F(x)$ and its derivative exists at $x = \pm 1$ which is always true, and we can use a condition like

$$\frac{y'_{x=1}}{y_{x=1}} = M < \infty \qquad (2.2.7)$$

to choose the regular solution of (2.2.5).

Returning to our original independent variable φ relation (2.2.7) corresponds to

$$\lim_{\varphi \to \frac{\pi}{2}} \frac{1}{\cos\varphi} \frac{\partial}{\partial \varphi} \psi_{Tz} - M \lim_{\varphi \to \frac{\pi}{2}} \psi_{Tz} = 0$$

From the finiteness of ψ_{Tz} one concludes then that a useful boundary condition, would be

$$\lim_{\varphi \to \frac{\pi}{2}} \frac{\partial}{\partial \varphi} \psi_{Tz} = 0 \qquad (2.2.8)$$

A completely similar analysis gives the same condition as $\varphi \longrightarrow -\frac{\pi}{2}$.

Once this choice is made as the boundary condition for equation (2.1.26) relation (2.2.4) suggests that the expression

$$\lim_{\varphi \to \frac{\pi}{2}} \frac{\partial}{\partial \varphi} \left(Q_{1z} - Q_{3z} \right) = 0 \qquad (2.2.9)$$

:an be used as a boundary condition for the prognostic relations 2. 2. 30) and (2. 1. 31) thereby avoiding the formation of thermal)oundary layers near the poles.

Equation (2. 1. 26) can be written as

$$\frac{\partial^2 \psi_{Tz}}{\partial \varphi^2} - \frac{\sin \varphi}{\cos \varphi} \frac{\partial \psi_{Tz}}{\partial \varphi} - a^2 q^2 \psi_{Tz} = \frac{a^2}{2} \left(Q_{1z} - Q_{3z} \right)$$

aking the limit as $\varphi \to \frac{\pi}{2}$ and using L'Hospital's rule and (2. 2. 2) ve get

$$\frac{2}{a^2} \frac{\partial^2 \psi_{Tz}}{\partial \varphi^2} - q^2 \psi_{Tz} = \frac{1}{2} \left(Q_{1z} - Q_{3z} \right) \qquad (2.2.10)$$

a relation that replaces (2. 1. 26) at the poles.

We now turn to the predictive relations. Equations 2. 1. 30) and (2. 1. 31) share a term of the form

$$\frac{1}{a^2 \cos \varphi} \frac{\partial}{\partial \varphi} \left[K \cos \varphi \frac{\partial Q}{\partial \varphi} \right] \equiv D$$

which can be written

$$a^2 D = K \frac{\partial^2 Q}{\partial \varphi^2} + \frac{\partial K}{\partial \varphi} - K \tan \varphi \frac{\partial Q}{\partial \varphi}$$

and the finiteness of the expression demands that $K \tan \varphi \frac{\partial Q}{\partial \varphi}$ remain)ounded as $\varphi \to \pi/2$. This requirement and relation (2. 2. 9) gives as boundary conditions

$$\lim_{\varphi \to \frac{\pi}{2}} \frac{\partial Q_{iz}}{\partial \varphi} = 0 \quad \text{or} \quad K_i = 0 \qquad (2.2.11)$$

The first alternative was chosen because it satisfies in a very simple way relation (2. 2. 9) , is quite adequate for an axisymmetric solution and because a vanishing eddy coefficient is not a very realistic representation for the polar cyclonic activity which although sporadic and weak still exists. L'Hospital rule then gives

$$\lim_{\varphi\to\frac{\pi}{2}} \frac{\sin\varphi}{\cos\varphi}\frac{\partial Q}{\partial\varphi} = -\lim_{\varphi\to\frac{\pi}{2}} \frac{\partial^2 Q}{\partial\varphi^2} = -\left.\frac{\partial^2 Q}{\partial\varphi^2}\right|_{\varphi=\frac{\pi}{2}}$$

and

$$\lim_{\varphi\to\frac{\pi}{2}} a^2 D = 2\left|K\frac{\partial^2 Q}{\partial\varphi^2}\right|_{\varphi=\pm\frac{\pi}{2}} - \left|\frac{\partial K}{\partial\varphi}\frac{\partial Q}{\partial\varphi}\right|_{\varphi=\pm\frac{\pi}{2}}$$

Then the two prognostic equations have as limit form over the poles

$$\frac{\partial Q_{1z}}{\partial t} = \frac{2K_1}{a^2}\frac{\partial^2 Q_{1z}}{\partial\varphi^2} + \frac{1}{a^2}\frac{\partial K_1}{\partial\varphi}\frac{\partial Q_{1z}}{\partial\varphi} - \lambda^2 H_{2z} - A\left(\zeta_{1z} - \zeta_{3z}\right) \qquad (2.2.12)$$

$$\frac{\partial Q_{3z}}{\partial t} = \frac{2K_3}{a^2}\frac{\partial^2 Q_{3z}}{\partial\varphi^2} + \frac{1}{a^2}\frac{\partial K_3}{\partial\varphi}\frac{\partial Q_{3z}}{\partial\varphi} + \lambda^2 H_{2z} + A\left(\zeta_{1z} - \zeta_{3z}\right) - \frac{\varepsilon}{2}\left(3\zeta_{3z} - \zeta_{1z}\right) \qquad (2.2.13)$$

The thermodynamic equation, (2. 1. 34) used to evaluate the meridional circulation, also presents this kind of term which by (2. 2. 8) is reduced so that the limit form of the equation for the pole is

$$\frac{\partial\psi_{Tz}}{\partial t} + \frac{2K_2}{a^2}\frac{\partial^2\psi_{Tz}}{\partial\varphi^2} + \frac{1}{a^2}\frac{\partial K_2}{\partial\varphi}\frac{\partial\psi_{Tz}}{\partial\varphi} - \frac{\bar{\sigma}\,p_s}{4f_0}\omega_{2z} = \frac{1}{2}\frac{R}{c_p}\frac{1}{f_0}H_{2z} \qquad (2.2.14)$$

2. 2. 2 Boundary Conditions at the Equator

Since any vorticity is by definition, at any level and time,

$$\zeta = \frac{1}{a\cos\varphi}\frac{\partial}{\partial\varphi}\left[\cos\varphi\frac{\partial\psi}{\partial\varphi}\right]$$

integrating from pole to pole one gets

$$\int_{\pi/2}^{\pi/2}\zeta\cos\varphi'\,d\varphi' = 0$$

If the integration is over one hemisphere only

$$\int_{0}^{\pi/2}\zeta\cos\varphi'\,d\varphi' = \frac{1}{a^2}\frac{\partial\psi}{\partial\varphi}\bigg|_{\varphi=0}$$

so that to retain a zero total vorticity, at any level and time, over the hemisphere we must set

$$\frac{\partial\psi}{\partial\varphi}\bigg|_{\varphi=0} = 0$$

indicating that convenient boundary conditions at the equator are

$$\frac{\partial\psi_{1z}}{\partial\varphi} = \frac{\partial\psi_{3z}}{\partial\varphi} = \frac{\partial\psi_{Tz}}{\partial\varphi} = \frac{\partial\psi_{2z}}{\partial\varphi} = 0 \qquad (2.2.15)$$

This also precludes heat fluxes across the equator, and makes

$$\int_{0}^{\pi/2}\left(Q_1 + Q_3\right)\cos\varphi'\,d\varphi' = 0$$

as can be easily shown from the definitions of Q_1 and Q_3. From the potential vorticity expressions one deduces that

$$\frac{\partial Q_1}{\partial \varphi} = 2\Omega + \frac{\partial \zeta_1}{\partial \varphi}$$

$$\frac{\partial Q_3}{\partial \varphi} = 2\Omega + \frac{\partial \zeta_3}{\partial \varphi} \qquad (2.2.16)$$

at the equator.

Adding the equations (2.1.30) and (2.1.31) multiplying by $\cos\varphi$ and integrating from pole to pole we get

$$\frac{\partial}{\partial t}\left[\int_{\pi/2}^{\pi/2}\left(Q_{1z}+Q_{3z}\right)\cos\varphi\, d\varphi\right] = 0$$

When the integration is performed over one hemisphere only, subject to (2.2.15) we obtain

$$\frac{\partial}{\partial t}\left[\int_{0}^{\pi/2}\left(Q_{1z}+Q_{3z}\right)\cos\varphi\, d\varphi\right] = \left| a^{-2} K_1 \frac{\partial Q_{1z}}{\partial \varphi} + K_3 \frac{\partial Q_{3z}}{\partial \varphi}\right|_{\varphi=0}$$

and to preserve the constancy of $(Q_{1z} + Q_{3z})$ over the hemisphere we have to assume

$$\left| K_1 \frac{\partial Q_{1z}}{\partial \varphi} + K_3 \frac{\partial Q_{3z}}{\partial \varphi}\right|_{\varphi=0} = 0$$

For arbitrary K_1 and K_3 this can be attained only if

$$\left.\frac{\partial Q_{1z}}{\partial \varphi}\right|_{\varphi=0} = \left.\frac{\partial Q_{3z}}{\partial \varphi}\right|_{\varphi=0} = 0 \qquad (2.2.17)$$

which is another convenient boundary condition at the equator. Then by (2. 2. 16)

$$\frac{\partial \zeta_1}{\partial \varphi} + 2\Omega = 0$$
$$\frac{\partial \zeta_3}{\partial \varphi} + 2\Omega = 0 \qquad (2.2.18)$$

at the equator.

These boundary conditions imply symmetry conditions with respect to the equator as can be seen from the power series solutions of (2. 2. 5) around the equator.

Equation (2. 2. 5) has as solutions around $\mu = 0$

$$y = 1 + a_1 x\left[1 + \frac{2+a^2q^2}{6}x^2 + \ldots\right] + \frac{a^2q^2}{2}x^2\left[1 + \frac{6+a^2q^2}{12}x^2 + \ldots\right]$$

and

$$y = x\left[1 + \frac{2+a^2q^2}{6}x^2 + \frac{2+a^2q^2}{6}\,\frac{12+a^2q^2}{20}x^4 + \cdots\right]$$

where a_1 is arbitrary. Imposing

$$\left.\frac{\partial y}{\partial x}\right|_{x=0} = 0$$

or in terms of φ

$$\left.\frac{\partial \psi_{Iz}}{\partial \varphi}\right|_{\varphi=0} = 0$$

we are picking an even solution around the equator for Ψ_{Tz} . An odd solution is not possible because of the physical interpretation of Ψ_{Tz} (proportional to mean atmospheric temperature), and points out that it is impossible to cross the equator with a formulation in terms of the geostrophic streamfunction. Since

$$RT_{2z} = 2f_0\Psi_{Tz}$$

and f_0 is discontinuous across the equator, the symmetry of Ψ_{Tz} implies a discontinuity of T_{2z} or vicerversa.

The diagnostic equation for Ψ_{Tz} at the equator becomes

$$\frac{\partial^2\Psi_{Tz}}{\partial\varphi^2} - a^2q^2\Psi_{Tz} = \frac{a^2}{2}\left(Q_{1z} - Q_{3z}\right) \qquad (2.2.19)$$

The potential vorticity equations are for $\varphi = \pm\frac{\pi}{2}$

$$\frac{\partial Q_{1z}}{\partial t} = \frac{K_1}{a^2}\frac{\partial^2 Q_{1z}}{\partial\varphi^2} - \lambda^2 H_{2z} - A\left[\zeta_{1z} - \zeta_{3z}\right] \qquad (2.2.20)$$

$$\frac{\partial Q_{3z}}{\partial t} = \frac{K_3}{a^2}\frac{\partial^2 Q_{3z}}{\partial\varphi^2} + \lambda^2 H_{2z} + A\left[\zeta_{1z} - \zeta_{3z}\right] - \frac{\varepsilon}{2}\left[3\zeta_{3z} - \zeta_{1z}\right] \qquad (2.2.21)$$

and the thermodynamic equation

$$\frac{\partial\Psi_{Tz}}{\partial t} - \frac{K_2}{a^2}\frac{\partial^2\Psi_{Tz}}{\partial\varphi^2} - \frac{\bar{\sigma}p_s}{4f_0}\omega_{2z} = \frac{1}{2}\frac{R}{C_p}\frac{1}{f_0}H_{2z} \qquad (2.2.22)$$

We have now given mathematical justification for the choice of boundary conditions at the poles. Conservation principles valid for the globe help to define them at the equator.

The boundary conditions at the pole include vanishing meridional first derivatives of the two potential vorticities. However to state the finite difference solution in a most economic fashion such conditions must be supplemented. Specifically to reduce the integration matrix to a tridiagonal one it is necessary to require a second order symmetry as polar boundary condition:

$$\frac{\partial^n Q_{1z}}{\partial \varphi^n} = \frac{\partial^n Q_{3z}}{\partial \varphi^n} = 0 \qquad n = 1,3 \tag{2. 2. 23}$$

which by (2. 2. 16) also implies

$$\frac{\partial^n \zeta_{1z}}{\partial \varphi^n} = \frac{\partial^n \zeta_{3z}}{\partial \varphi^n} = 0 \qquad n = 1,3 \tag{2. 2. 24}$$

2. 3 ENERGETICS OF THE MODEL

Under this heading we consider first the meridional transports of angular momentum and heat to continue with that part of the energy cycle linked to the zonal kinetic and available potential energies.

2. 3. 1 Momentum Transport

In a quasi-geostrophic model with continuous vertical structure potential vorticity is defined from equation (2. 1. 12) as

$$Q = f + \zeta + \frac{\partial}{\partial p}\left(\frac{f_o^2}{\bar{\sigma}} \frac{\partial \psi}{\partial p}\right) \qquad (2.3.1)$$

The transport of potential vorticity is obtained from this definition multiplied by the meridional velocity, v, and zonally averaged. If the transport of relative vorticity is expressed in terms of the convergence of momentum and the temperature is substituted for the streamfunction, by using the hydrostatic relation we obtain

$$\left[v Q\right]_z = \frac{1}{\cos^2\varphi} \frac{\partial}{a\,\partial\varphi}\left\{\left[uv\right]_z \cos^2\varphi\right\} - \frac{\partial}{\partial p}\left\{\frac{f_o R}{\bar{\sigma} p}\left[vT\right]_z\right\} \qquad (2.3.2)$$

The substitution for the fluxes of heat and potential vorticities by expressions in terms of the eddy coefficient for quasi-conservative quantities, K, whose uniqueness was proved by Bretherton (1966b), provide after some simplification

$$\frac{1}{a\cos^2\varphi} \frac{\partial}{\partial\varphi}\left\{\left[uv\right]_z \cos^2\varphi\right\} = K \frac{\partial[f+\zeta]}{a\,\partial\varphi} + \frac{f_o R}{\bar{\sigma} p} \frac{\partial K}{\partial p} \frac{\partial T}{a\,\partial\varphi} \qquad (2.3.3)$$

This equation shows that the vertical variation of the exchange coefficient K is linked to the evolution of the dependent variables. It also suggests that momentum transport can be modelled indirectly if parameterizations of the heat and potential vorticity transports are available and that these parameterizations are not completely independent of each other, but have to satisfy the integral constraints of

the transport of angular momentum. Assuming steady state conditions, integrating over the complete atmospheric column and remembering that in steady state or for annual mean conditions the total divergence of angular momentum equals the surface torque exerted by the air on the earth one obtains:

$$-g\tau_s = \int_0^{p_s} K \frac{\partial [f+\zeta]_z}{a\,\partial\varphi} dp + \int_0^{p_s} \frac{f_0 R}{\bar{\sigma} p} \frac{\partial T}{a\,\partial\varphi} \frac{\partial K}{\partial p} dp \qquad (2.3.4)$$

Under the assumption that deviations from steadiness are small and considering that τ_s is proportional to the surface wind where surface westerlies prevail, the second integral must be negative and dominate the right hand side of the equation. The first integral is positive because under quasi-geostrophic conditions $f >> \zeta_z$.

If we now integrate (2.3.3) with respect to latitude from pole to pole after multiplying by $\cos^2\varphi$ we get:

$$\int_{-\pi/2}^{\pi/2} \left\{ K \frac{\partial [f+\zeta]}{a\,\partial\varphi} + \frac{f_0 R}{\bar{\sigma} p} \frac{\partial K}{\partial p} \frac{\partial T}{a\,\partial\varphi} \right\} \cos^2\varphi \, d\varphi = 0 \qquad (2.3.5)$$

This is a condition that has to be satisfied on any isobaric surface and is also valid for the hemispheric case if the boundary conditions imply a vanishing transport across the equator.

Since quasi-geostrophy implies a misrepresentation in the low latitude regions and vanishing mean meridional motions, the important transfer of angular momentum by the Hadley cell is underestimated and one has to expect a large negative residual in the hemispheric balance of momentum. Within a quasi-geostrophic framework it is illusory to comply with relation (2.3.5).

Let us now turn to our two-level model. From the definitions of potential vorticities (2. 1. 18) and (2. 1. 19) one can deduce the relations

$$-\frac{1}{a\cos^2\varphi}\frac{\partial}{\partial\varphi}\left\{\left[u_1v_1\right]_z\cos^2\varphi\right\}=\left[v_1Q_1\right]_z+q^2\left[v_2\psi_T\right]_z \qquad (2.3.6)$$

$$-\frac{1}{a\cos^2\varphi}\frac{\partial}{\partial\varphi}\left\{\left[u_3v_3\right]_z\cos^2\varphi\right\}=\left[v_3Q_3\right]_z-q^2\left[v_2\psi_T\right]_z \qquad (2.3.7)$$

that relate the transports of potential vorticities to those of momentum and heat. In obtaining these expressions use has been made of integration by parts and the vanishing advection of temperature by the thermal wind.

In view of the parameterizations introduced by equations (2. 1. 28), (2. 1. 29), and (2. 1. 36) these relations can be cast in the form

$$-\frac{1}{a\cos^2\varphi}\frac{\partial}{\partial\varphi}\left\{\left[u_1v_1\right]_z\cos^2\varphi\right\}=-K_1\frac{\partial Q_{1z}}{\partial\varphi}-q^2K_2\frac{\partial\psi_{Tz}}{\partial\varphi} \qquad (2.3.8)$$

$$-\frac{1}{a\cos^2\varphi}\frac{\partial}{\partial\varphi}\left\{\left[u_3v_3\right]_z\cos^2\varphi\right\}=-K_2\frac{\partial Q_{3z}}{\partial\varphi}+q^2K_2\frac{\partial\psi_{Tz}}{\partial\varphi} \qquad (2.3.9)$$

If we multiply by $a\cdot\cos^2\varphi$ and integrate these equations from pole to pole we obtain

$$\int_{-\pi/2}^{\pi/2}\left\{\frac{\partial Q_{1z}}{\partial\varphi}+q^2K_2\frac{\partial\psi_{Tz}}{\partial\varphi}\right\}\cos^2\varphi\,d\varphi=0 \qquad (2.3.10)$$

$$\int_{-\pi/2}^{\pi/2}\left\{\frac{\partial Q_{3z}}{\partial\varphi}-q^2K_2\frac{\partial\psi_{Tz}}{\partial\varphi}\right\}\cos^2\varphi\,d\varphi=0 \qquad (2.3.11)$$

These integral constraints show that the use of time independent values for K_1, K_2 and K_3 introduces some inconsistency. In hemispheric models these constraints reduce to

$$\int_0^{\pi/2} \left\{ K_1 \frac{\partial Q_{1z}}{\partial \varphi} + q^2 K_2 \frac{\partial \psi_{Tz}}{\partial \varphi} \right\} \cos^2\varphi \, d\varphi = - \left[u_1 v_1 \right]_z \Big|_{\varphi=0} = 0 \qquad (2.3.12)$$

$$\int_0^{\pi/2} \left\{ K_3 \frac{\partial Q_{3z}}{\partial \varphi} - q^2 K_2 \frac{\partial \psi_{Tz}}{\partial \varphi} \right\} \cos^2\varphi \, d\varphi = - \left[u_3 v_3 \right]_z \Big|_{\varphi=0} = 0 \qquad (2.3.13)$$

The last equality is based on boundary conditions which isolate one hemisphere from the other: $v_1(\varphi=0) = v_3(\varphi=0) = 0$. Addition of these relations gives

$$\int_0^{\pi/2} \left\{ K_1 \frac{\partial Q_{1z}}{\partial \varphi} + K_3 \frac{\partial Q_{3z}}{\partial \varphi} \right\} \cos^2\varphi \, d\varphi = 0 \qquad (2.3.14)$$

If we add equations (2.3.6) and (2.3.7) to obtain the vertically integrated divergence of momentum, by the same procedure we got the relation (2.3.4) for the continuous case, the two-level model gives after some arrangements and substitutions

$$-2\varepsilon u_{4z} = (K_3 + K_1) \frac{\partial}{a \partial \varphi} (Q_{3z} + Q_{1z}) + (K_3 - K_1) \frac{\partial}{a \partial \varphi} (Q_{3z} - Q_{1z}) \qquad (2.3.15)$$

a relation that must be satisfied under steady conditions or over a typical year. As far as the zonal flow is concerned this cannot be attained by adding a constant velocity to the flow at all levels. Such additions implies a change in vorticity so that the corrected solution

is not compatible with the governing differential equations and the boundary conditions. Such a correction was evaluated for each year so as to make the atmospheric torque on the earth vanish, but is not included in the results presented later.

The angular momentum transport will be evaluated from an integration, from a given latitude to the pole, of equations (2. 3. 8) and (2. 3. 9):

$$\left[u_1 v_1\right]_z \cos\varphi \Big|_\varphi = -\frac{a}{\cos\varphi}\int_\varphi^{\pi/2}\left\{K_1\frac{\partial Q_{1z}}{\partial\varphi} + q^2 K_2\frac{\partial \psi_{Tz}}{\partial\varphi}\right\}\cos^2\varphi\, d\varphi$$

$$\left[u_3 v_3\right]_z \cos\varphi \Big|_\varphi = -\frac{a}{\cos\varphi}\int_\varphi^{\pi/2}\left\{K_3\frac{\partial Q_{3z}}{\partial\varphi} - q^2 K_2\frac{\partial \psi_{Tz}}{\partial\varphi}\right\}\cos^2\varphi\, d\varphi$$

The angular momentum transported poleward across the latitude circle φ in the upper half of the atmosphere is, using the thermal wind $u_{Tz} = -\frac{\partial \psi_{Tz}}{a\,\partial\varphi}$

$$M_1 = -\frac{\pi a^2 p_s}{g}\int_\varphi^{\pi/2}\left\{K_1\frac{\partial Q_{1z}}{\partial\varphi} - q^2 K_2 a\, u_{Tz}\right\}\cos^2\varphi\, d\varphi \qquad (2.3.16)$$

and below 50 cb we obtain a similar relation:

$$M_3 = -\frac{\pi a^2 p_s}{g}\int_\varphi^{\pi/2}\left\{K_3\frac{\partial Q_{3z}}{\partial\varphi} + q^2 K_2 a\, u_{Tz}\right\}\cos^2\varphi\, d\varphi \qquad (2.3.17)$$

giving a total amount for the whole column:

$$M = -\frac{\pi a^2 p_s}{g}\int_{\varphi}^{\pi/2}\left\{K_1\frac{\partial Q_{1z}}{\partial\varphi} + K_3\frac{\partial Q_{3z}}{\partial\varphi}\right\}\cos^2\varphi\, d\varphi \qquad (2.3.18)$$

2.3.2 Heat Transport

By definition the heat transport is given by

$$\left[HT\right]_2 = \left(v_2 T_2\right)_z c_p = c_p \frac{2f_0}{R}\left(v_2 \psi_T\right)_z$$

Using the eddy exchange parameterization (2.1.36) we get

$$\left(HT\right)_2 = -\frac{2f_0}{aR} K_2 \frac{\partial \psi_{Tz}}{\partial\varphi} c_p$$

or in terms of the zonal thermal wind

$$\left(HT\right)_2 = c_p \frac{2f_0}{R} K_2 u_{Tz}$$

For the whole atmospheric column we finally obtain

$$\left(HT\right) = 2\pi a\cos\varphi \frac{p_s}{g} c_p \frac{2f_0}{R} K_2 u_{Tz}$$

$$= 4\pi \frac{a p_s c_p f_0}{g R} K_2 u_{Tz}\cos\varphi \qquad (2.3.19)$$

2.3.3 Energy Balance

Through 2.1 we have described briefly the various approximations behind equations (2.1.30), (2.1.31), (2.1.26) and (2.1.27). Several of these simplifications have been justified from an order of

magnitude viewpoint. Such an approach seems justified for short range prediction purposes, but it may not be suitable when integrations are performed over long periods of time. Lorenz (1960) has introduced one procedure which through energy invariants attains inner consistency of the equations and avoids unbalanced sources of energy. Following the same idea we will perform a detailed analysis of the expressions describing energy conversions and will match the outcome of the equations of motion and the thermodynamics first principle. This procedure will also help to define quadrature schemes for integration in pressure which in a two-level model are heavily truncated.

In the model we are using, the available potential and the kinetic energy enter the only invariant since the static stability is not allowed to vary (Lorenz, 1960).

Kinetic energy is evaluated more precisely from the zonal velocities directly, instead of vorticities, because those are the outcome of an integration which in general will tend to compensate errors. The model provides zonal velocities at two levels and these will enter in a quadratic form in the kinetic energy evaluation.

Available potential energy, on the other hand, can be evaluated from isobaric deviations of the thermal streamfunction which is given at one level only. Again the form involved is quadratic. Hence we have more and better information for the kinetic energy than for the available potential energy. On these grounds it was decided to choose the kinetic energy expression and adjust the potential energy formula so that conservation of energy prevails in the system in the adiabatic, frictionless case.

The kinetic energy of the model is expressed in terms of the solenoidal component of the isobaric flow only. This is a consequence of the hydrostatic and geostrophic assumptions mentioned in Section 2. 1. a. If we choose a trapezoidal rule for a quadrature scheme in pressure we can define the kinetic energy for the atmosphere by

$$K = \frac{p_s}{2g} \int_S \frac{1}{2} \left\{ \mathbb{V}_1 \cdot \mathbb{V}_1 + \mathbb{V}_3 \cdot \mathbb{V}_3 \right\} dS$$

where the integration is performed over an isobaric surface. Considering zonal means and their deviations

$$\mathbb{V}_i = \mathbb{V}_{iz} + \mathbb{V}_{iE} \qquad i = 1,3$$

the total kinetic energy can be expressed as $K = K_z + K_E$

where

$$K_E = \frac{p_s}{2g} \int_S \left\{ \frac{1}{2} \mathbb{V}_{1E} \cdot \mathbb{V}_{1E} + \mathbb{V}_{3E} \cdot \mathbb{V}_{3E} \right\} dS$$

$$K_z = \frac{p_s}{2g} \int_S \left\{ \frac{1}{2} \mathbb{V}_{1z} \cdot \mathbb{V}_{1z} + \mathbb{V}_{3z} \cdot \mathbb{V}_{3z} \right\} dS \qquad (2.3.20)$$

In terms of the streamfunction after an integration by parts we obtain

$$K_z = - \frac{p_s}{2g} \int_S \frac{1}{2} \left\{ \psi_{1z} \zeta_{1z} + \psi_{3z} \zeta_{3z} \right\} dS ;$$

then

$$\frac{dK_z}{dt} = - \frac{p_s}{2g} \int_S \left\{ \psi_{1z} \frac{\partial \zeta_{1z}}{\partial t} + \psi_{3z} \frac{\partial \zeta_{3z}}{\partial t} \right\} dS$$

This expression is suitable for use with the vorticity equations of the model. Remembering that the winds V_1 and V_3 in equations (2. 1. 13) and (2. 1. 14) are solenoidal the zonal mean of the advection terms can be written

$$\left\{ V\cdot\nabla(\zeta+f) \right\}_z = \frac{1}{a\cos\varphi}\frac{\partial}{\partial\varphi}\left\{ (\zeta v)_z \cos\varphi \right\} \qquad (2.3.21)$$

Noting that by the solenoidal condition and after some arrangements we can obtain

$$(\zeta v)_z = -\frac{1}{a\cos^2\varphi}\frac{\partial}{\partial\varphi}\left\{ (uv)_z \cos^2\varphi \right\} \qquad (2.3.22)$$

Substitution of (2. 3. 21) and (2. 3.22) in the zonal mean of (2. 1. 13) and (2. 1. 14) gives

$$\frac{\partial \zeta_{iz}}{\partial t} = -\frac{1}{a\cos\varphi}\frac{\partial}{\partial\varphi}\left\{ \frac{1}{a\cos\varphi}\frac{\partial}{\partial\varphi}\left[(u_i v_i)_z \cos^2\varphi \right] \right\} + \delta\frac{2f_0}{p_s}\omega_{2z} + F_i$$

where $i = 1, 3$

$$\delta = \begin{cases} 1 & i=1 \\ -1 & i=3 \end{cases}$$

$$F_i = \begin{cases} -\ 2A\zeta_{Tz} & i=1 \\ -\ \frac{1}{2}\left[\varepsilon(3\zeta_{3z}-\zeta_{1z}) - 4A\zeta_{Tz}\right] & i=3 \end{cases}$$

Forming the expression for the time variation of the zonal mean kinetic energy and after some manipulation we obtain

$$\frac{dK_z}{dt} = -\frac{p_s}{2g}\int_S \frac{dS}{a\cos^2\varphi}\left\{\sum_{i=1,3} u_{iz}\frac{\partial}{\partial\varphi}\left[\left(u_i v_i\right)_z \cos^2\varphi\right]\right\}$$

$$-\frac{2f_0}{g}\int_S \omega_{2z}\,\psi_{Tz}\,dS$$

$$+\int_S \left\{2A u_{Tz}^2 + \frac{\varepsilon}{2}u_{3z}\left(3u_{3z}-u_{1z}\right)\right\}dS \qquad (2.3.23)$$

The interpretation of each term in the right hand side is evident. The conversion of zonal available potential to kinetic energy can be written as

$$C\left(A_z, K_z\right) = -\frac{2f_0}{g}\int_S \omega_{2z}\,\psi_{Tz}\,dS \qquad (2.3.24)$$

and the dissipation of kinetic energy by friction

$$D\left(K_z\right) = \int_S \left\{2A u_{Tz}^2 + \frac{\varepsilon}{2}u_{3z}\left(3u_{3z}-u_{1z}\right)\right\}dS \qquad (2.3.25)$$

In order to express the conversion of eddy to zonal kinetic energy in terms of zonal mean quantities we will make use of the relations

$$-\frac{1}{a\cos^2\varphi}\frac{\partial}{\partial\varphi}\left\{\left(u_i v_i\right)_z \cos^2\varphi\right\} = \left(v_{iE}Q_{iE}\right)_z + \\ + \delta q^2 \left(v_{iE}\psi_{TE}\right)_z \qquad i = 1,3 \qquad (2.3.26)$$

which are deduced from the definitions of potential vorticities (2.1.18) and (2.1.19) making use of (2.3.22). Then the eddy flux parameterizations (2.1.28), (2.1.29) and (2.1.36) allows us to write down the first term on the right hand side of (2.3.23) as

$$C\left(K_E, K_z\right) = -\frac{p_s}{2g}\int_S \sum\left\{u_{iz}K_i \frac{\partial Q_{iz}}{a\,\partial\varphi}\right\} dS + \\ + \frac{p_s}{g} q^2 \int_S K_z u_{Tz}^2 \, dS \qquad (2.3.27)$$

The thermodynamic equation (2.1.34) can be used to obtain an expression for the rate of change of available potential energy. Since this is related to the isobaric variance of the thermal field (Lorenz, 1955) as a first step let us take the isobaric mean of (2.1.34) and subtract it from the original equation to obtain

$$\frac{\partial \psi_T'}{\partial t} + \nabla\cdot\left(V_2 \psi_T\right) - \frac{\bar{\sigma} p_s}{4 f_0}\omega_2 = \frac{R}{2 f_0 c_p} H_2' \qquad (2.3.28)$$

where primes indicate isobaric deviations.

Taking zonal mean of (2. 3. 28) we get

$$\frac{\partial \psi'_{Tz}}{\partial t} + \frac{1}{a\cos\varphi}\frac{\partial}{\partial \varphi}\left(v_z \psi_T\right)_z \cos\varphi - \frac{\bar{\sigma} p_s}{4 f_o}\omega_{2z} = \frac{R}{2 f_o c_p} H'_{2z}$$

According to (2. 3. 24), which links the zonal kinetic to the zonal potential energy the conversion, $C(A_z, K_z)$ must be generated from the vertical velocity term. To obtain the same form as in (2. 3. 18) we have to multiply by $\frac{8 f_o^2}{g p_s \bar{\sigma}} \psi'_{Tz}$ and integrate. In this connection we must remember that $\omega_{2z} = \omega'_{2z}$ by conservation of mass so that $\psi_{Tz}\omega_{2z} = \psi'_{Tz}\omega_{2z}$. Introducing (2. 1. 36) we obtain

$$\frac{dA_z}{dt} = -C\left(A_z, A_E\right) - C\left(A_z, K_z\right) + G\left(A_z\right)$$

where

$$G\left(A_z\right) = \frac{4 R f_o}{g c_p \bar{\sigma} p_s}\int_S H'_{2z}\psi'_{Tz}\, dS \qquad (2.3.29)$$

$$C\left(A_z, A_E\right) = \frac{p_s}{g} q^2 \int_S K_z u^2_{Tz}\, dS \qquad (2.3.30)$$

and the zonal available potential energy must be defined as

$$A_z = \frac{p_s}{2g} q^2 \int_S \psi'^2_{Tz}\, dS \qquad (2.3.31)$$

CHAPTER III

DIABATIC HEATING

3.1 INTRODUCTION

The purpose of this section is the design of a heating model suitable for a zonally averaged, two-level model with a time resolution adequate to simulate annual variations. This heating function must be as close as possible to reality in order to minimize its effect as a source of errors and permit a validation of results by comparison with observations. We will not hesitate to make use of climatological information to obtain this goal and therefore the thermal forcing to be formulated is of little value for climate simulation purposes.

In the standard form, the two-level model possess a constant static stability which fixes the value of the lapse rate and limits the representation of the infrared vertical fluxes to some function of the mean atmospheric temperature. Another shortcoming of the dynamic model, from a radiative point of view, is the location of the level where thermodynamic variables are evaluated. If the atmosphere is to be considered a grey body a temperature representative of the lower troposphere is more relevant than the 50 cb value, since the most active absorber and thick clouds are found there. However, Smagorinsky (1963), Saltzman (1967 and 1968) and Saltzman and Vernekar (1971) have dealt successfully with this problem and provide us with useful basic information.

The driving force of atmospheric motions is the radiative transfer of energy. As a consequence, radiative processes play a central role in the forcing of the dynamical model. Radiative processes

depend strongly upon temperatures at the earth's surface and in the atmosphere. The latter is specified initially and subsequently forecasted by the two-level model. The surface temperature has to be determined. For this purpose use is made of the heat balance of a thin surface layer with negligible heat capacity. Admittedly this is an idealization which is not supported by reality over the oceans, where solar radiation penetrates several meters while long wave radiation, evaporation and turbulent transfer of heat are actual surface processes. Thus our "thin" layer is several meters thick and has an important heat capacity. This complication will be disregarded in this attempt. As a matter of fact temperatures at 100 cb will be used as surface values.

When the surface temperature is known, the diabatic heating can be obtained from the energy balance of the air column.

Simplicity and the nature of the dynamical model dictate a climatological water balance independent of vertical motions which the model determines poorly in tropical regions, where the release of latent heat is important.

3.2 HEAT BALANCE FOR AN ATMOSPHERIC COLUMN

Considering a unit vertical column of air as a whole, five processes contribute to its diabatic heating (Fig. 3.2.1):

i) Shortwave solar incoming radiation
ii) Atmospheric longwave emission
iii) Terrestrial longwave emission
iv) Transport of sensible heat across the earth surface
v) Latent heat released by condensation

Following Saltzman (1968) these five processes will be labelled $H_a^{(i)}$, $i = 1, 2, 3, 4, 5$. The analytical expression for some of them will be those used by several authors, Smagorinsky

(1963), Saltzman (1968) and Saltzman and Vernekar (1971), namely

$$H_a^{(1)} = \chi (1 - r_a) R_o$$

$$H_a^{(2)} = (\nu_1 + \nu_2) \sigma T_2^4 \qquad (3.2.1)$$

$$H_a^{(3)} = \Gamma \sigma T_4^4$$

where χ is the atmospheric opacity to solar radiation, r_a is the atmospheric albedo, ν_1 is the downward emissivity of the atmosphere, ν_2 is the upward emissivity of the atmosphere, Γ is the atmospheric absorptivity to long wave radiation, R_o is the incoming solar radiation at the top of the atmosphere, T_2 the mean tropospheric temperature and T_4 the surface temperature.

Specific analytical expressions for the transfer of sensible heat and latent heat release will be considered in the next section.

To evaluate the diabatic heating consider the vertical divergence of the fluxes through the whole column. At the top of the atmosphere the net flux is

$$F_t = - \left[R_o (1-r_a) - r_s (1-r_a) (1-\chi) R_o \right] + \nu_2 \sigma T_2^4 + (1 - \Gamma) \sigma T_4^4$$

the upward net flux across the surface is

$$F_b = - R_o (1-r_a) (1-r_s) (1-\chi) - \nu_1 \sigma T_2^4 + \sigma T_4^4$$

The only important heat source to be considered is the release of latent heat by consensation processes $H_a^{(5)}$. Other heating

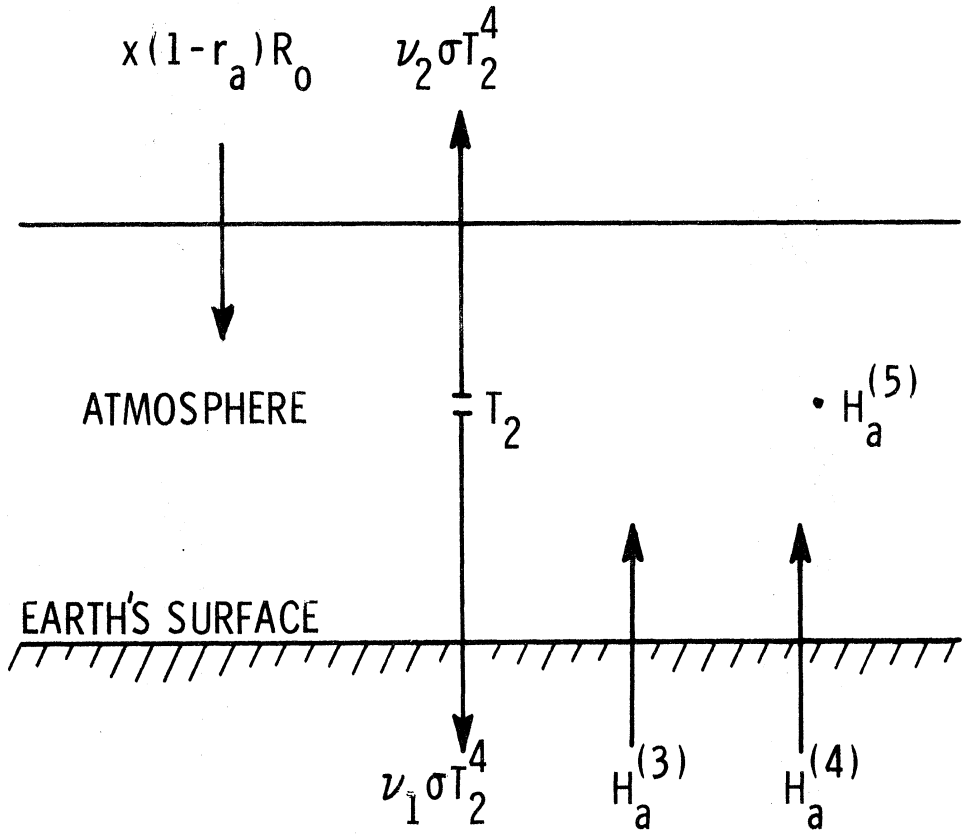

Figure 3.2.1 Energy fluxes related to the diabatic heating of the atmosphere.

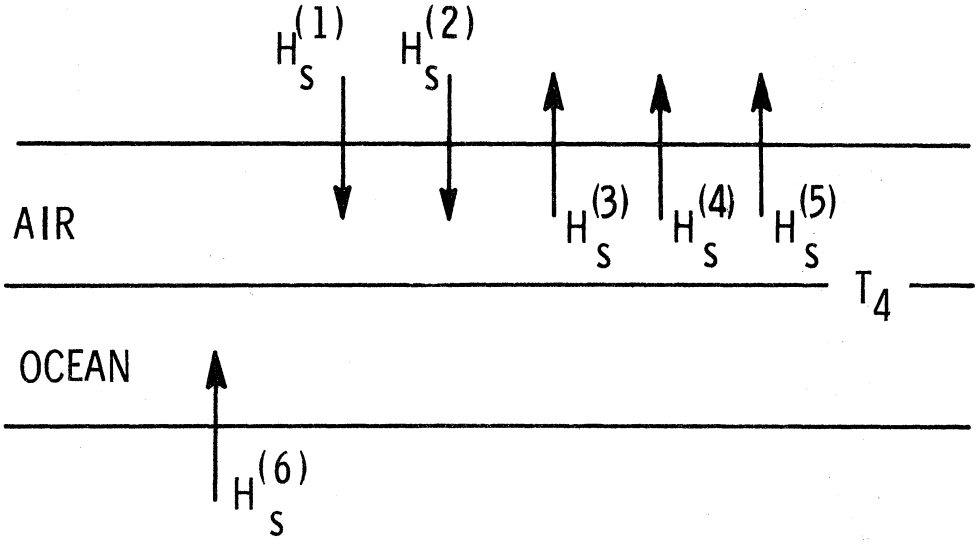

Figure 3.3.1 Energy fluxes related to the surface layer.

processes affect only small fractions of the total mass of the column. Hence the heating of the whole atmospheric column is given by

$$H_a = -(F_t - F_b)$$

or

$$H_a = \chi(1 - r_a) R_o - (\nu_1 + \nu_2)\ \sigma T_2^4 + \Gamma \sigma T_4^4 + H_a^{(4)} + H_a^{(5)}$$

or (3.2.2)

$$H_a = H_a^{(1)} - H_a^{(2)} + H_a^{(3)} + H_a^{(4)} + H_a^{(5)}$$

The evaluation of the surface temperature T_4 will be done using the surface heat balance

3.3 SURFACE HEAT BALANCE

Consider now a thin layer around the surface of the earth such that its heat capacity can be ignored. Energy fluxes to be considered are

i) Shortwave solar radiation
ii) Atmospheric longwave emission
iii) Terrestrial longwave emission
iv) Vertical transfer of sensible heat
v) Evaporation
vi) Subsurface heat conduction

The time integration of the equations of motion is done with time steps of 12 hours and for such a short time the surface layer cannot be considered in thermal equilibrium, therefore it is necessary to use a layer with negligible thermal inertia. The vertical divergence of energy fluxes and the sources satisfy then a time independent continuity equation for energy.

If the surface under consideration is the ocean surface the sixth process mentioned above becomes of paramount importance and cannot be neglected. The oceans receive heat in low latitudes throughout the year, while in middle latitudes they store heat from the warm to the cold season. The excess of heat received in low latitudes is transported poleward by the general circulation of the oceans. This is a fact that should be accounted for in the model. In the oceanic case the balance of the thin layer presents an additional problem, due to penetration of solar energy to appreciable depths. This difficulty will be overlooked and the entire incident solar radiation will be assumed absorbed at the surface. The horizontal advection of heat within the layer is negligible since by previous assumption its heat capacity can be disregarded. Ignoring, in addition, surface heat sources (such as dew) the heat balance for the surface becomes (Fig. 3.3.1):

$$- \left[(- H_s^{(1)} - H_s^{(2)} + H_s^{(3)} + H_s^{(4)} + H_s^{(5)} - H_s^{(6)}) \right] = 0 \qquad (3.3.1)$$

with

$$H_s^{(1)} = (1 - \chi)(1 - r_a)(1 - r_s) R_o$$

$$H_s^{(2)} = \nu_1 \sigma T_2^4$$

$$H_s^{(3)} = \sigma T_4^4$$

and where r_s is the albedo of the earth surface. Substituting in (3.3.1) we obtain

$$(1 - \chi)(1 - r_a)(1 - r_s) R_o + \nu_1 \sigma T_2^4 - \sigma T_4^4 - H_s^{(4)} - H_s^{(5)} - H_s^{(6)} = 0 \qquad (3.3.2)$$

3.4. VERTICAL TRANSFER PROCESSES AND THE WATER BALANCE

Eddy processes which transfer water vapor and sensible heat to the atmosphere are due to turbulence generated by thermal and mechanical instabilities. Direct observation of this phenomena has so far been made only on a local scale and global figures given in the present literature are determined as small residues required for balance in a climatological time scale. Therefore, these are not well known quantities, especially over the oceans where observations are scanty. There are some indications that seasonal variations of sensible heat transport are relatively small when compared with similar variations in other items of the energy budget (Davies, 1963). Some authors have used parameterizations which depend linearly on the temperature difference between the atmosphere and the earth surface. It is difficult to ascertain the representation of such formulations since they certainly bear no relation with mechanically generated turbulence and as far as convective processes are concerned they are difficult to evaluate from observations due to the intermittent character of convection in time and space.

Because of these uncertainties and for convenience, annual mean values of heat transfer and evaporation for each latitude will be used throughout the year, i.e.,

$$H_s^{(4)} = b(\varphi) = - H_a^{(4)}$$

$$H_s^{(5)} = E\, L$$

Here b is the annual mean value of the sensible heat transfer as a function of latitude, E the evaporation, L the latent heat for water.

This simple formulation has the additional advantage of making evaporation time independent, facilitating a formulation for latent heat release, a most important process in generating zonal available potential energy.

A third turbulent transfer mechanism to be considered is the subsurface conduction of heat. This phenomenon is important only over the seas, since, by comparison, the heat capacity of continents is negligible. An analytical expression

$$H_s^{(6)} = - k(\epsilon T_4 - T_D) \tag{3.4.1}$$

was chosen. Here T_D is an empirical temperature to which a loose physical meaning can be attached only when $T_D < T_4$, i.e., when the stratification is stable. It is better to consider k and T_D as empirical factors to be determined from observations and the nature of the surface. ϵ is a factor, time dependent, which relates the mean temperature at 100 cb, T_4, with the surface ocean temperature at a given latitude. The factor k, a measure of thermal conductivity, was computed from

$$k = k_* \left(j_1 + \frac{1}{200} j_2 + \frac{1}{250} j_3 + \frac{1}{1000} j_4 \right) \tag{3.4.2}$$

after Saltzman (1968) where k_* is a constant and j_1, j_2, j_3 and j_4 are the fractions of the globe covered by oceans, sea-ice, continents and snow-ice, respectively. The relative importance of the different kinds of surfaces was fixed using values provided in Laikhtman et. al. (1970).

This extremely crude parameterization endeavors to represent the ocean behavior as a heat storage for the atmosphere. Although nobody can feel satisfied with this approximation it gives fairly good values for the oceanic heat transport towards the poles, Fig. (3. 6. 2), and a qualitatively correct ocean behavior, Fig. (3. 6. 3).

The release of latent heat $H_a^{(5)}$ can be parameterized using the water balance and the observed rainfall distribution in time and space. From rainfall values at a given time a set of factors was computed in such a way that they are proportional to the amount of rain and its integral over the hemisphere, at any time, equals one. Using then

$$H_a^{(5)} = m(\varphi, t) \int_0^{\frac{\pi}{2}} E \cos\varphi \, d\varphi$$

the release of latent heat has a distribution similar to rainfall and in every unit time condenses as much water as has been evaporated. Hence, there is no variation of water storage in the atmosphere. Representing the last integral by I

$$H_a^{(5)} = m\, I$$

All the processes present in the heat balances have been parameterized and equations (3. 2. 2) and (3. 3. 2) can be written in their final forms

$$H_a = \chi(1-r_a)\, R_o - (\nu_1 + \nu_2)\sigma T_2^4 + \Gamma\sigma T_4^4 + b + mI \qquad (3.4.3)$$

$$(1-\chi)(1-r_a)(1-r_s)\, R_o + \nu_1\sigma T_2^4 - \sigma T_4^4 - b - E - k(\epsilon T_4 - T_D) = 0 \qquad (3.4.4)$$

As already stated seasonal variations are the main goal of the study. However data availability and simplicity dictates the inclusion of time dependence only where it seems to be of importance. Thus R_o, T_2, T_4, T_D, m and ϵ will be considered as functions of time and space, while χ, r_a, r_s, Γ, ν_1, ν_2, b and E are functions of latitude only; I is a constant.

The values of k will depend on latitude through the fractional cover factors j_i.

3.5 COMPUTATION OF THE HEATING FUNCTION

The amount of heat available to an atmospheric column with unit cross section per unit time is given by (3.4.3). Given T_2, the only obstacle to compute H_a is the unknown T_4. To determine the surface temperature we can use equation (3.4.4). Reordering this equation according to powers of T_4 we obtain

$$\sigma T_4^4 + k \epsilon T_4 + C = 0$$

where

$$C = -(1-\chi)(1-r_a)(1-r_s)R_o - \nu_1 \sigma T_2^4 + b + E - kT_D$$

This fourth order equation has the following properties: the function of T_4 so defined has always positive curvature since σ is always positive, the only real extremum is a minimum which is in the negative T_4 half plane. Thus the function has at most two real roots, one of which is always negative. Henceforth, if we use Newton's method, a real positive guess is sufficient to pick the physically meaningful root of the equation. The coefficient of the fourth power is an absolute constant while the other two coefficients are functions

of latitude and time. Considering the right hand side of equation (3. 4. 3), the first and last two terms are functions of latitude and time, while the coefficients of T_2^4 and T_4^4 are functions of latitude only. In order to compute the heating function H_a, we need to interpolate three quantities in time and latitude and three others in latitude only.

Latitude interpolation will be performed using a spline scheme (see Appendix II) with vanishing first derivative as boundary conditions. This choice seems sensible for the poles where symmetry is required. At the equator it was chosen for simplicity, since physical reasoning is of no help. Time interpolation was also done using the spline technique choosing ends where the linear estimation of the first derivatives is accurate, i. e., near the inflexion points of the seasonal fluctuation for middle latitudes. The quantities

$$L_1 = \sigma \nu_1$$

$$L_2 = -\sigma (\nu_1 + \nu_2)$$

$$L_3 = \sigma \Gamma$$

were interpolated in latitude only, so that values for every five degrees were available. The quantities

$$LT_1 = k \epsilon$$

$$LT_2 = -(1-\chi)(1-r_a)(1-r_s)R_o + b + E - kT_D$$

$$LT_3 = \chi(1-r_a)R_o + b + m I$$

were interpolated in latitude first and then spline coefficients were stored for interpolation in time as close as necessary.

3.6 TUNING OF THE HEATING MODEL

The diabatic heating of an atmospheric column has been expressed in terms of a set of constants and parameters whose values has to be determined. Some of them are easily found in the literature but have to be adjusted to the specifications of the model. There are others which are not available explicitly. However, the whole set of parameters has to be consistent, so that the present state of the earth-atmosphere system is compatible with their values. They also have to satisfy some global constraints. For instance, the atmospheric heating integrated over the globe and the year, must be very small. There must also exist an annual balance between the space and the earth atmosphere system, and the oceans must receive as much heat as they release over the year.

In general terms we can divide the set of parameters and constants in four groups:

(a) Those determined by geographical and astronomical conditions: R_o.

(b) Those determined directly by climatological observations: b, m, E, ϵ.

(c) Those determined from global constraints: k, T_D.

(d) Those determined by fitting observational results: Γ, ν_1, ν_2, χ, r_a, r_s.

Once determinations of groups (a), (b), and (d) are performed an adjustment is done so that mean monthly observed values of surface and mean tropospheric temperatures satisfy the global constraints with good approximation.

Some words about the use of mean monthly temperatures for tuning purposes are necessary. These temperatures enter the

heating function in a nonlinear fashion so the use of mean values is not strictly correct in the determination of the parameters. At any time:

$$T_i = \overline{T}_i + T_i' \qquad i = 2, 4$$

where $\overline{T}_i$ is the mean value over say a month and T_i' the corresponding deviation. Temperatures affect the heating function nonlinearly through the long wave emission terms where it appears raised to the fourth power, so

$$T^4 = \overline{T}^4 + 4\,\overline{T}^3\,T' + 6\,\overline{T}^2\,T'^2 + 4\,\overline{T}\,T'^3 + T'^4$$

taking monthly average

$$\overline{T^4} = \overline{T}^4 \left\{ 1 + 6\left(\frac{T'}{\overline{T}}\right)^2 + \ldots \right\}$$

Since we are using zonal averages daily and local extrema are smoothed out (except near the poles), the error made when substituting mean monthly values is very small and for a month in which the mean daily temperature changes as much as 20°K around a 250° mean amounts to less than 1%.

3.6.1 Numerical Procedure

Computation for the tuning of the zonally averaged heating model were performed in latitude with an interval of 10 degrees, with the first point at the equator and the last at the pole: values at latitudes 0, 10, 20, . . . , 80, 90 degrees were computed.

Global integrations were performed using the trapezoidal rule, and global balances were satisfied with an error less than 1 ℓy/day. To use the tuned heating model in the dynamic time integration, values were interpolated to every five degrees of latitude. The interpolation scheme, designed to give a smooth variation, did not preserve integrals, so a better accuracy in the global balance would not be justified on these grounds and also because of the approximate knowledge of the magnitudes of the energy fluxes.

3.6.2 Determination of Parameters

Incoming solar radiation R_o: This quantity was obtained from List (1951), Table 132, interpolating with a spline scheme (see Appendix II) for twelve equally spaced centered points along the year. To ease the computational procedure in the integration of the initial value problem, a fictitious time unit was chosen such that 360 of them are equivalent to 365, 25 common days. Thus the year is divided into twelve equal fictitious months, each composed of 30 fictitious days. Each fictitious day equals to 1.01458 days so that the correction is small. However, R_o values were multiplied by this factor. Before applying this correction, R_o values were adjusted to integrate, over the globe and a year, to one fourth of the solar constant, taken as 1.95 cal/cm^2 min approximately.

Radiative fluxes were changed to the new time unit by a slight modification of Boltzman's constant σ Turbulent transfers and latent heat released were not modified due to their approximate character.

Evaporation, E: This process was taken as time independent. Seasonal variations of the zonal mean evaporation are not

TABLE 3.6.1

Boundary layer vertical transfers (ly day^{-1})

Latitude	Evaporation		Sensible Heat Transfer	
	N. H.	S. H.	N. H.	S. H.
0	210	197	28	28
10	213	224	36	28
20	215	237	55	38
30	188	217	68	37
40	140	180	57	27
50	96	121	43	29
60	64	58	31	32
70	32	21	11	16
80	9	6	-16	-26
90	0	0	-36	-38

Source: Newton (1972)

as small as the sensible heat, but its parameterization is particularly difficult in a simple model as the one used here. Attempts were made to use the temperature difference between ocean surface and 100 cb level without success. Fig. 9.15 from Newton (1972), gives an idea of the seasonal variations involved. They are somehow important in the NH subtropics, but nowhere reach the variations shown by precipitation in low latitudes. This approximation will not affect directly the heating function but will modify the surface temperatures which in turn enter in the heating determination. The values shown in Table 3.6.1 were interpolated from Newton (1972).

Transfer of sensible heat, b: This process is considered as time independent and annual mean values for each latitude were taken from Newton (1972) for both hemispheres. The validity of this approximation is substantiated by Fig. 3 in Davies (1967), which shows seasonal variations of this term together with latent heat release for some latitudes of the Northern Hemisphere.

Distribution factor for latent heat release, m : For the computation of this factor the basic assumption is a constant water vapor storage for the hemispheric atmosphere. The amount of water evaporated per unit time is condensed in the same time interval with a geographical distribution m dependent on the season. An additional, less stringent assumption is used, namely that latent heat release can be estimated through the rainfall, i.e., water precipitates as soon as condensation occurs. With these two suppositions at any instant the release of latent heat can be expressed as

$$H_a^{(5)} = m \int_0^{\frac{\pi}{2}} H_s^{(5)} \cos\varphi \, d\varphi \qquad (3.6.1)$$

TABLE 3.6.2

Latent heat release normalization factor: m

Latitude	Jan	Feb	Mar	Apr	May	June	July	Aug	Sep	Oct	Nov	Dec
90 N	0.137	0.114	0.117	0.119	0.087	0.103	0.151	0.160	0.194	0.178	0.166	0.158
80	0.171	0.153	0.143	0.146	0.137	0.137	0.192	0.197	0.240	0.225	0.205	0.201
70	0.285	0.242	0.234	0.225	0.224	0.228	0.313	0.310	0.333	0.337	0.331	0.317
60	0.763	0.700	0.651	0.597	0.511	0.526	0.524	0.572	0.648	0.730	0.779	0.813
50	0.945	1.018	1.041	1.061	1.034	0.994	0.908	0.863	0.860	0.871	0.896	0.929
40	1.014	1.107	1.145	1.180	1.121	0.983	0.827	0.770	0.777	0.824	0.887	0.971
30	0.820	0.955	1.002	1.008	0.897	0.811	0.787	0.816	0.758	0.721	0.731	0.739
20	0.569	0.446	0.390	0.464	0.623	0.800	1.009	1.032	0.953	0.871	0.779	0.633
10	1.822	1.527	1.301	1.193	1.370	1.542	1.715	1.877	2.035	2.060	2.026	2.006
0	1.594	2.036	2.473	2.519	2.279	2.000	1.584	1.267	1.092	1.096	1.150	1.256
0	1.613	1.704	1.759	1.765	1.706	1.594	1.452	1.319	1.238	1.254	1.364	1.497
10 S	1.613	1.539	1.393	1.224	1.071	0.947	0.865	0.848	0.933	1.128	1.378	1.558
20	1.251	1.178	1.033	0.880	0.769	0.697	0.650	0.625	0.663	0.807	1.025	1.195
30	0.576	0.603	0.674	0.756	0.821	0.870	0.907	0.933	0.920	0.845	0.722	0.620
40	0.732	0.793	0.960	1.146	1.300	1.418	1.510	1.570	1.538	1.357	1.067	0.830
50	1.012	1.032	1.108	1.232	1.398	1.575	1.709	1.736	1.636	1.439	1.224	1.074
60	0.737	0.749	0.769	0.790	0.808	0.826	0.849	0.879	0.896	0.872	0.810	0.755
70	0.214	0.228	0.248	0.258	0.242	0.215	0.199	0.218	0.255	0.273	0.252	0.225
80	0.037	0.039	0.042	0.043	0.041	0.038	0.037	0.038	0.042	0.044	0.041	0.038
90	0.012	0.013	0.013	0.013	0.012	0.011	0.010	0.010	0.010	0.011	0.011	0.012

Using the constant storage condition

$$\int_0^{\pi/2} H_a^{(5)} \cos\varphi \, d\varphi = \int_0^{\pi/2} H_s^{(5)} \cos\varphi \, d\varphi \qquad (3.6.2)$$

for any time the integration of (3.6.1) gives

$$\int_0^{\pi/2} m \cos\varphi \, d\varphi = 1$$

The second assumption mentioned before, permit us to write

$$H_a^{(5)} = Lr \qquad (3.6.3)$$

where r stands for rainfall and L is the water latent heat. Then (3.6.1), (3.6.2) and (3.6.3) give

$$m = \frac{H_a^{(5)}}{\int H_a^{(5)} \cos\varphi \, d\varphi} = \frac{r}{\int r \cos\varphi \, d\varphi}$$

and so m can be computed from a knowledge of $r(\varphi)$ for any time. Taking then $r(\varphi)$ for different months one can get $m(\varphi, t)$, Table 3.6.2. Monthly rainfall data for the Northern Hemisphere were taken from London (1957) and for the Southern Hemisphere from Möller (1951).

Oceans surface temperature factor, ϵ : This factor reduces the 100 cb zonal mean temperature to the oceanic surface

temperature at the same latitude and month. Using values of ocean surface temperatures, T_{SS}, as provided by Neumann and Pierson (1966) Table 14.3, for the North and South Atlantic Ocean and 100 cb temperatures given by Oort and Rasmusson (1971) for the Northern Hemisphere and by Jenne et al. (1968) for the Southern Hemisphere, values were computed for each month and every 10 degrees of latitude.

Subsurface condition, T_D and k: One of the most uncertain factors in the heating budget is the subsurface conduction. This process is very important over the oceans. In comparison it can be neglected over the continents and ice covered oceans. To determine the seasonal behavior of this process the following procedure was applied. Using values of T_2, T_4, T_{SS} from the sources mentioned above, the surface balance equation (3.4.4) was used to determine the amount of heat conducted downward, $H_s^{(6)}$, as a function of latitude and month of the year. We chose to give a form like (3.4.1) to the process, where k is determined by (3.4.2) and k_* was given the value 10 ly day^{-1}deg^{-1}. Then, suitable values of $T_D(\varphi, t)$ were computed. It must be stressed that k and T_D have no physical meaning attached to them; they only serve the purpose of proper evaluation of $H_s^{(6)}$.

In very high latitudes where there is no ocean coverage this term is absent, and the surface budget was approximately balanced by modifications of the radiative parameters.

Radiation parameters: All six radiation parameters, r_s, r_a, Γ, ν_1, ν_2, χ are considered latitude dependent only. This represents a fairly good approximation for some of them like Γ, χ, ν_2, r_a, but for ν_1 and r_s the approximation is less reliable in high latitudes.

The short wave parameters χ , r_a , r_s , were evaluated using studies of London (1957) and Smagorinsky (1963) for the Northern Hemisphere, and of Sasamori et. al. (1972) for the Southern Hemisphere Results presented in these articles allow an individual determination of χ , r_a , r_s , for the year as a whole and for individual seasons.

For the long wave part, results of Smagorinsky (1962) were used for the NH. The study of Sasamori et. al. (1972) allows a determination of ν_1 and a relation between ν_2 and Γ : the atmospheric flux divergence. Assuming values for Γ , which in the literature do not vary much, values for ν_2 were fixed so as to satisfy the observed values for the long wave flux divergence. In this process again monthly mean values of surface and tropospheric temperature as observed were used.

Once all the parameters were computed as described, small adjustments were made to satisfy the global annual equilibrium of the atmosphere and the earth-atmosphere system within a 1 ly / day tolerance.

The outcome of this process for the Northern and Southern Hemispheres is shown in Table 3. 6. 3 . Satellite observations have provided evidence for lower tropical albedos than those shown, (Vonder Haar and Suomi, 1971 , and London and Sasamori, 1971), but no detailed radiation balance based on them was available to us. The values shown are to a large extent in agreement with the already mentioned sources.

3. 6. 3 Characteristics of the Tuned Heating Function

The behaviour of the heating function can be appreciated from the following results. Using observed mean monthly temperatures

TABLE 3.6.3

Radiation Parameters

r_a : atmospheric albedo

r_s : earth surface albedo

r_{ss} : ocean surface albedo (used only for oceanic heat transport estimate)

χ : atmospheric opacity to solar radiation

Γ : atmospheric absorptivity to longwave radiation

ν_1 : atmospheric downward emissivity

ν_2 : atmospheric upward emissivity

Northern Hemisphere

Lat.	Γ	ν_1	ν_2	r_a	r_s	r_{ss}	χ
EQ	0.96	1.35	0.77	0.27	0.07	0.06	0.30
10	0.96	1.35	0.78	0.29	0.06	0.06	0.30
20	0.96	1.35	0.79	0.26	0.07	0.06	0.29
30	0.96	1.33	0.80	0.28	0.08	0.07	0.26
40	0.96	1.30	0.81	0.31	0.08	0.08	0.27
50	0.96	1.29	0.83	0.36	0.08	0.09	0.29
60	0.96	1.26	0.84	0.38	0.10	0.10	0.30
70	0.96	1.20	0.84	0.41	0.20	0.11	0.36
80	0.96	1.20	0.85	0.42	0.63	0.63	0.38
NP	0.96	1.09	0.87	0.40	0.63	0.63	0.39

Southern Hemisphere

Lat.	Γ	ν_1	ν_2	r_a	r_s	r_{ss}	χ
EQ	0.96	1.35	0.77	0.25	0.07	0.06	0.30
10	0.96	1.33	0.78	0.25	0.07	0.06	0.29
20	0.96	1.32	0.80	0.25	0.08	0.06	0.29
30	0.96	1.35	0.82	0.25	0.08	0.07	0.28
40	0.96	1.37	0.84	0.34	0.05	0.08	0.28
50	0.96	1.39	0.88	0.42	0.05	0.09	0.34
60	0.96	1.37	0.90	0.51	0.10	0.10	0.37
70	0.95	1.16	0.86	0.41	0.45	0.15	0.27
80	0.95	0.82	0.83	0.30	0.80	0.65	0.23
SP	0.95	0.66	0.70	0.26	0.80	0.70	0.23

at 50 and 100 cb and the evaluated parameters the annual hemispheric energy budget was computed. The results, including observed values, are shown in Table 3. 6. 4. The agreement is quite good showing that, in this sense at least, the modifications performed to satisfy global constraints have not introduced substantial changes.

The energy budget for the whole earth-atmosphere system is shown in Fig. 3. 6. 1 as a function of latitude. When one compares with observations of Vonder Haar and Suomi (1971) both curves are somewhat low in the intertropical region with a net excess of absorbed energy. Towards the north pole the agreement is very close. In the Southern Hemisphere the absorption is slightly underestimated. Discrepancies in the tropical region are due to the different albedos considered. The mean planetary albedos in the model are 34. 2% and 34. 6 % for the Northern and Southern Hemispheres, respectively, while a value of 30% reported by Vonder Haar and Suomi (1971). This difference is mainly due to the intertropical region.

The poleward transport of heat by the oceans was estimated using the zonal mean values given in Table 3. 6. 1 for the turbulent transfer of heat and water vapor. Oceanic albedos, shown in Table 3. 6. 3, were taken from Manabe (1969), and the oceanic coverage factor was used to estimate the amount of heat that has to be conducted across the surface. An integration in latitude provides the transport polewards, if no heat is transferred across the equator. Fig. 3. 6. 2 shows the curves thus obtained. As expected, both hemispheres shows a net loss which is larger in the Northern Hemisphere where the mean turbulent transfers are less representative of oceanic conditions. The uncertainty in observations of these fluxes is very large, especially

TABLE 3.6.4

	N.H.		S.H.		Globe
	London 1957	Model	Sasamori et. al. 1972	Model	London & Sasamori 1972
I	100	100	100	100	100
AA	17.5	20.1	20.7	20.5	20.7
SA	47.5	45.5	44.6	44.7	44.6
AR SR	35.	34.2	34.8	34.7	34.8
AE	153.	161.	152.8	159.	
AEU	56.5	60.8		60.7	
SES	5.5	4.6	66.5	4.6	66.5
SE	114.5	117.3	111.8	115.2	111.8
AED	96.5	100.1	96.1	98.4	96.1
SEA	109.	112.7		110.4	
SHT	11.	6.		4.1	
E	18.5	22.		24.	

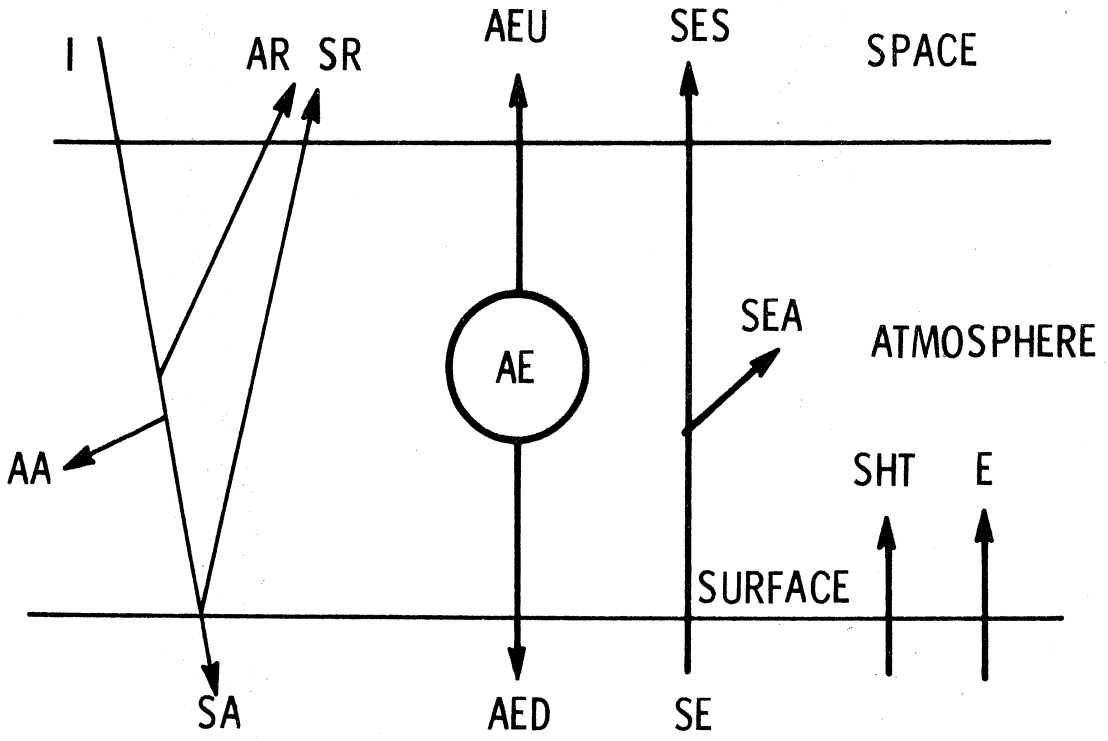

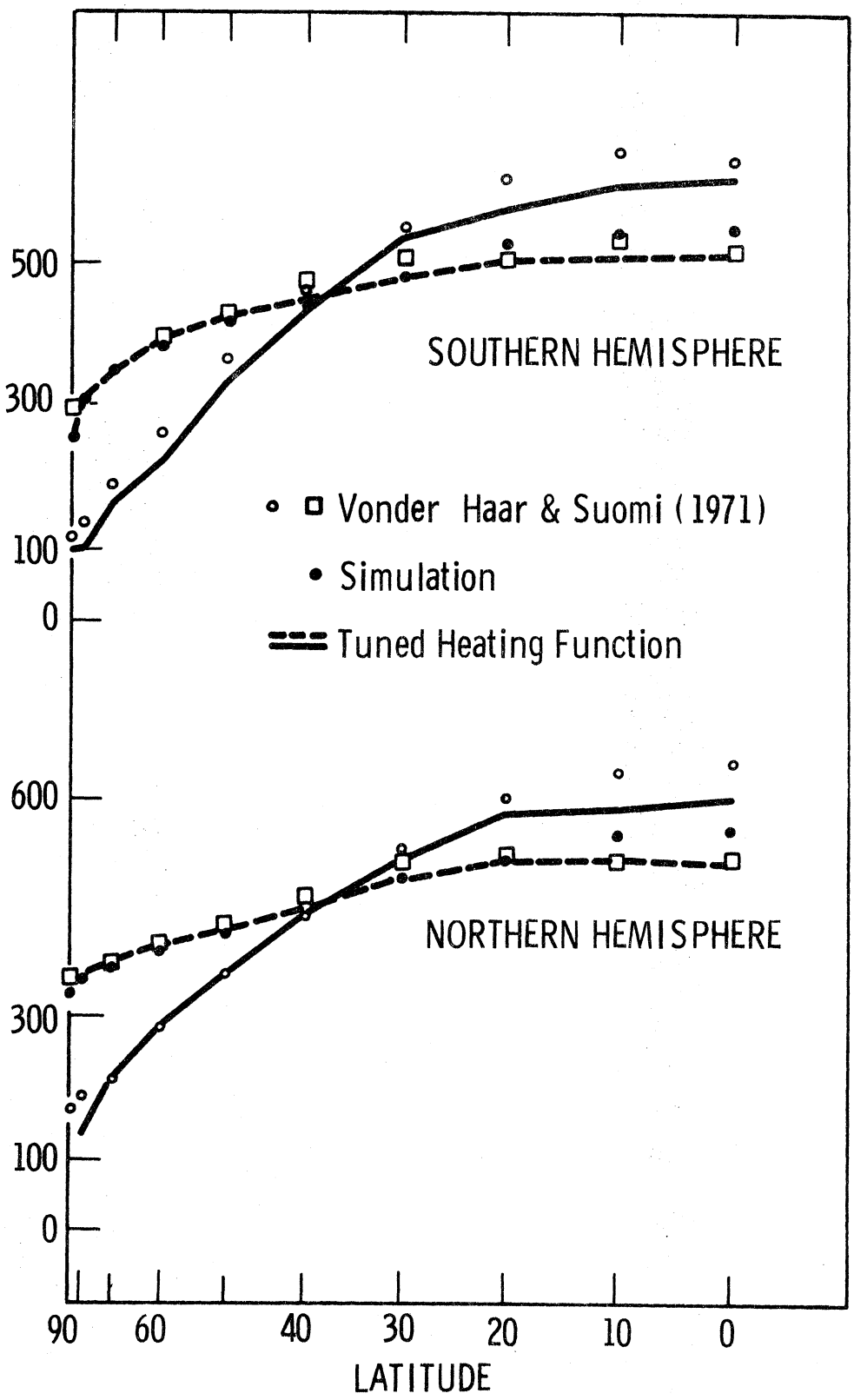

Figure 3.6.1 Energy balance of the earth-atmosphere system. Solar energy absorbed in the tuning is shown by the continuous line. Long-wave emission in the tuning is shown by the dashed line. Values obtained in the simulation and observations as indicated. Units: ly/day.

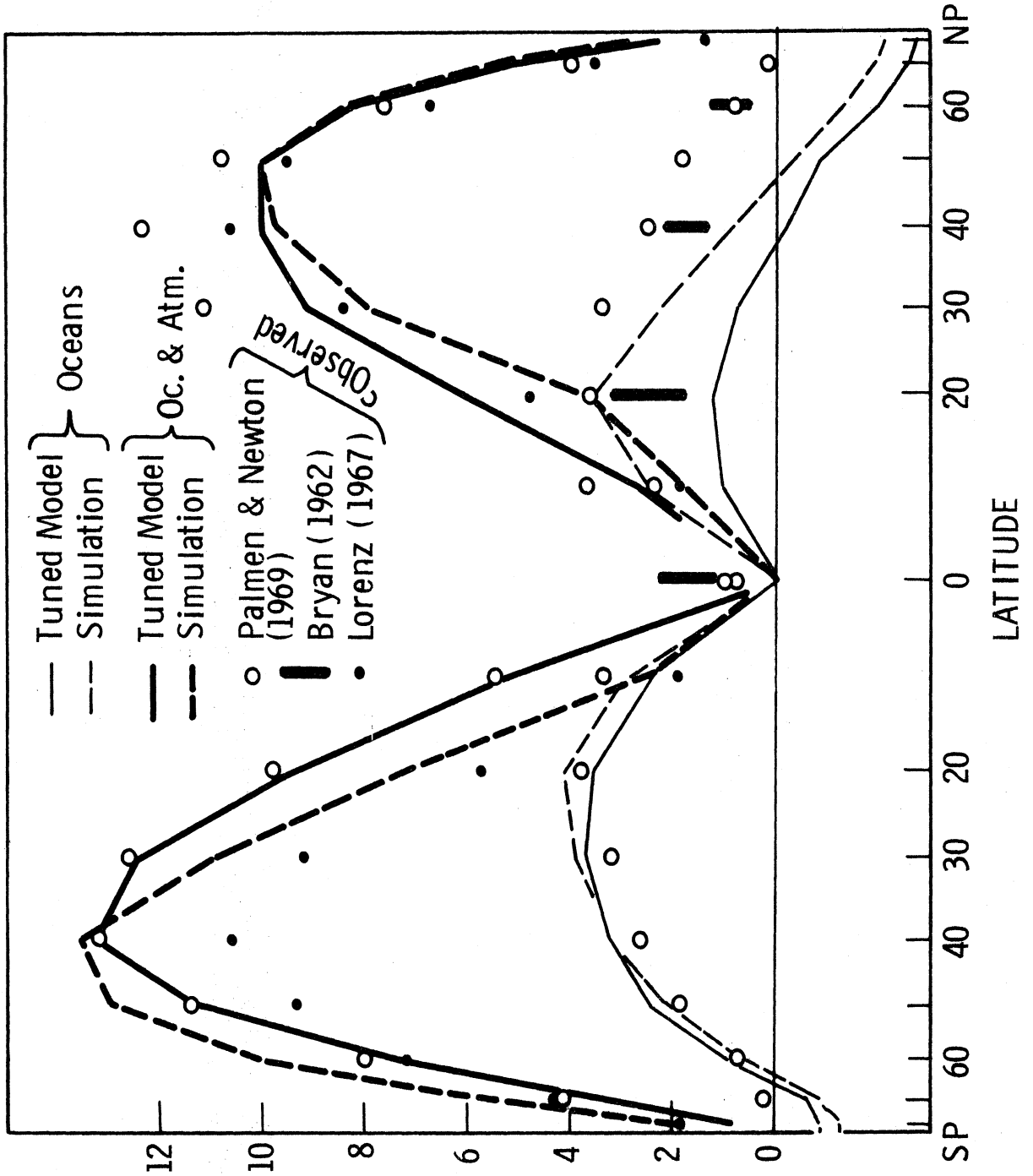

Figure 3.6.2 Poleward heat transport by the ocean-atmosphere system and by the oceans. Continuous lines show values attained in the tuning while dashed lines are those obtained in the simulation. Observations as indicated. Units: 10^{14} cal /sec.

with the low values for the tropical albedos (Vonder Haar and Oort, 1973). The profiles obtained should be compared with those evaluated with high albedos, for instance as shown by Bryan (1962). The order of magnitude and general shape of the curves are similar. There exists a maximum between 20 to 30 degrees and improvements in the right direction are to be expected from a proper account of the turbulent processes. Another source of uncertainty in the observed values is the equatorial flux, which seems to be from South to North.

The time behaviour of the subsurface conduction (3. 4. 1) is presented in Fig. 3. 6. 3. Roughly speaking the oceans store heat from March to September in the Northern Hemisphere, to release it in the rest of the year. In very low latitudes there is no cycle, the sea gaining heat throughout the year.

The annual mean heating function of the tuned model for the Northern Hemisphere is shown in Fig. 3. 6. 4, together with those obtained from observations by several authors. The main discrepancy occurs at latitudes 20 and 30 where the model overestimates the cooling. Otherwise the curve falls among the observations, in particular at high latitudes. Fig. 3. 6. 5 shows how this mean heating is formed by the processes represented in equation (3. 4. 3). It is remarkable to what extent the release of latent heat by condensation determines the meridional variations of diabatic heating. In this regard a thermal forcing that does not include latent heat effect will be in error. Newell et. al. (1969) have estimated the heating for the four seasons. Fig. 3. 6. 6 compares the tuned heating function with their results. The modelling for the Northern Hemisphere is in good agreement with the observations except at the equator. In the Southern Hemisphere the fitting is poorer

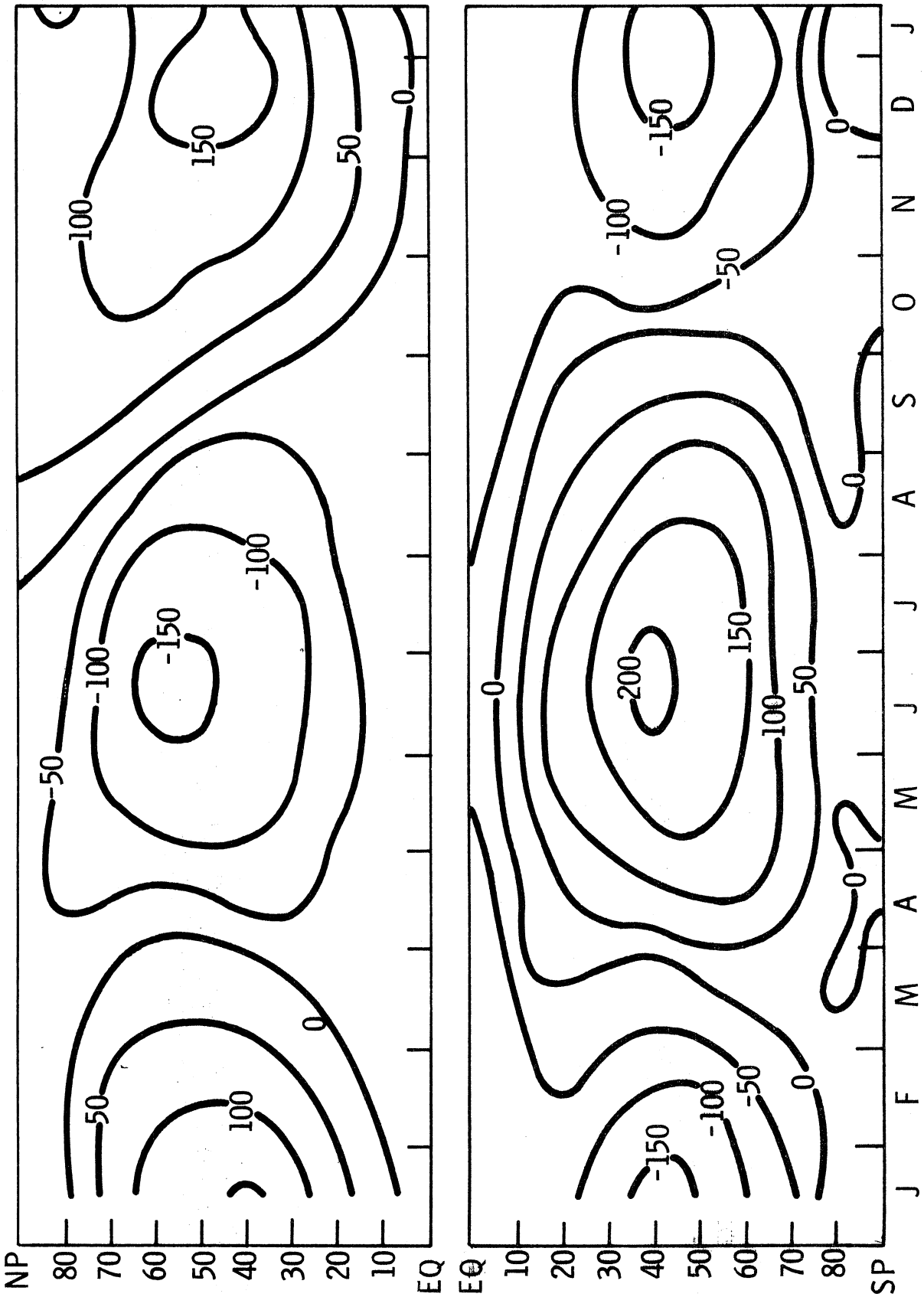

Figure 3.6.3 Heat released by the oceans. Upper part corresponds to the Northern Hemisphere while the lower part belongs to the Southern Hemisphere. Units : ly/day.

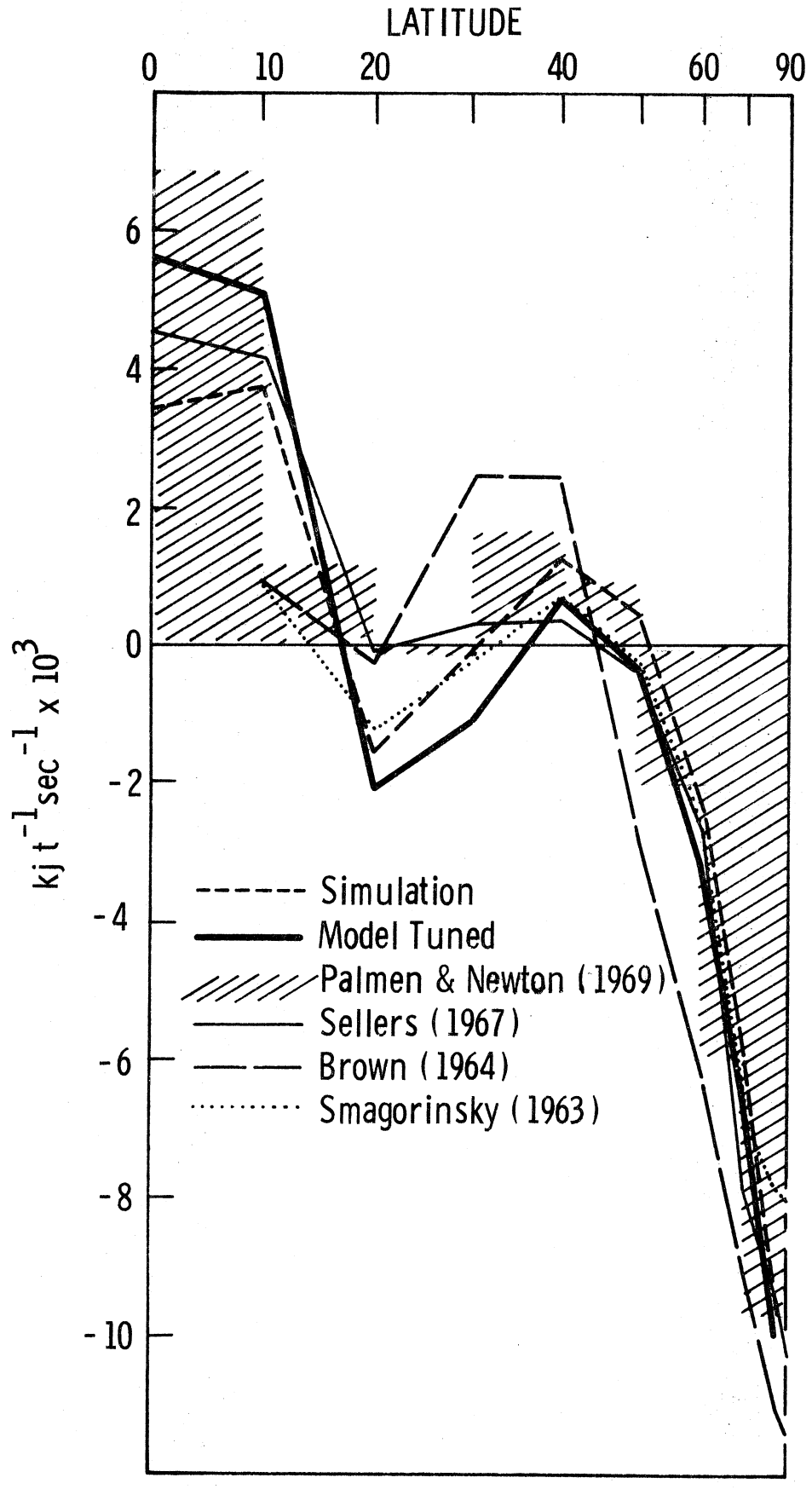

Figure 3.6.4 Mean annual heating function. Results of tuning, simulation and observations are shown as indicated. Units : 10^3 kj/(t sec).

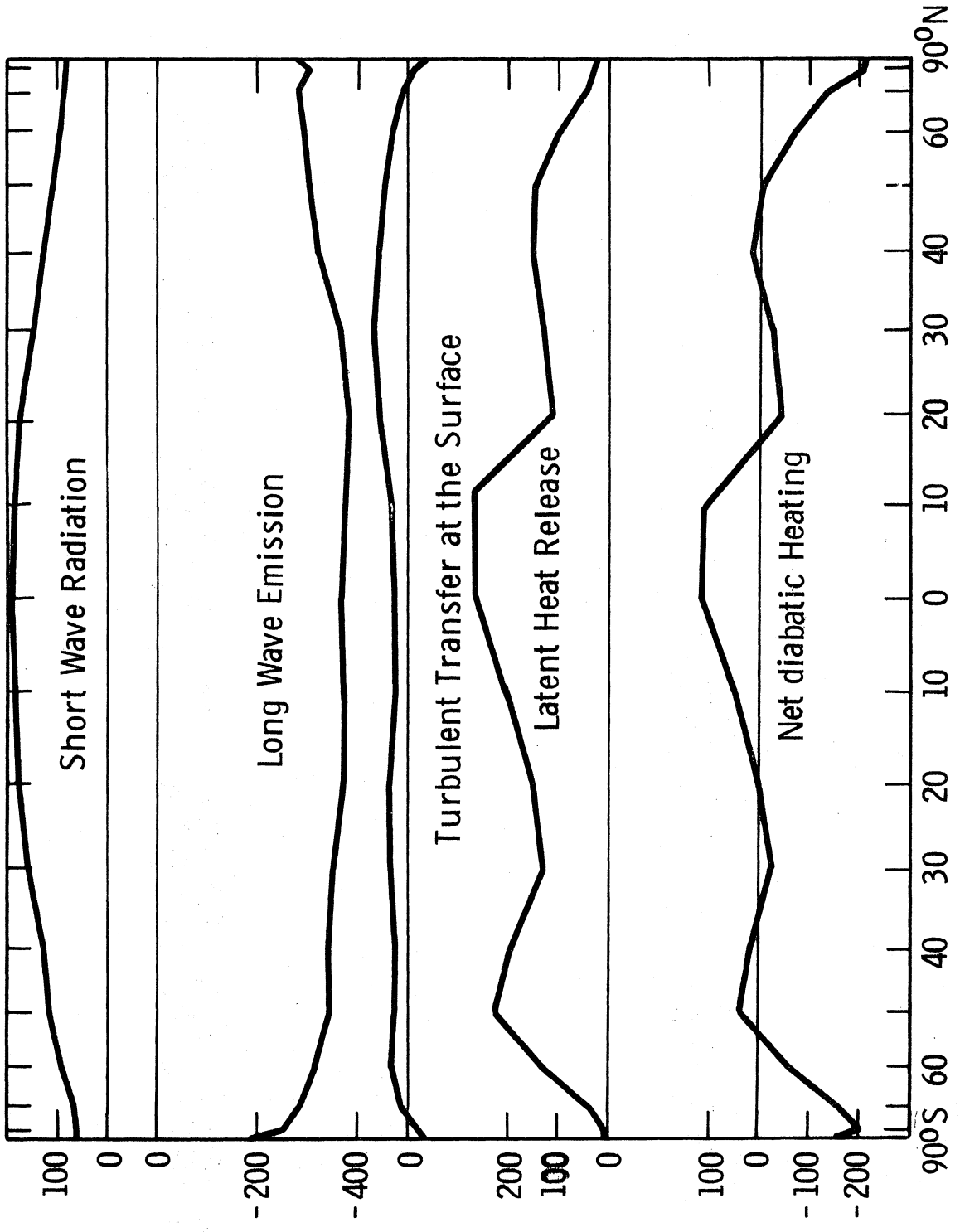

Figure 3.6.5 Atmospheric heat budget. The mean annual diabatic heating of an atmospheric column and its components according to latitude. Units : ly/day.

at all latitudes, with some evidence of the model marching somewhat ahead. Finally Fig. 3.6.7 shows the time and space variation of the diabatic heating for the actual atmospheric temperatures.

3.6.4 Diabatic Heating in the Simulation

The dynamical model was unable to reproduce the observed temperatures and reached a different quasi-steady state. In the Southern Hemisphere the annual mean heating remained about the same at all latitudes with exception of the equator, see Fig. 3.6.8. This is not the case in the seasonal apportionment, Fig. 3.6.6. The hemispheric balance remained small. In the Northern Hemisphere the mean annual values remain fairly close to the tuned profile with discrepancies in low latitudes and some improvements near the tropic, Fig. 3.6.4. The seasonal fluctuations were retained with a good accuracy northward of latitude 10^{o}N. The hemispheric imbalance increased to 1.7 ly day, a quantity small enough as to generate little variation between the second and third year of simulation. For instance, the maximum zonal wind at 25 cb in January increased from 34.98 to 35.03 m sec^{-1} and the temperature at level 2, latitude 40, in January, changed only by one 1/100 of degree Kelvin. The available potential energy went from 4837.9 to 4838.9 kj m^{-2}. These amounts are in all cases negligible allowing us to state that the model reached a steady state for almost all purposes.

The differences between the tuned heating function and the simulation function are most prominent near the equator. This is a consequence of the two main shortcomings of the model. First the diagnostic values of the eddy exchange coefficients were evaluated (Wiin-Nielsen and Sela, 1971) under the quasi-geostrophic assumption,

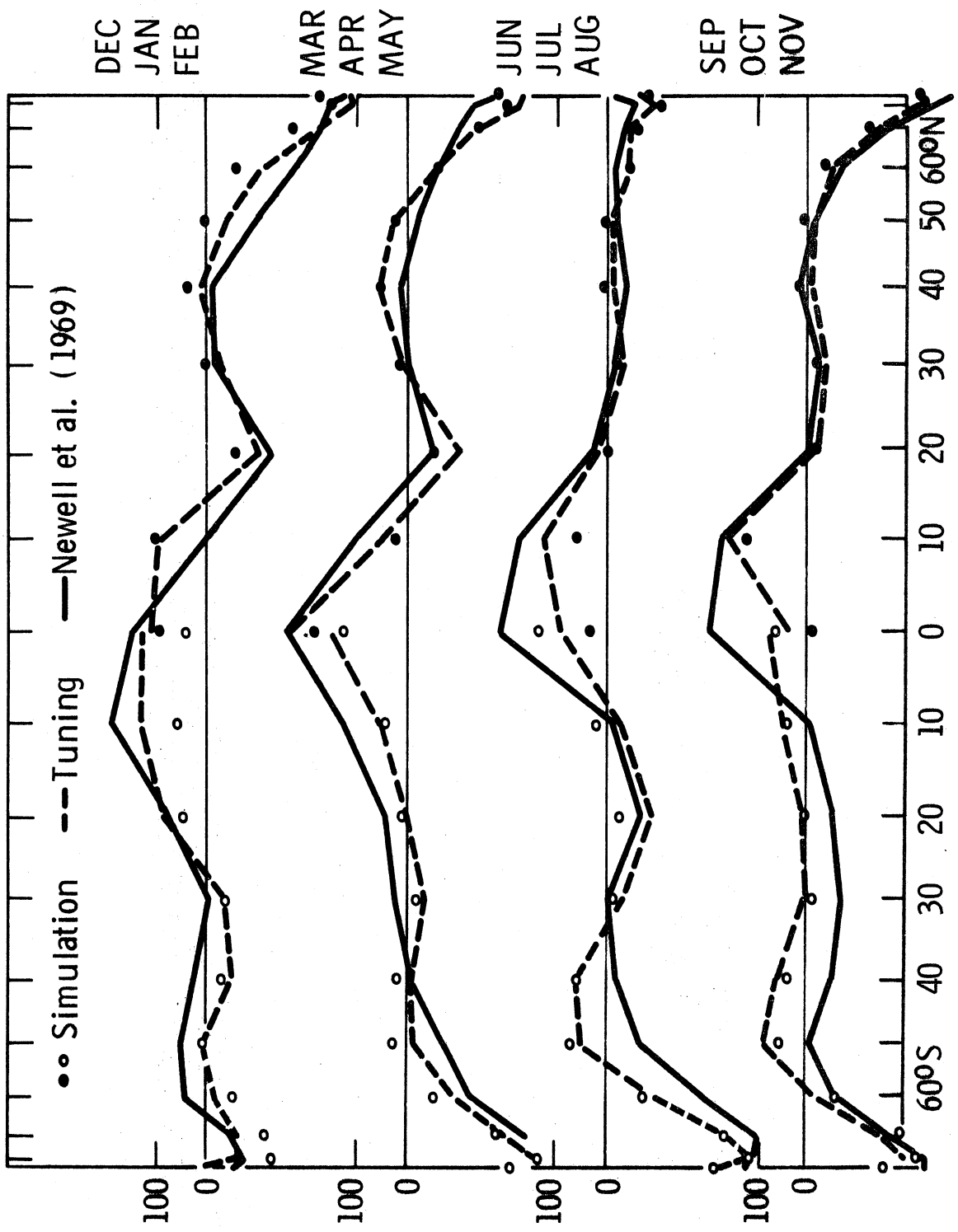

Figure 3.6.6 Seasonal distribution of the diabatic heating of an atmospheric column. Dashed line indicates values in the tuning. Dots and circles are values from the simulation. Observational values by Newell et al. (1969) are shown by a continuous line. Units : ly/day.

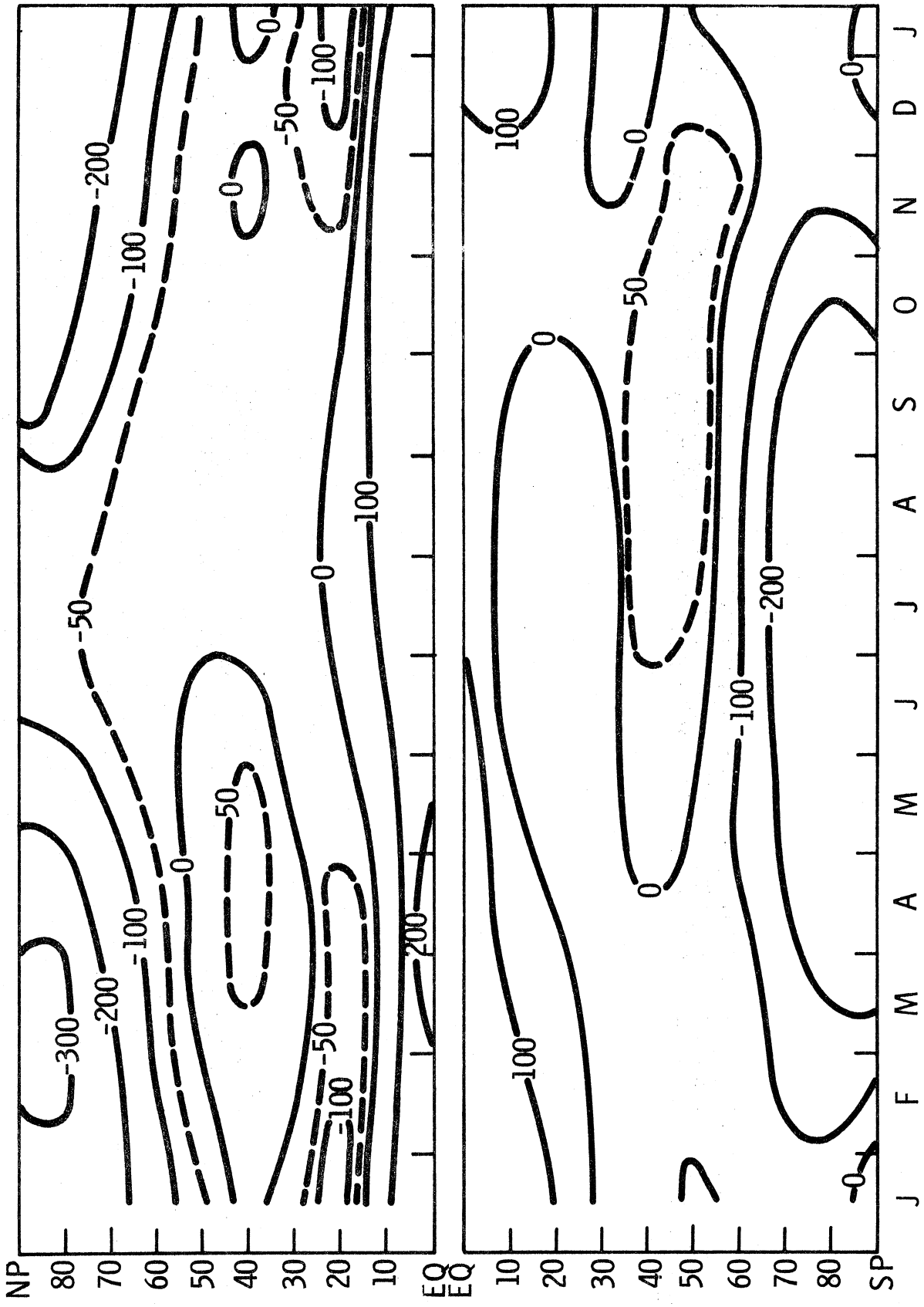

Figure 3.6.7 Diabatic heating of an atmospheric column. Upper part corresponds to the Northern Hemisphere and the lower part to the Southern Hemisphere. Units : ly/day.

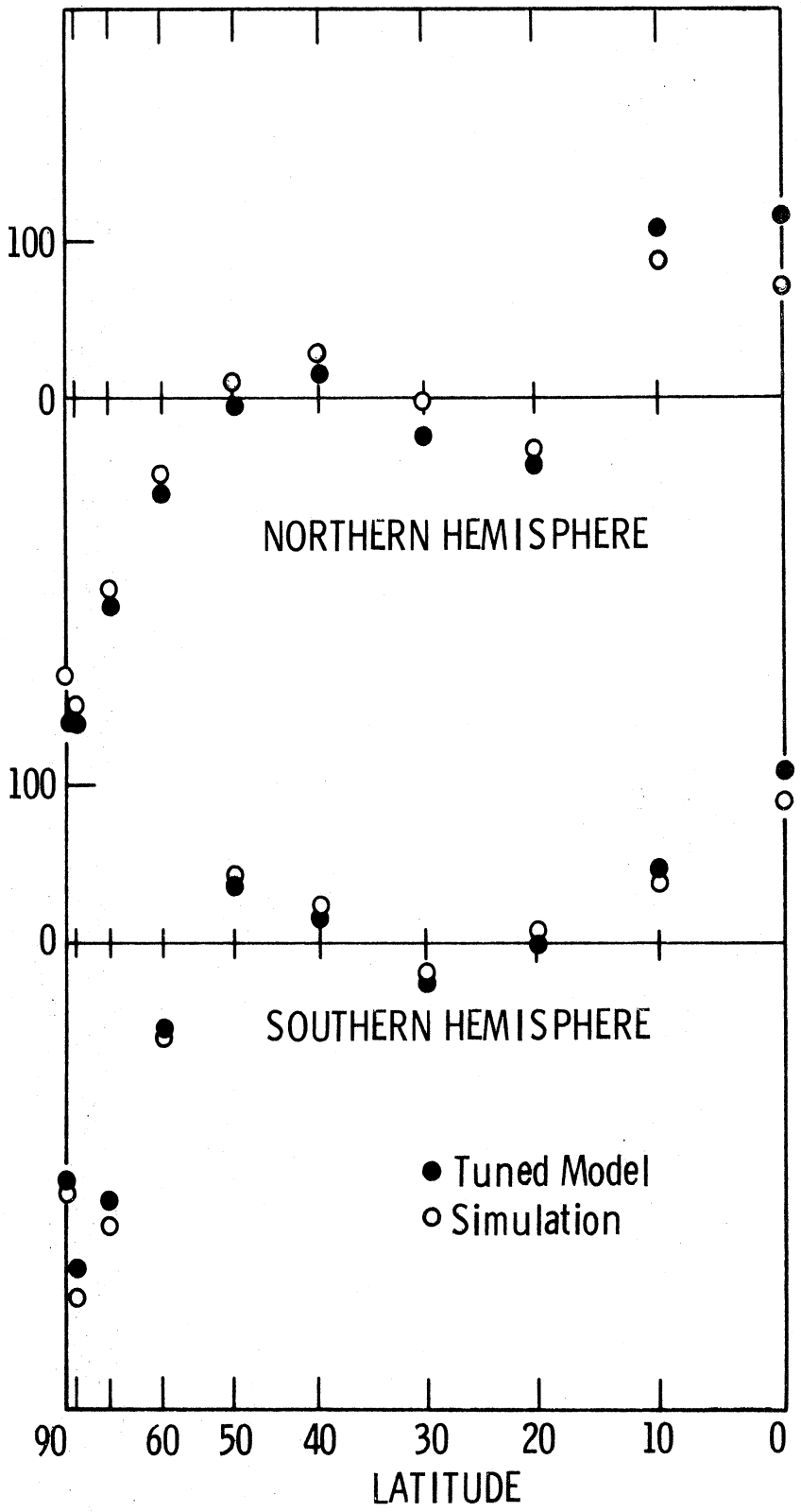

Figure 3.6.8 Comparison of mean annual heating obtained in the simulation and the tuning. Upper part Northern Hemisphere. Lower part Southern Hemisphere. Units : ly/day.

so that they are unable to account for mean meridional circulations, which are the most effective agents of transport in low latitudes. Besides, the model itself is quasi-geostrophic and ignores all mean meridional circulations, as far as transport effects are concerned (see for instance relation 2. 1. 36). The second reason for the misrepresentation in low latitudes is due to the artificial boundary at the equator, which does not allow heat fluxes across.

The energy balance of Table 3. 6. 4 is maintained to a remarkable extent. The largest modification amounts to . 5%. Modifications in the transports of heat are shown in Fig. 3. 6. 2, next to observational results of Palmen and Newton (1969) and Sellers as quoted by Lorentz (1967).

As a final comment, Figures 3. 6. 2 and 3. 6. 4 show that observational values cover a wide range, specially if one considers the new values for tropical albedos. The heating function model we are going to use falls within these variations everywhere but near the equator, fitting observation quite well in middle and high latitudes of the Northern Hemisphere.

CHAPTER IV

LINEAR SIMULATIONS

Equations (2. 1. 30) and (2. 1. 31) were integrated over three years using diagnostic values for the eddy exchange coefficients for heat and potential vorticities. These depend only on latitude and appear in Fig. 2 of Sela and Wiin-Nielsen (1971). This integration was performed for each hemisphere separately. The same values of the eddy coefficients were used in both cases due to a lack of information about the southern half of the globe.

A schematic flow chart of the computation procedure is shown in Fig. 4. 0. 1 for the time step n . The computation was performed with a grid interval of 5 degrees of latitude (550 km. approximately) and a time step of twelve hours.

The initial condition, of little importance for our purposes, was a motionless and isothermal ($T_{2Z} = 273^{\circ}K$) state. The spin up of the model took about 200 time steps ($3\frac{1}{2}$ months) after which the seasonal fluctuation repeated almost exactly in the second and third simulated year. This periodicity also serves as a control of truncation errors.

The computational stability of the time integration was insured by an implicit scheme (Crank-Nicholson, see Appendix I). In exchange for this advantage the thermal forcing and the dissipation had to be used with a half time step lag with respect to the other terms in Equations (2. 1. 30) and (2. 1. 31). This lag of 6 hours in the forcing is assumed to be of little consequence on the results which have a much longer typical time scale.

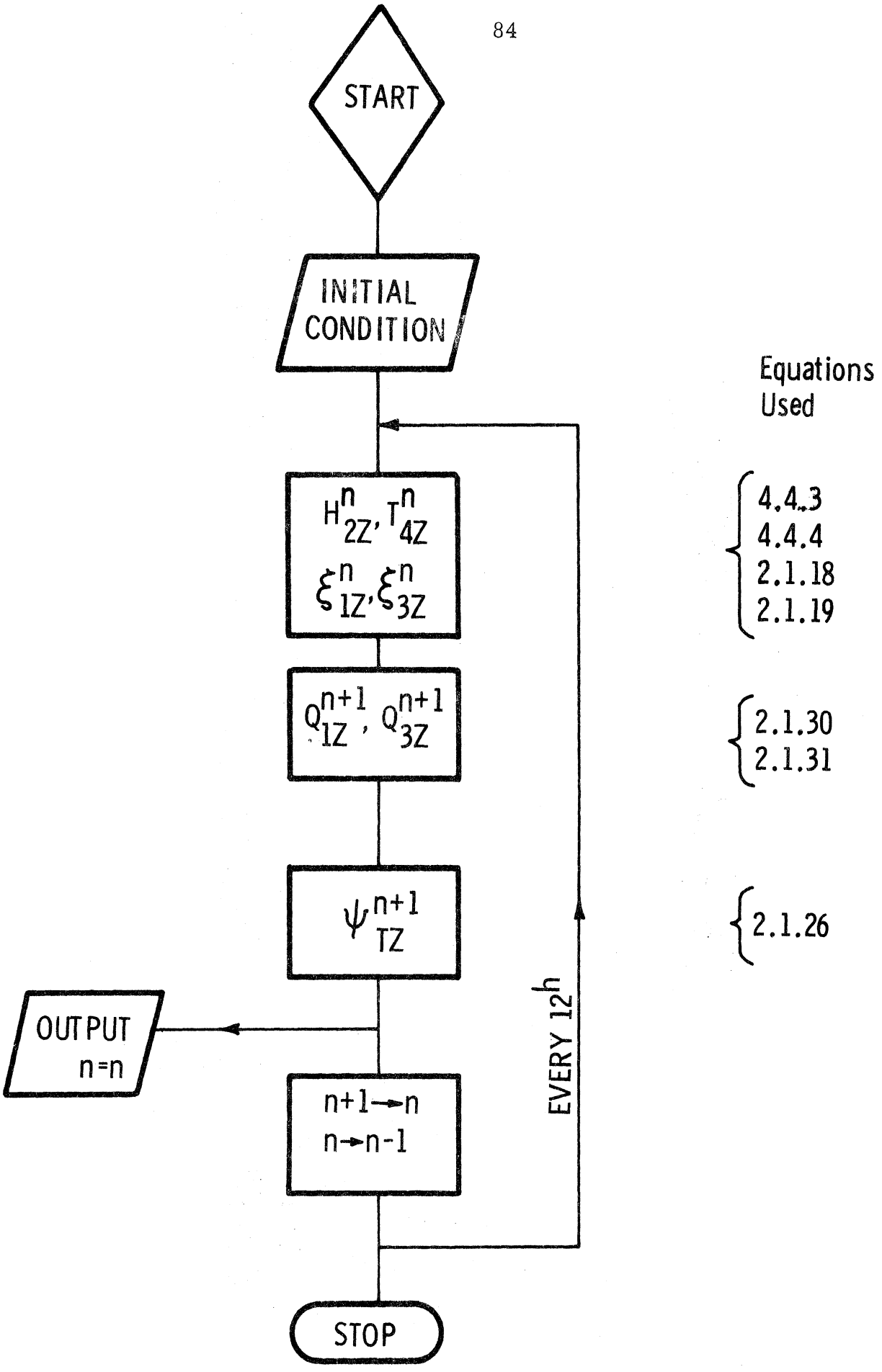

Figure 4.0.1 Flow chart for computation of linear simulations.

The basic cycle in the computation was the following:

i) With Q_{1z}^n, Q_{3z}^n, ψ_{Tz}^n given by initial conditions or a previous time step, equation (3. 4. 4) provides the surface temperature, T_4^n. Then equation (3. 4. 3) gives the diabatic heating of an atmospheric column, H_{2z}^n, and the potential vorticities definitions allow the calculation of the relative vorticities ζ_{1z}^n and ζ_{3z}^n.

ii) Equations (2. 1. 30) and (2. 1. 31) are integrated, using boundary contitions described in Section 2. 2. The numerical procedure is developed in Appendix I. Thus we obtain Q_{1z}^{n+1} and Q_{3z}^{n+1}.

iii) Equation (2. 1. 26) is integrated with boundary conditions (2. 1. 10) and (2. 1. 22) and by the technique described in Appendix I, to give ψ_{Tz}^{n+1}.

iv) If desired at this point one can evaluate the three dimensional flow, temperature at 50 cb, heat and angular momentum transport and energy conversions by the relations deduced in Chapter 2. This was done once every six time steps (once every three days).

v) Return to i) and repeat as long as necessary.

A three-year simulation took 112 sec of CPU time in an IBM 360/67 computer.

4. 1 NORTHERN HEMISPHERE SIMULATION

Results for the Northern Hemisphere are represented in Figs. 4. 1. 1 to 4. 1. 13.

4. 1. 1 Temperature Field

The model provides temperature values for 50 and 100 cb, which are shown in Fig. 4. 1. 1 and 4. 1. 2 respectively. The field at 50 cb represents a drastic improvement over that obtained by Sela and Wiin-Nielsen (1971) hereafter referred to as S-WN. The results show

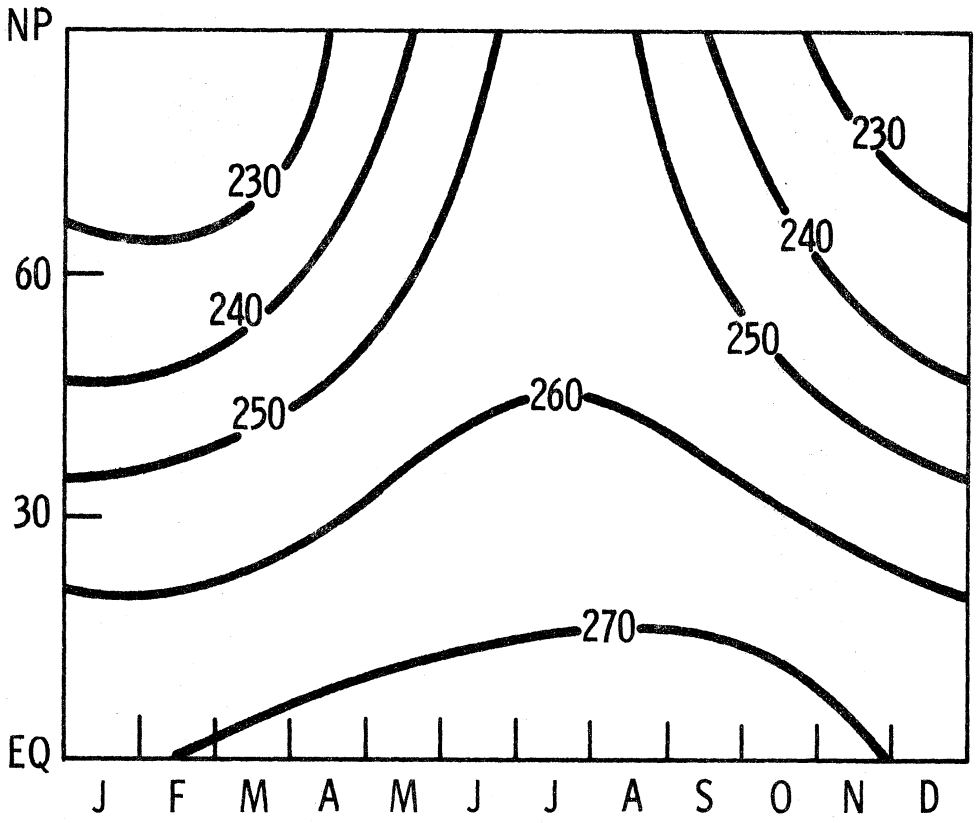

Figure 4.1.1 Thermal field at 50 cb for the Northern Hemisphere in the linear simulation. Units : ^{o}K.

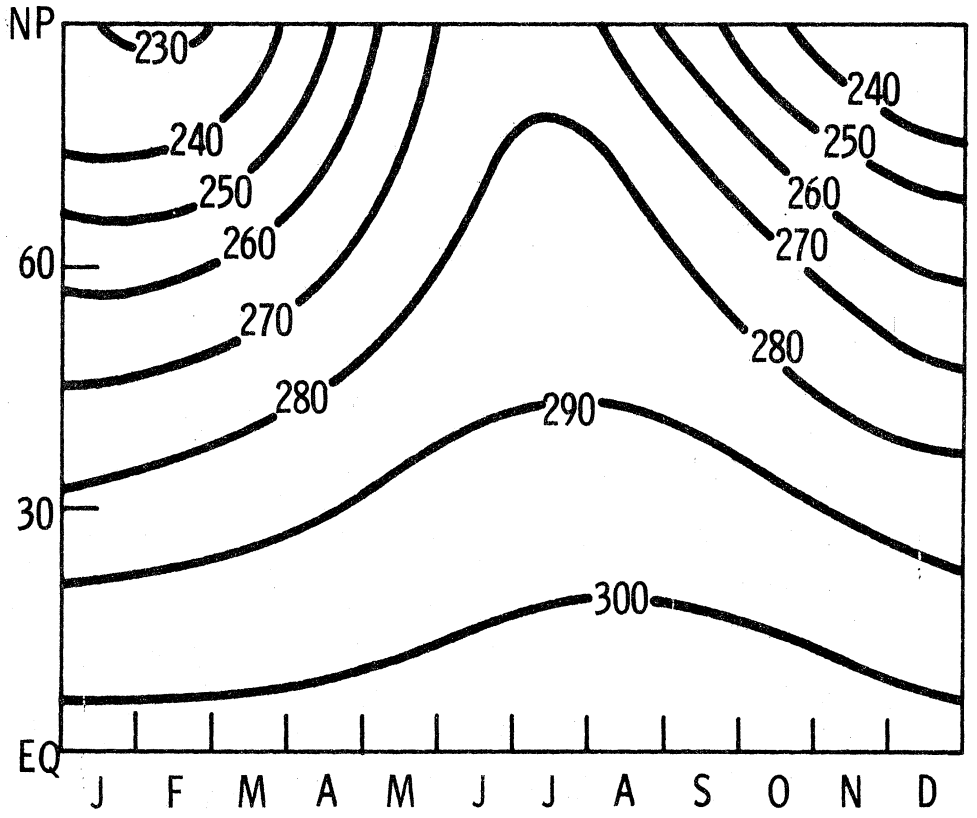

Figure 4.1.2 Same as Figure 4.1.1 but at 100 cb.

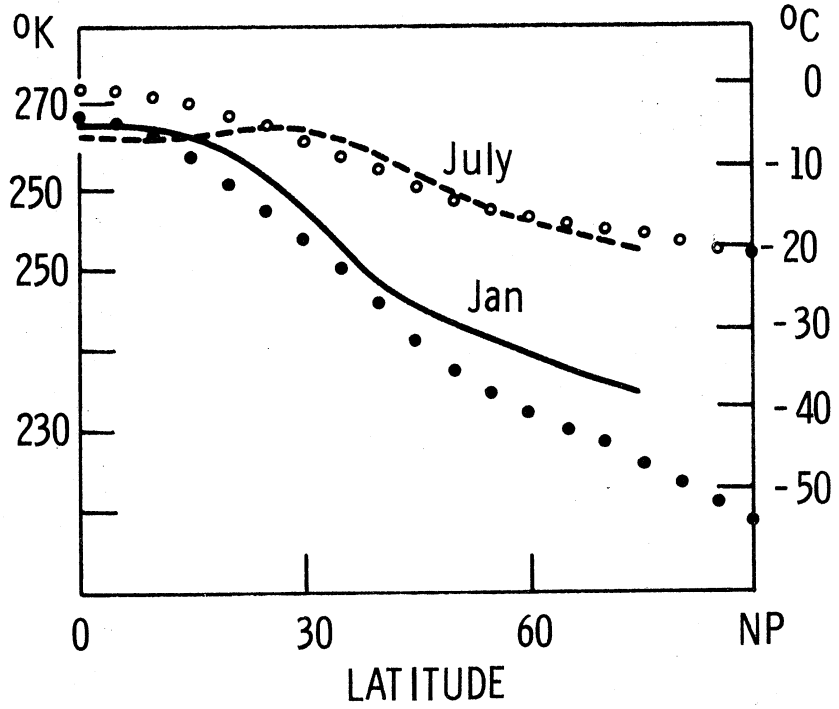

Figure 4.1.3 Meridional temperature profile for July and January at 50 cb , Northern Hemisphere. Simulation values shown by dots and circles. Observed values after Oort & Rasmusson (1971) shown by the continuous and dashed lines.

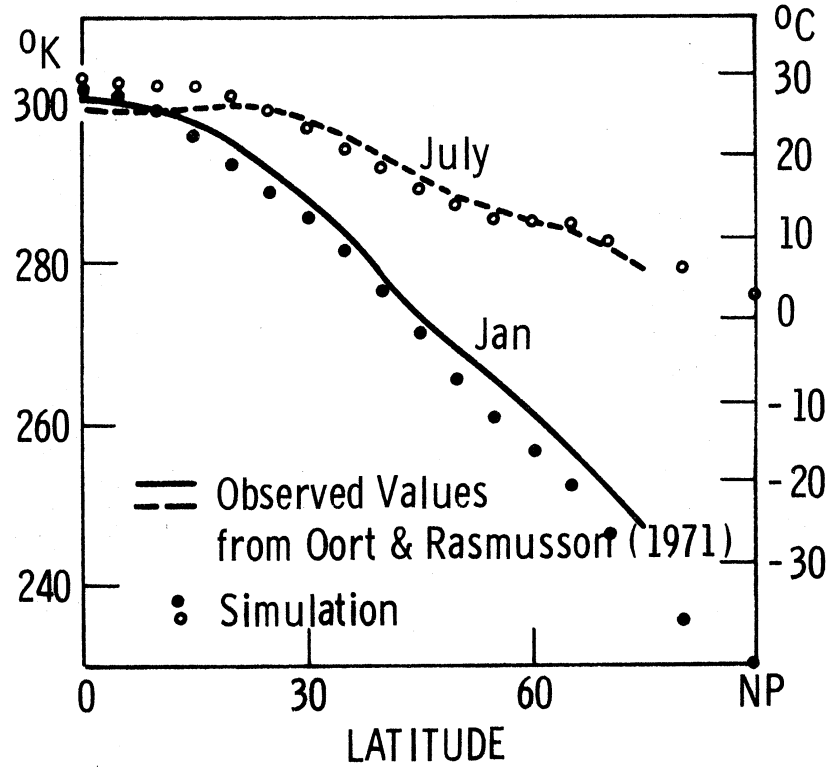

Figure 4.1.4 Same as Figure 4.1.3 but for 100 cb.

that most of their discrepancies with observations were due to the oversimplified thermal forcing. However the weak meridional circulation in low latitudes manifests itself in excessive thermal gradient, especially in the summer. See Fig. 4.1.3 for a comparison with observations. At this level the model produces a larger temperature gradient in middle and high latitudes in winter as if the eddy exchange were not as strong as observations suggest.

Surface temperatures, shown in Figs. 4.1.2 and 4.1.4, seem to be better simulated than 50 cb values. Again low latitudes show disagreement to be blamed on a weak Hadley cell in summer.

In Figs. 4.1.1 and 4.1.2 it is interesting to note that the date of maximum temperature lags the summer solstice by a larger amount the lower the latitude is. This is a consequence of the oceans behaviour shown in Fig. (3.6.5).

4.1.2 Zonal Motion

The model specifies the zonal wind at 25 and 75 cb (the 100 cb wind is obtained through a linear extrapolation in pressure). These are shown in Figs. 4.1.5 and 4.1.6. The flow at the upper level simulates the observed variations in some aspects such as the trade winds appearance in summer and the intensity of the jet stream. On the other hand polar easterlies are present during a short period of time and reach higher latitudes than shown by observations. The maximum wind in summer is too low by about 10 m/sec and does not move to lower latitudes in winter.

At 75 cb, Fig. 4.1.6, the zonal flow shows a summer anomaly due to the inconsistency introduced by the time independence assumption of the exchange coefficients (see 2.3.a). The winter

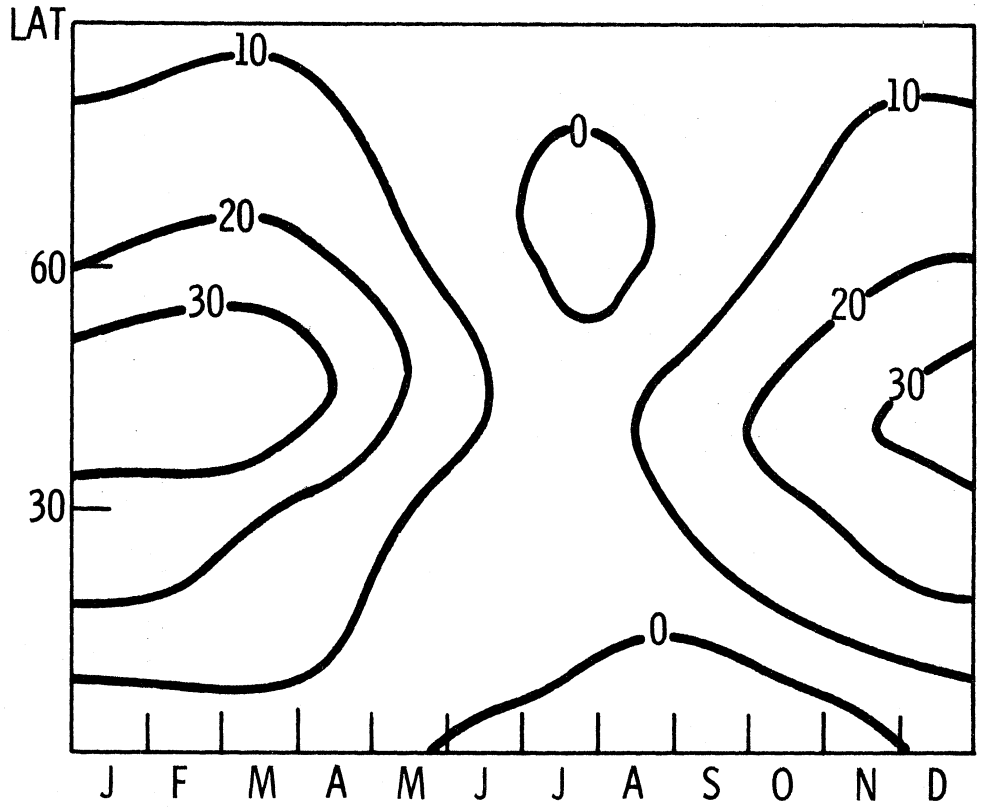

Figure 4.1.5 Zonal flow at 25 cb for the Northern Hemisphere in the linear simulation. Velocity correction for annual angular momentum balance : 3.4 m/sec. Units : m/sec.

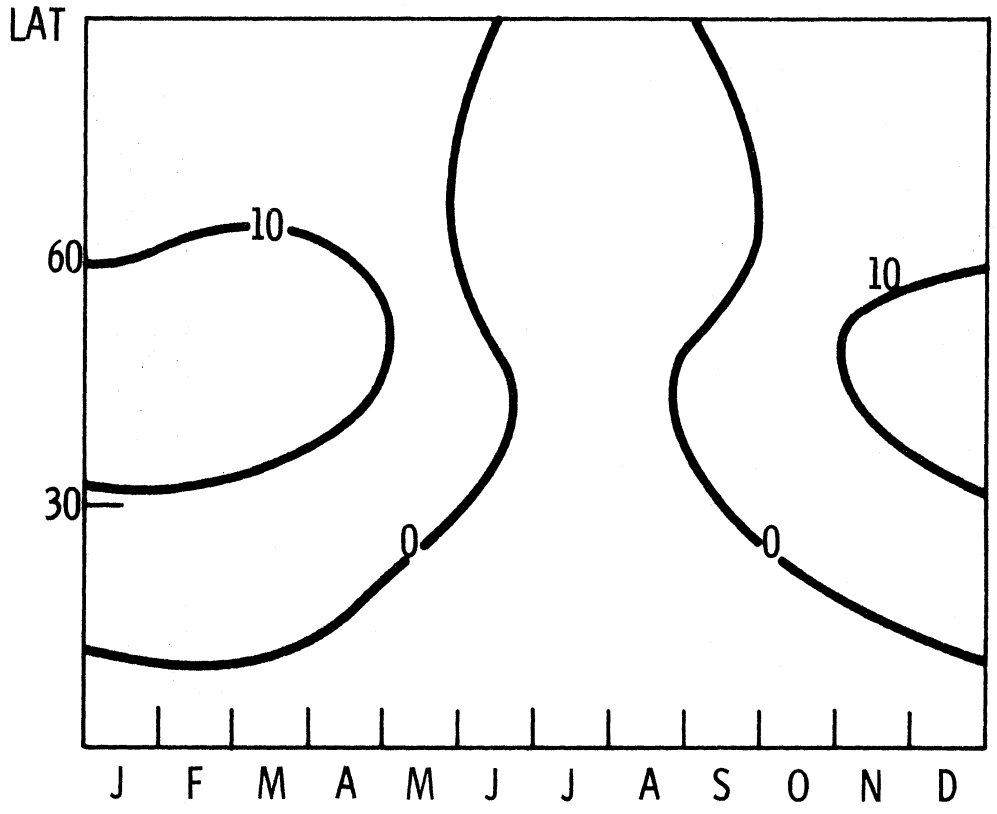

Figure 4.1.6 Same as Figure 4.1.5 but at 75 cb.

magnitudes are correct, but in summer, easterlies appear at all latitudes. The extrapolation at 100 cb shows the same feature. The figures improve if we correct the zonal velocities by a constant amount (3.4 m/sec) such that the torque on the earth surface vanishes, when integrated over the hemisphere and the year. At 75 cb we obtain some westerlies between 25 and 50 degrees of latitude. However, such correction alters the fields of vorticities and therefore is illegitimate.

In comparing with S-WN there is improvement in the magnitudes of the zonal flow. Most of the defects just mentioned are also present in their work and to this extent can be attributed to the values assigned to the exchange coefficients.

4.1.3 Meridional Circulation

The meridional circulation can be shown through the meridional flow or the vertical motion since they are related by the continuity equation (2.1.38). Fig. 4.1.7 presents the vertical motion in the isobaric system of reference, so that negative values indicate ascent. There exists a three cell configuration all year long with some variations in intensity but little in geographical location. When these results are compared with the observations of Oort and Rasmusson (1971), hereafter referred to as O-R, two discrepancies are apparent. First the tropical ascent is too weak and in middle latitudes the upward motion is too strong. Second, seasonal variations of the extension of easterlies and westerlies are not well simulated.

S-WN did not obtain a three cell system which again must be due to the simplified thermal forcing.

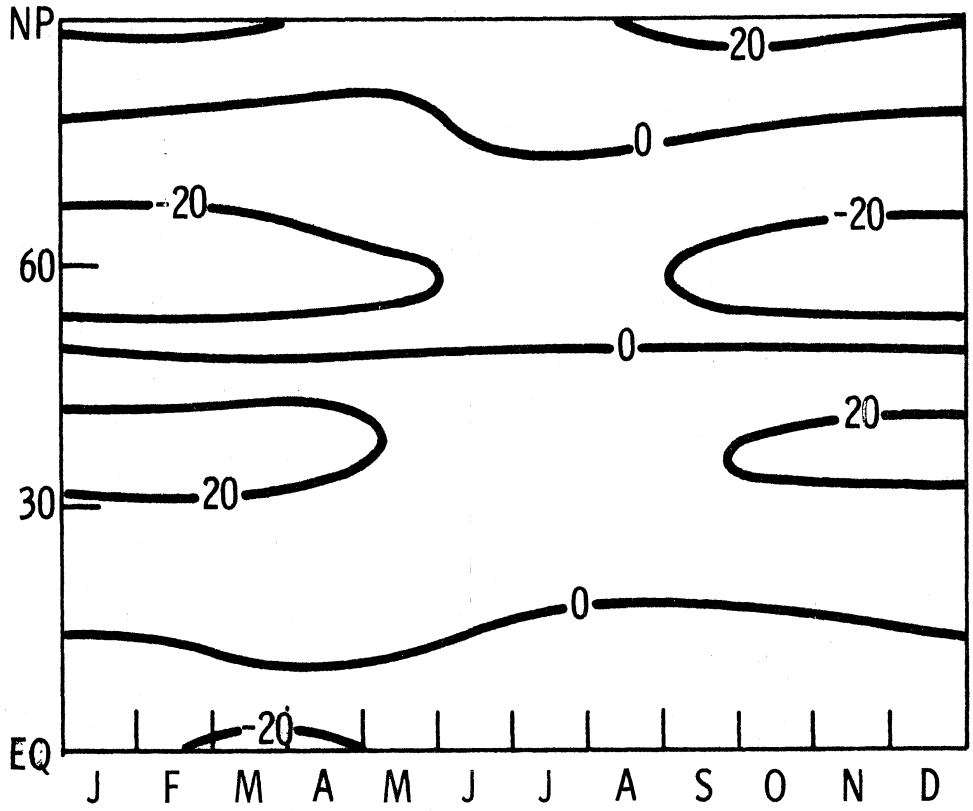

Figure 4.1.7 Vertical velocity at 50 cb for the Northern Hemisphere in the linear simulation. Units : 10^{-6} cb/sec.

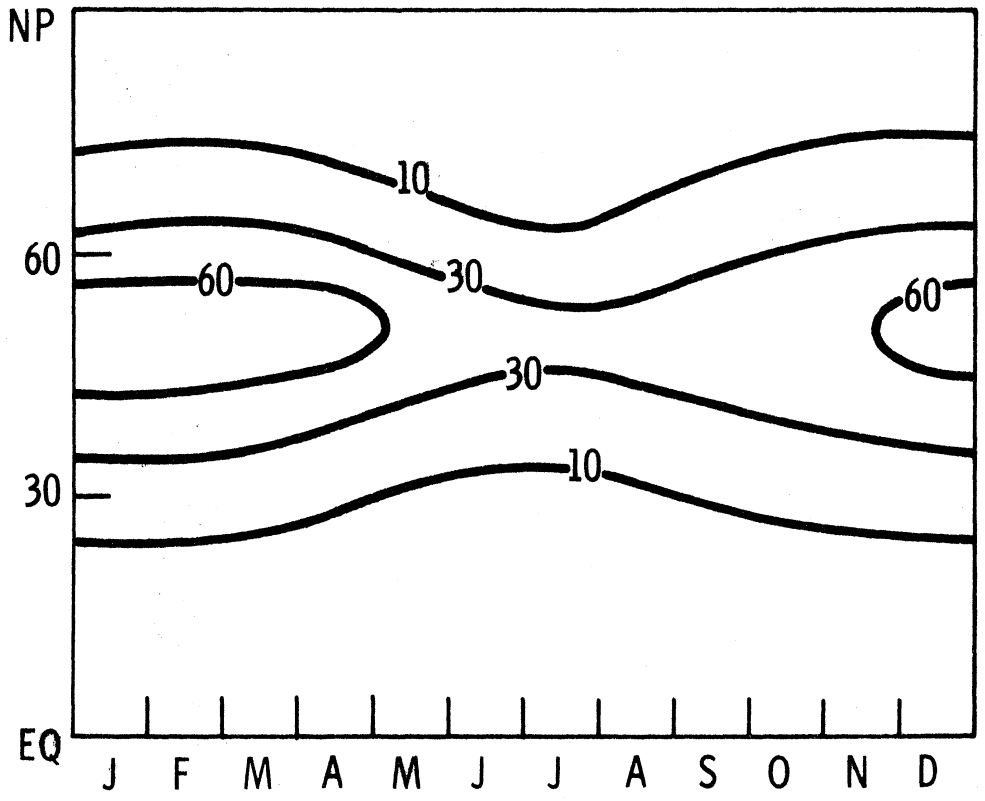

Figure 4.1.8 Heat transport by the atmosphere for the Northern Hemisphere in the linear simulation. Units : 10^{11} kj/sec.

4.1.4 Transport of Heat and Momentum

The transport of heat shown in Fig. 4.2.8 compares quite well with observed estimates of the annual mean as provided by Lorenz (1967). This is a new check on the suitability of the heat transport parameterization. The seasonal and geographical variation is also in good agreement with results reported by O-R.

Angular momentum transport is not well modelled, particularly in summer. In winter months this transport shows the deficiencies of the Hadley cell. Fig. 4.1.9 shows the actually computed curve for January (dashed line) and the variation adjusted so as to get zero transport across the equator (continuous curve). This last one is a very good representation of the annual mean both in magnitude and latitudinal variation, see Lorenz (loc. cit). In summer, the transport becomes negative at all latitudes and the adjustment decreases their magnitude but does not alter the sign. This behaviour is in agreement with the zonal flow features already commented. It seems that the diagnostic values of the eddy exchange coefficients may be adequate for winter conditions but not for modelling summer features.

4.1.5 Energetics

Energy amounts and conversions between them were computed once every third day. Fig. 4.1.10 shows the time variation of zonal available potential and kinetic energies computed by equations (2.3.31) and (2.2.20) respectively. To judge the quality of the modelling we can compare with results of observational studies by Wiin-Nielsen (1967), Krueger, Winston and Haines (1965), Newell et. al. (1969) and Oort (1964), hereafter referred to as WN, KWH, NVDFK

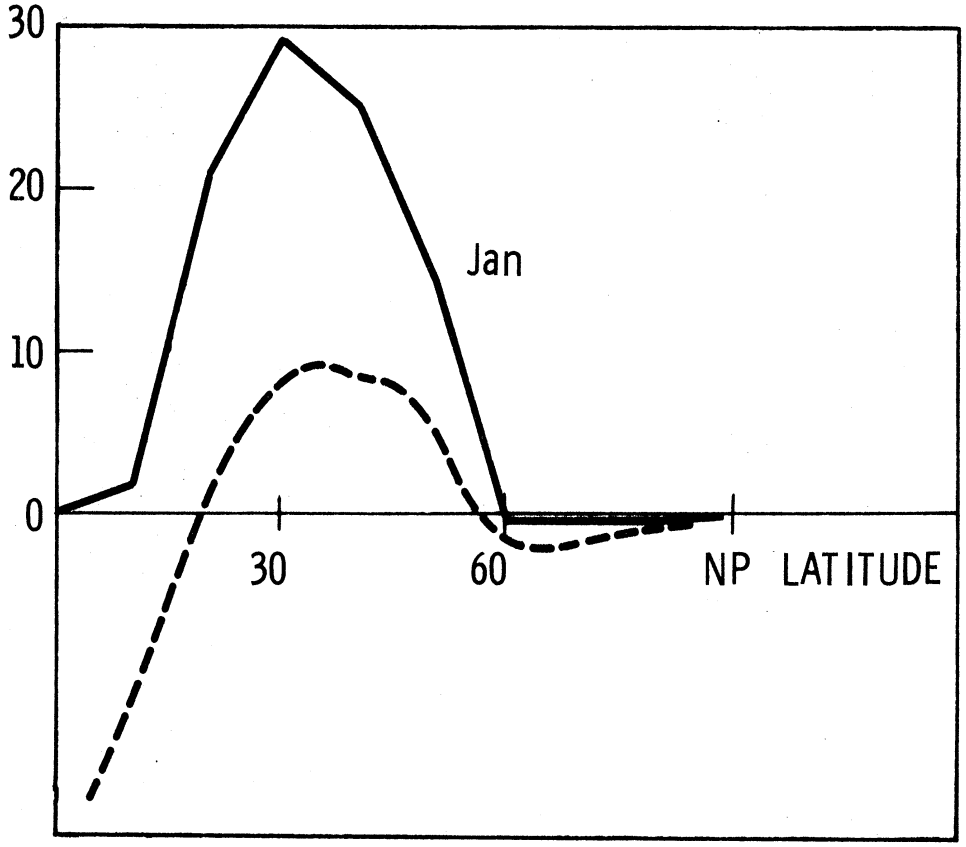

Figure 4.1.9 Angular momentum transport for the Northern Hemisphere in January. Dashed line shows the values obtained in the simulation. Continuous line are values corrected as to obtain zero cross equator flux. Units : 10^{15} ton m^2/sec^2.

and O respectively. WN based his calculations on a one-year data sample for the Northern Hemisphere including the atmosphere below 10 cb. KWH used a five-year data sample containing information of the 85 and 5C cb levels only and for latitudes north of 20^{o}N. NVDFK collected data from a number of sources covering the globe and up to 10 cb. Oort's article is a review paper and includes results of several authors for the Northern Hemisphere.

Available potential energy showed a wave with the maximum in the first week of February. The springtime decrease occurs with a larger rate than the fall build up. The amplitude of the variation amounts to about 3500 kj/m^2 around a mean level of almost 5000 kj/m^2 In a qualitative sense this is in excellent agreement with results of WN. The mean level is somewhat high compared with Oort's estimate of 4000 ± 1000 kj/m^2, but the discrepancy is larger with results of WN and NVDFK which are around 3000-3500 kj/m^2. However, the annual mean is very sensitive to the value assigned to the static stability, and the streamfunction constant, f_o. In particular the latter has been given arbitrarily the value 10^{-4} sec^{-1} which is used in models with cartesian geometry. Had we considered all latitudes weighted according to area a more proper value would have been 0.729 x 10^{-4} sec^{-1} which reduces the value of A_z to about one half of its original magnitude. Therefore the value obtained is within the range that can be expected from the model. Besides, the poor modelling of the Hadley cell tend to increase the available potential energy. The amplitude seems too large by a factor of three. In this respect the results of KWH are helpful because they have been evaluated for latitudes north of 20^{o}N and exclude most of the tropical regions. The seasonal fluctuation of available potential energy for the 85 to 50 layer is reported

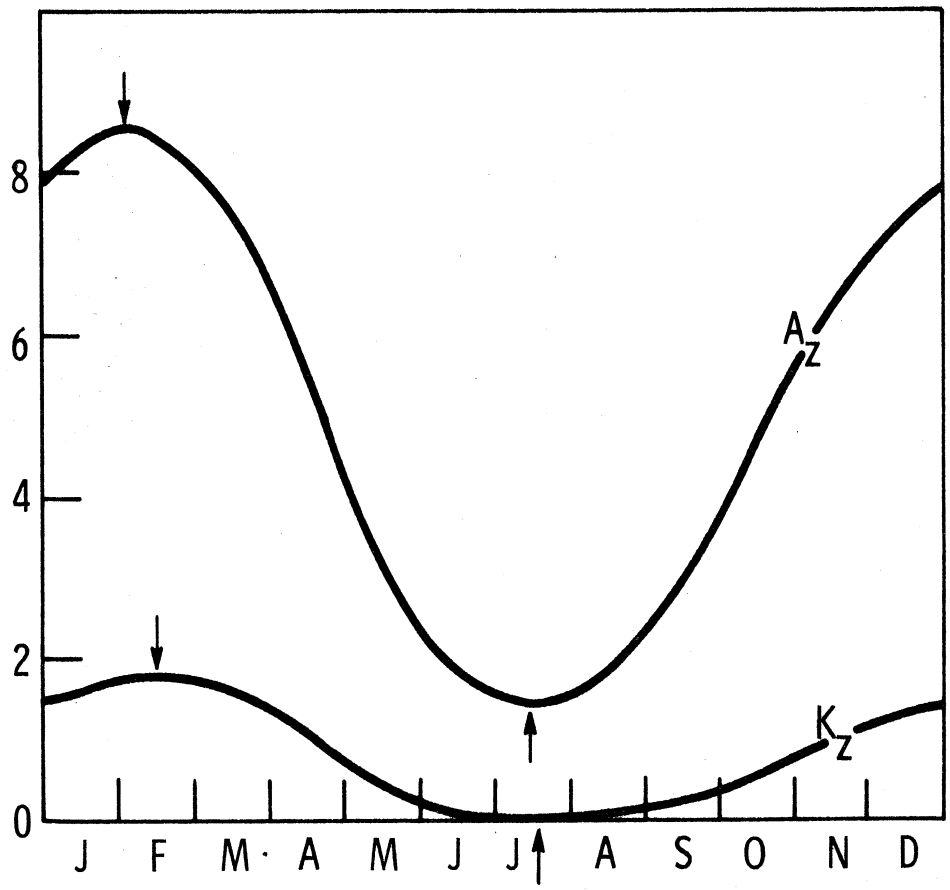

Figure 4.1.10 Simulated variations of zonal available potential energy (A_Z) and zonal kinetic energy (K_Z) along the year for the Northern Hemisphere. Units : 10^6 kj/m^2.

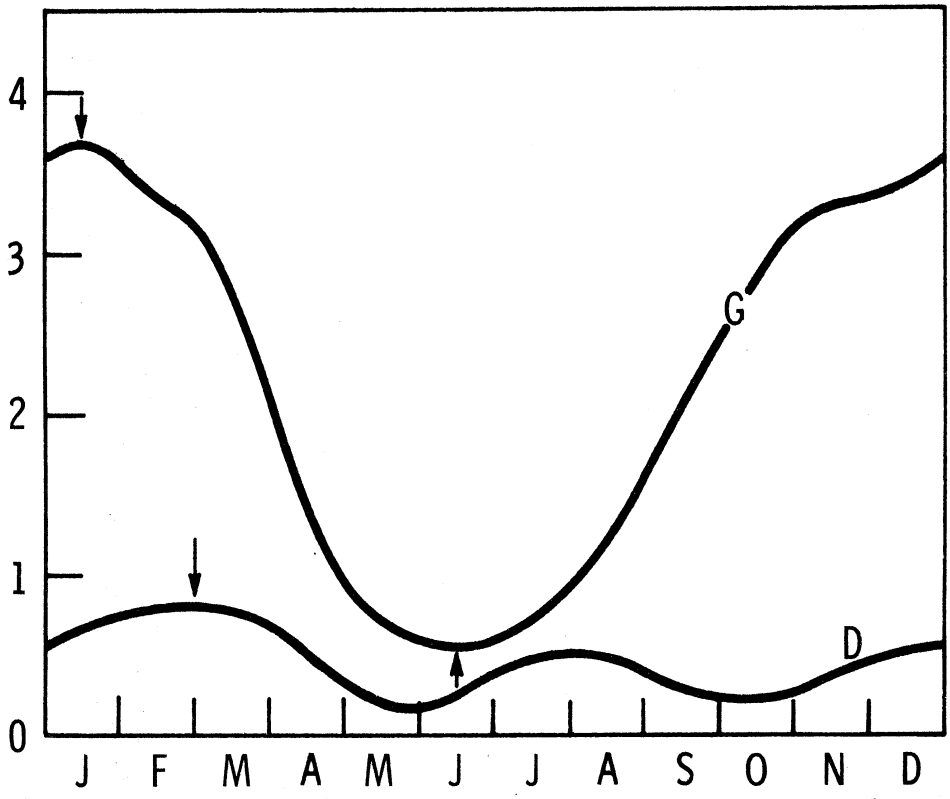

Figure 4.1.11 Simulated variation of the generation of zonal available potential energy (G) and dissipation of zonal kinetic energy (D) along the year for Northern Hemisphere. Units : watts/m^2.

with an amplitude of 1200 kj/m^2, which compares well with the value obtained from the model for the whole atmospheric column.

With respect to S-WN's results, the available potential energy variation shows a smaller amplitude and higher values in the summer months but a somewhat higher mean value. In other aspects they are similar.

The kinetic energy, see Fig. 4.1.10, also represents a simple wave variation. The maximum lags that of the available potential energy by about 12 days. The amplitude reaches about 850 kj/m^2, about the same value as the annual mean. Observed values provided by WN are in very good agreement with the simulation in all respects. This is also valid for values reported by O and KWH. This is an indication that the zonal kinetic energy of the tropical regions is correctly represented. Results of NVDFK do not agree with those cited above, they are about one half smaller.

The results obtained represent a considerable improvement over those reported by S-WN both in amplitude and mean value.

The generation of available potential energy is represented in Fig. 4.1.11 beside the dissipation of kinetic energy. Their maximums occur approximately by January 15 and February 30 so there exists a 1.5 months lag as in S-WN's results. It is to be noted that WN, KWH, and S-WN, computed generations and dissipations as residual terms, while in our case equations (2.3.23) and (2.3.19) were used. The mean values of both quantities over the year agree with estimates by O. The seasonal fluctuation of the generation has an amplitude similar to those reported by NVDFK and somewhat smaller values than those of KWH. Results of WN are not directly

comparable because they are in terms of generation of total potential energy, but do not contradict the outcome of the simulation. The general features of the seasonal fluctuation of both quantities reported by S-WN agree with our simulation, with the exception that neither the generation nor the dissipation attain negative values in our case.

The three energy conversions that are present in the model are shown in Fig. 4.1.12. That from zonal to eddy available potential energy, $C(A_Z, A_E)$, is related to the meridional transport of heat and its maximum is around January according to KWH and WN. The simulation peaks in mid February. The annual mean agrees with values reported by O, KWH and WN; those of NVDFK are again lower. With respect to S-WN's results, there is a slight improvement, mainly in the summer months.

The conversion between eddy and zonal kinetic energies $C(K_E, K_Z)$, presents fluctuations which do not agree with those reported by WN and NVDFK. Both authors find that a maximum is attained in the fall while this simulation and that of S-WN show a maximum in winter. The location of the minimum is less clear. For NVDFK it is in the summer, being positive, while in WN's results it appears in winter and is negative. This transfer was evaluated through equation (2.3.21) and therefore presents one basic difficulty because it is a small residue obtained by subtraction of two relatively large quantities. Furthermore these quantities depend on parameterizations which are not valid in tropical regions (which cover about one half of the earth). At this point there is one indication that tends to support our parameterization. KWH have estimated energy diagrams for each season from 20^{o}N to the pole. Taking the annual mean diagram and

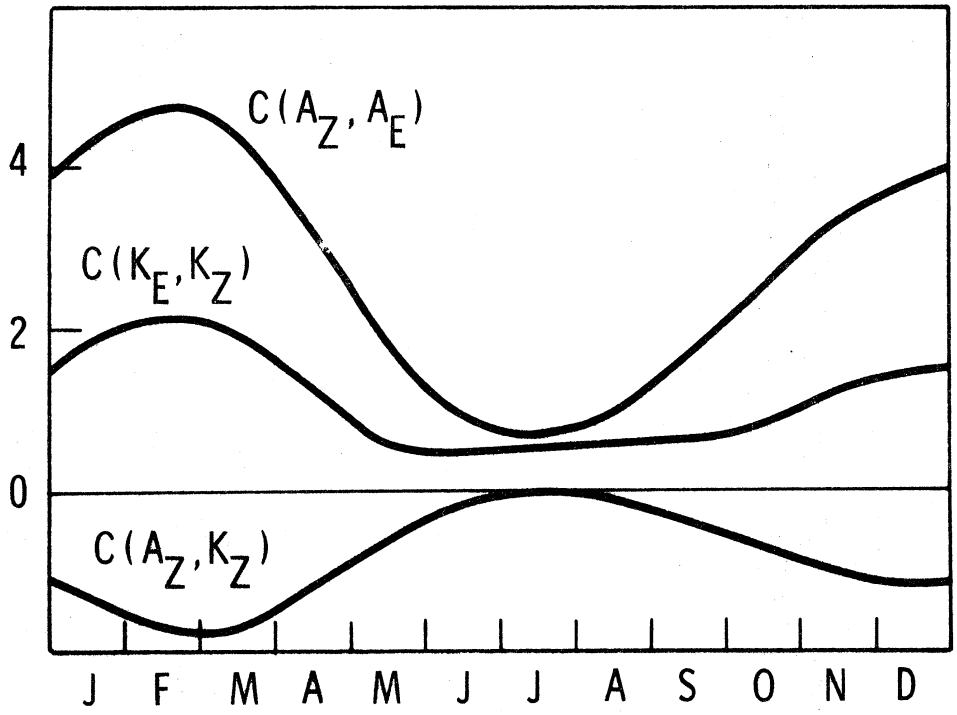

Figure 4.1.12 Simulated annual variations of the conversions between zonal and eddy available potential energies $C(A_Z, A_E)$; eddy and zonal kinetic energies $C(K_E, K_Z)$, and between zonal available potential to zonal kinetic energies $C(A_Z, K_Z)$ for the Northern Hemisphere. Units: watts/m^2.

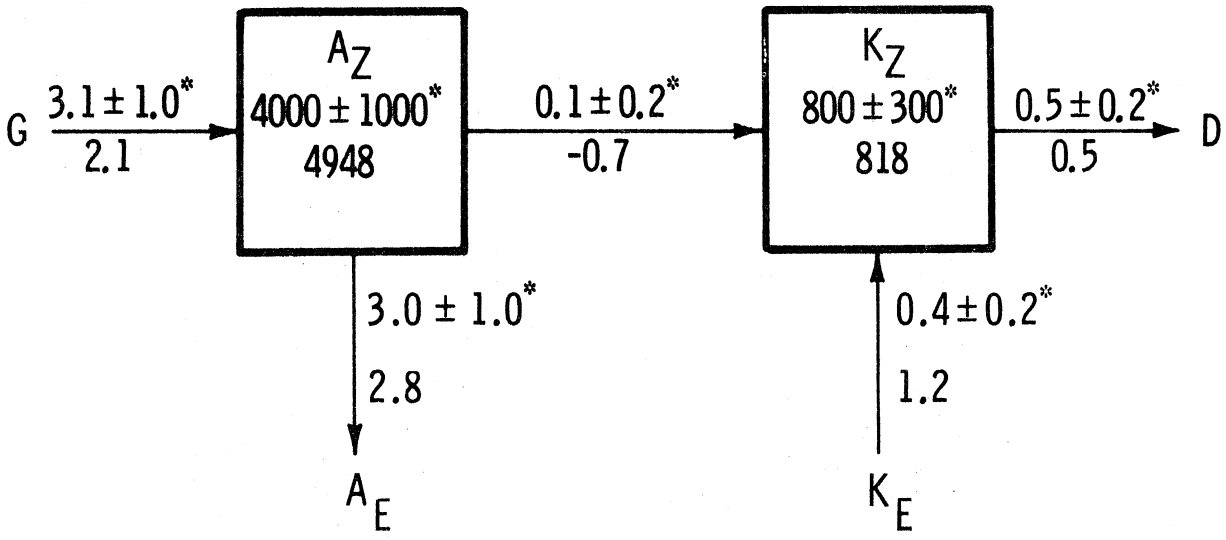

Figure 4.1.13 Simulated energy box diagram in a typical year for the Northern Hemisphere, zonal available potential energy (A_Z) and zonal kinetic energy (K_Z) in kj/m^2. Generation (G), dissipation (D) and conversions in watts/m^2. Observed values after Oort (1964) with asterisk.

introducing the value for the zonal kinetic energy dissipation of say 0.5 watts/m^2, a generally accepted value which must remain unchanged or increase when the tropical regions are omitted, it turns out from the principle of conservation of energy that a value of 1.16 watts/m for $C(K_E, K_Z)$ is obtained. Applying the same procedure to each season we obtain

	$D(K_Z)$	+	$C(K_Z, A_Z)$	= $C(K_E, K_Z)$
Winter	0.5		.83	= 1.33
Spring	0.5		.77	= 1.27
Summer	0.5		.40	= 0.90
Autumn	0.5		.74	= 1.24
Year	0.5		.66	= 1.16

This shows that the modelling is in agreement with the observation in extratropical latitudes. S-WN obtained negative values for this conversion during the spring and summer months. This is contrary to results of NVDFK and KWH, but presents some agreement with the analysis of WN.

The same piece of information provided by KWH is useful in appreciating the results shown for the conversion of zonal available potential to kinetic energy, $C(A_Z, K_Z)$. When compared with hemispheric averages the values shown have the wrong sign and are about one order of magnitude too large, but estimates of KWH show that when the tropical regions are not included, the values obtained in the simulation agree, in magnitude, sign and seasonal fluctuation, with observations. S-WN provided an annual mean value which agreed quite close with observations. Nevertheless, they were unable to obtain a

realistic field of vertical motion, a fact that detracts from their result.

Finally, Fig. 4.1.13 shows the annual mean energy diagram obtained from the study together with observed values from Oort (1964). The agreement is good except for the two conversions just discussed. In the light of the results of KWH one can conclude that the model simulates the middle and high latitudes quite well as far as the energetics is concerned.

4.2 SOUTHERN HEMISPHERE SIMULATION

When dicussing the modelling of the Southern Hemisphere it is necessary to keep in mind that the eddy exchange coefficients were estimated from Northern Hemisphere data so that to some extent we are assuming the same cyclonic activity in both places.

The simulation was completely analogous to the northern counterpart and it differs only in one aspect related to the presence of the Antarctic continent. The tuning of the thermal forcing function was performed with surface temperatures as given by Jenne et. al. (1968), instead of 100 cb values.

4.2.1 Temperature Field

At 50 cb, Fig. 4.2.1, the thermal fields behaves very much like the Northern Hemisphere's. Again the maximum meridional gradient fluctuates anomalously, from about 30^{o} in the winter to 40^{o} in the summer. Similarly the maximum temperature date is between the end of July to mid August in low latitudes.

The field at 100 cb, Fig. 4.2.2, shows some substantial differences with respect to its northern counterpart. The oceanic coverage produces a more homogeneous regime. This is apparent

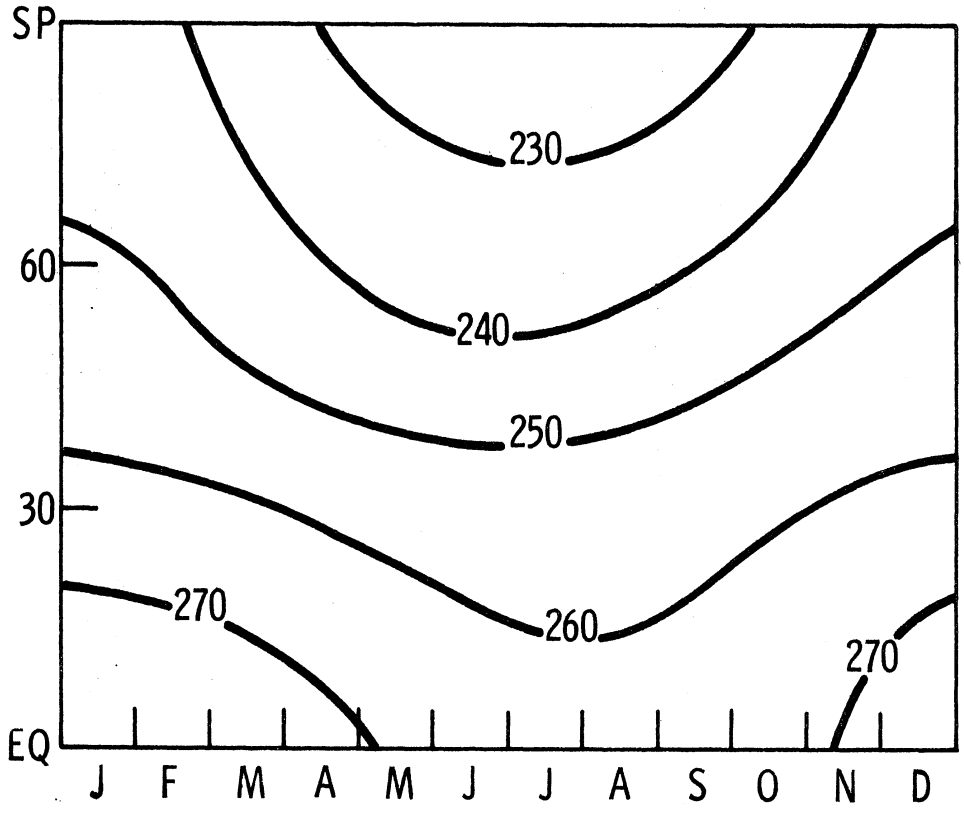

Figure 4.2.1 Same as Figure 4.1.1 but for Southern Hemisphere.

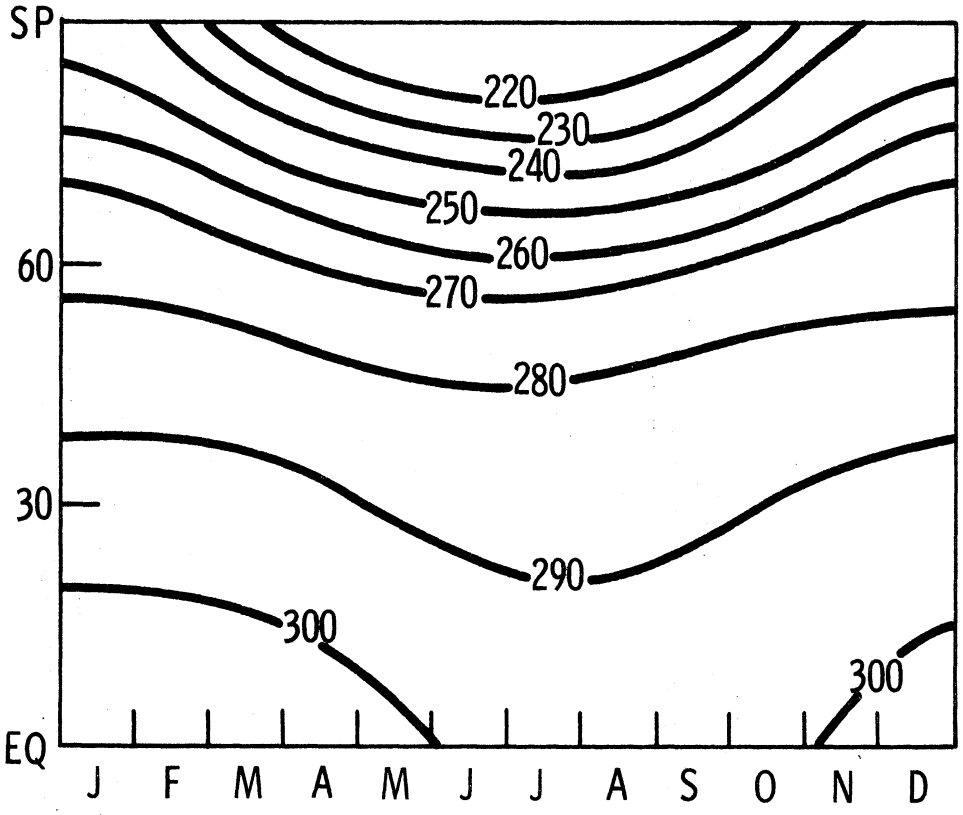

Figure 4.2.2 Same as Figure 4.1.2 but for Southern Hemisphere.

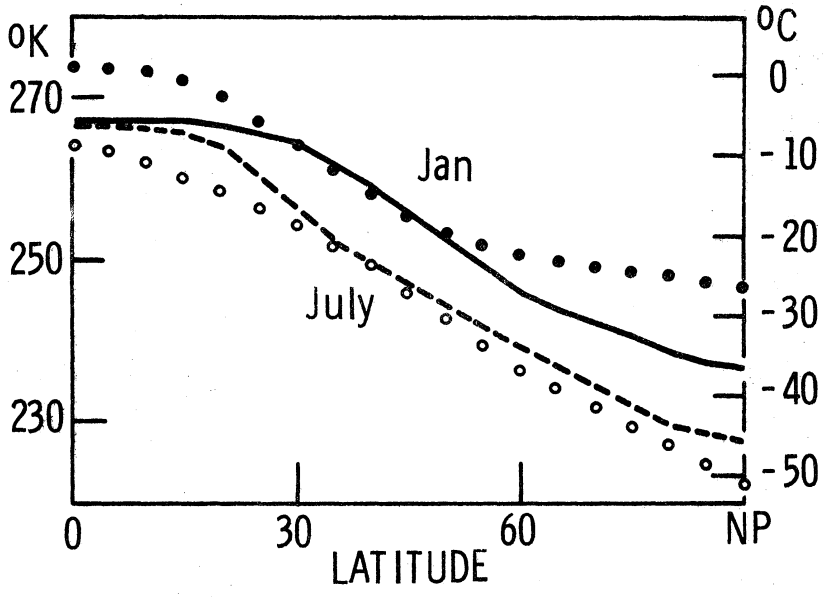

Figure 4.2.3 Same as Figure 4.1.3 but for Southern Hemisphere. Observed values after Jenne et al. (1968).

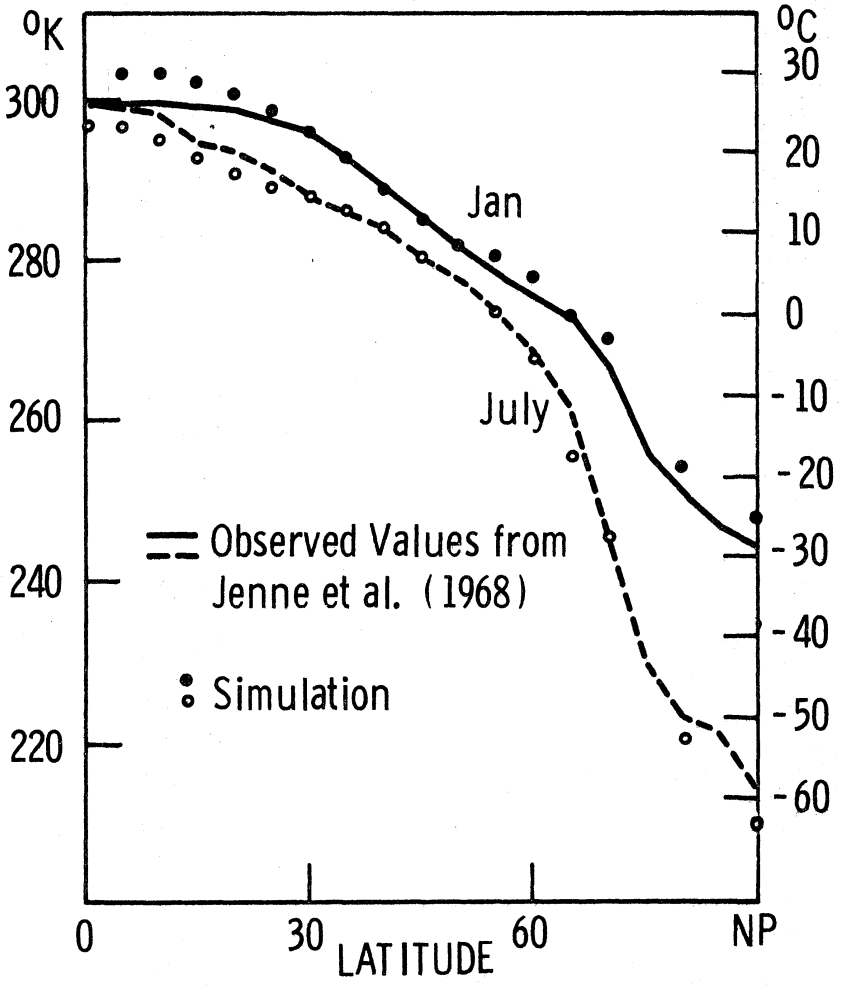

Figure 4.2.4 Same as Figure 4.1.4 but for Southern Hemisphere. Observed values after Jenne et al. (1968).

from a comparison of isotherm 280°K, for instance. In general the whole field in high latitudes follows a smaller amplitude variation; the larger latitudinal gradient is due to the orography effect included in the tuning of the heating function. The model reproduces the flat minimum winter typical of the Antartic stations. Fig. 4. 2. 3 and 4. 2. 4 compare latitudinal variations with observation for the months of January and July. The same characteristics discussed in Section 4. 1. 1 appear, namely, misrepresentation in the low latitudes and better adjustment in surface values.

4. 2. 2 Zonal Motion

Figs. 4. 2. 5 and 4. 2. 6 show the zonal flow at 25 and 75 cb respectively. The seasonal fluctuation is somewhat less than in the Northern Hemisphere in agreement with the smaller seasonal change in the thermal field. This agrees with observations. However, the wind maximum is smaller and its seasonal variation in latitude is 6 months out of phase with observation. The trades behave properly, and there are no polar easterlies.

At 75 cb the simulation is in fair agreement with observation. Polar easterlies begin at 65°S in summer and 72°S in the winter according to Van Loon (1972). In this respect the model attains better agreement with observations in the Southern than in the Northern Hemisphere.

The extrapolated flow at 100 cb does not show substantial differences between the two hemispheres except that the area covered by westerlies is smaller in the austral case.

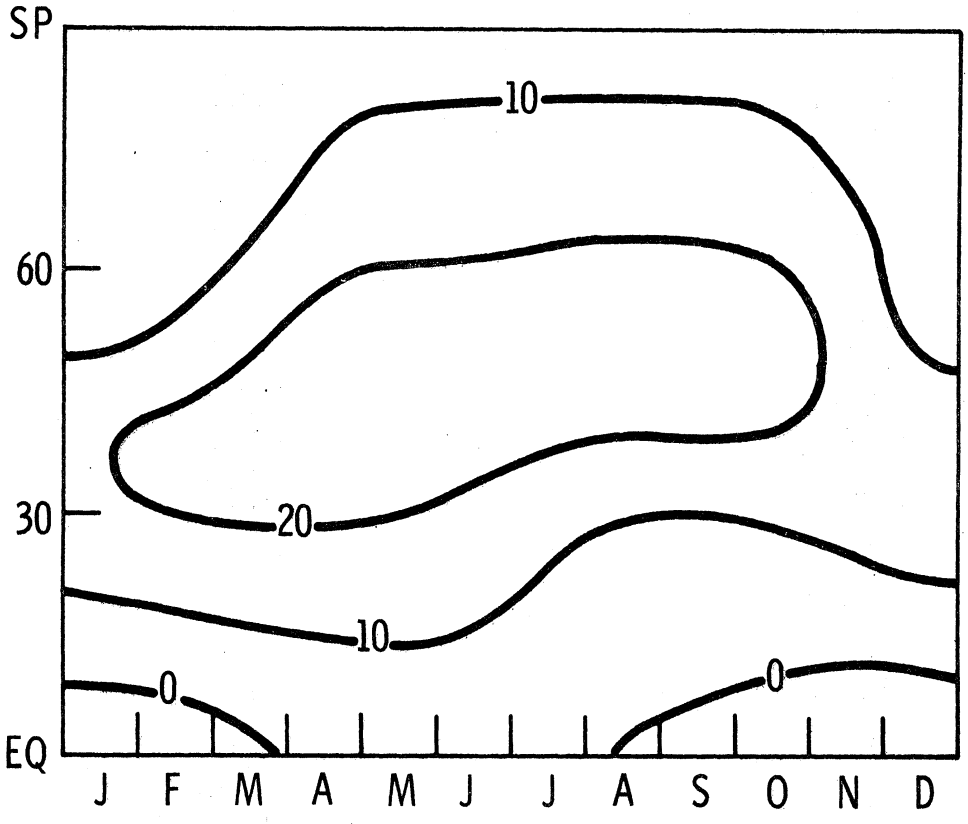

Figure 4.2.5 Same as Figure 4.1.5 but for Southern Hemisphere. Velocity correction 3.6 m/sec.

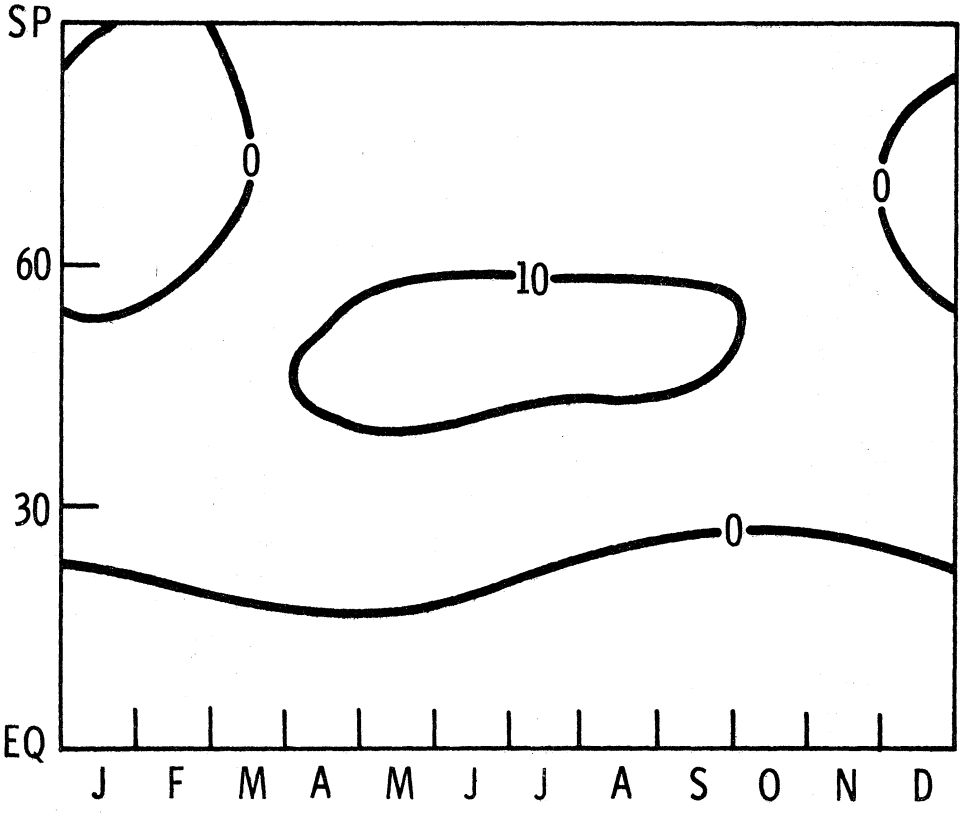

Figure 4.2.6 Same as Figure 4.1.6 but for Southern Hemisphere. Velocity correction 3.6 m/sec.

4. 2. 3 Meridional Circulations

The only observational study that contains information about the zonal mean meridional circulation of the Southern Hemisphere is Newell et. al. (1969). This source reveals that the Hadley cell is much stronger than the other two meridional cells in the fall, winter and spring and almost vanishes in the summer. Fig. 4. 2. 7 shows that the seasonal fluctuation is not reproduced and that the tropical circulation is too weak. The three cell structure is very steady in location and intensity.

4. 2. 4 Transport of Heat and Momentum

Fig. 4. 2. 8 shows the transport of heat by the atmosphere through the year. A comparison with the Northern Hemsiphere, Fig. 4. 1. 8, shows that the major difference is a more moderate seasonal fluctuation, a consequence of the oceanic coverage. The mean level of the transport is in agreement with results of Sellers (1965), but is somewhat larger than the results by Newton (1972). This last author also presents seasonal fluctuations which are about one third of those in the Northern Hemisphere.

The angular momentum transport, Fig. 4. 2. 9, shows the same defects that appear in the Northern Hemisphere. The main difference is a smaller maximum, a fact that does not seem supported by observation, Newton (1972).

4. 2. 5 Energetics

Seasonal variations of energy amounts and conversions are shown in Fig. (4. 2. 10) to (4. 2. 12). It is apparent that the whole energetic picture is characterized by smaller seasonal variations than the

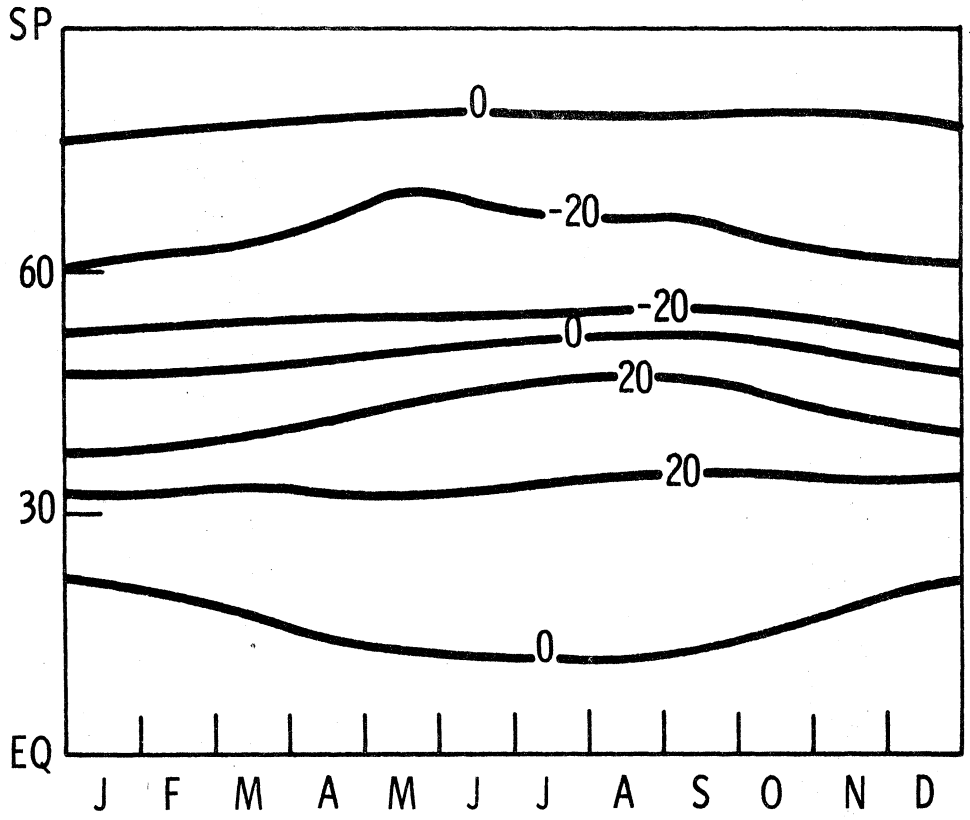

Figure 4.2.7 Same as Figure 4.1.7 but for the Southern Hemisphere.

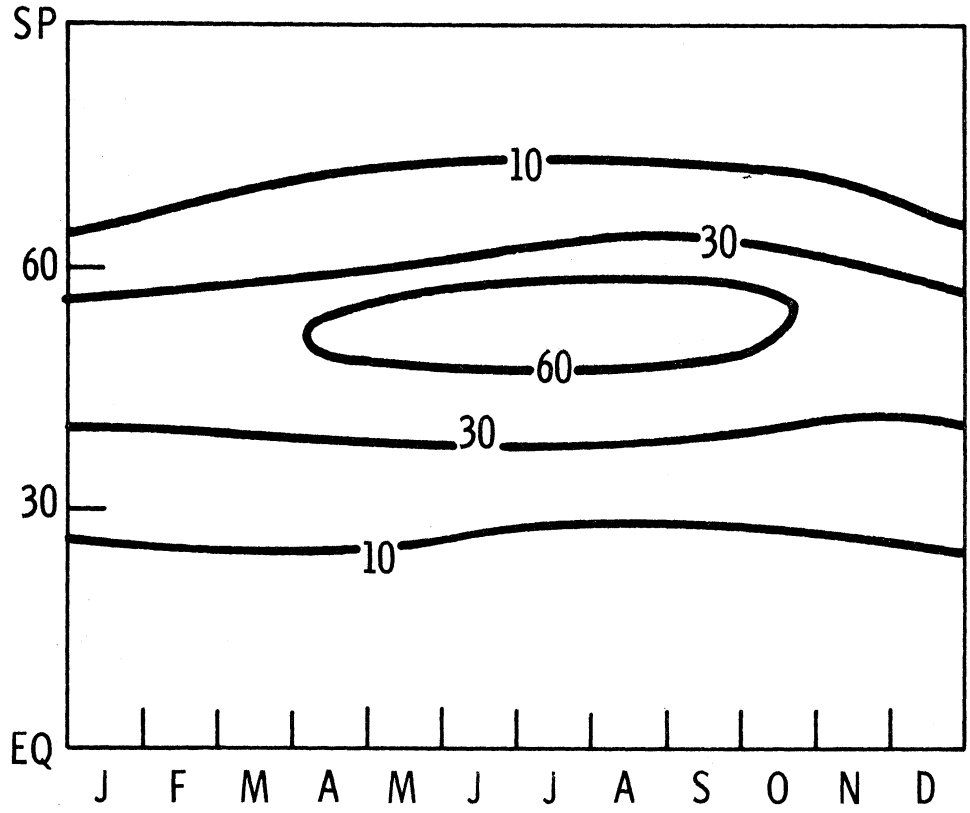

Figure 4.2.8 Same as Figure 4.1.8 but for Southern Hemisphere.

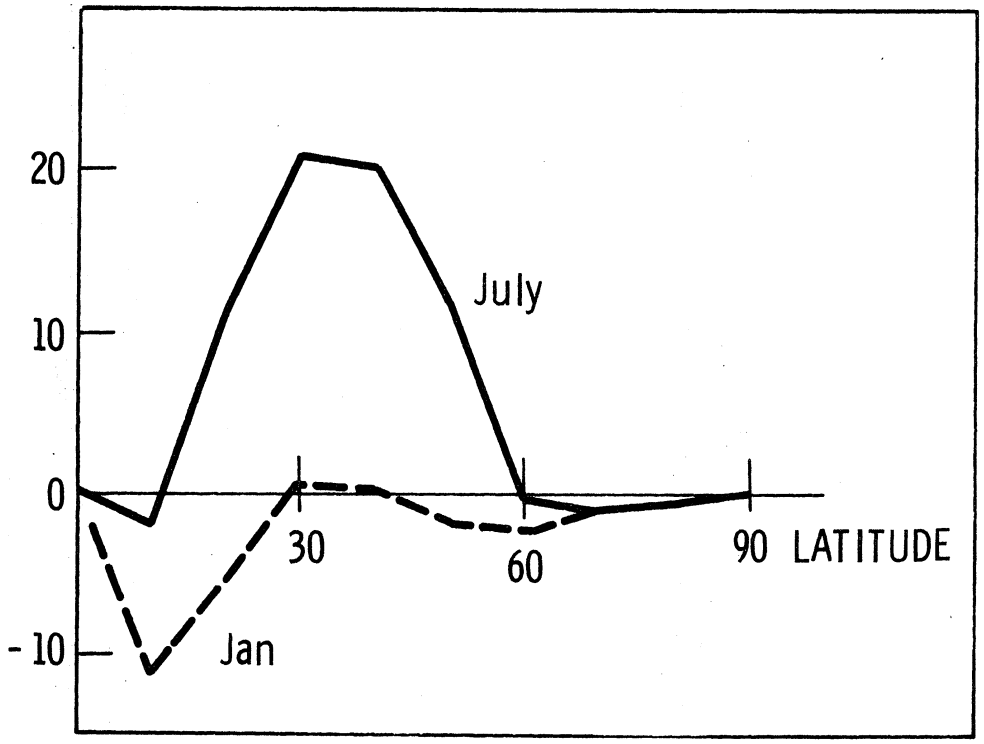

Figure 4.2.9 Angular momentum transport for the Southern Hemisphere in January and July. Both corrected for zero cross-equator flux. Units : 10^{15} ton m^2/sec^2.

Northern Hemisphere. A peculiar feature is the early maximum in generation of zonal potential energy with respect to the summer solstice. The maxima of available potential and kinetic energy follow with time lags very much as those of the other hemisphere. The mean levels of generation and the two energies are in very good agreement with observed values, Fig. (4. 2. 13). However, the aforementioned time lag is not supported by observations, Newell et. al. (1969). This discrepancy can be traced back to the thermal forcing shown in Fig. (3. 6. 6). It is seen there that the heating function in the simulation (small circles) tend to underestimate the correlation between temperature and the diabatic heating in the fall and winter months. In low latitudes this is probably due to an incorrect assessment of the release of latent heat and its seasonal fluctuations. The only source for this data was Möller (1951), who presents the information on a seasonal rather than monthly basis.

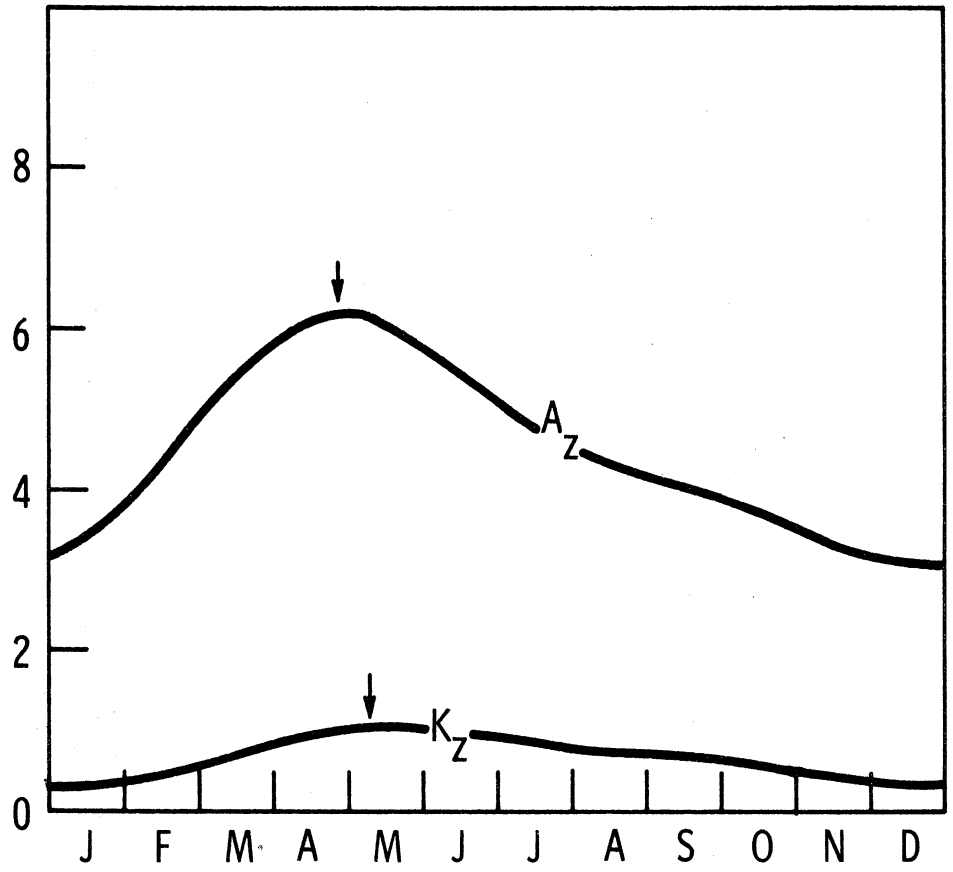

Figure 4.2.10 Same as Figure 4.1.10 but for Southern Hemisphere.

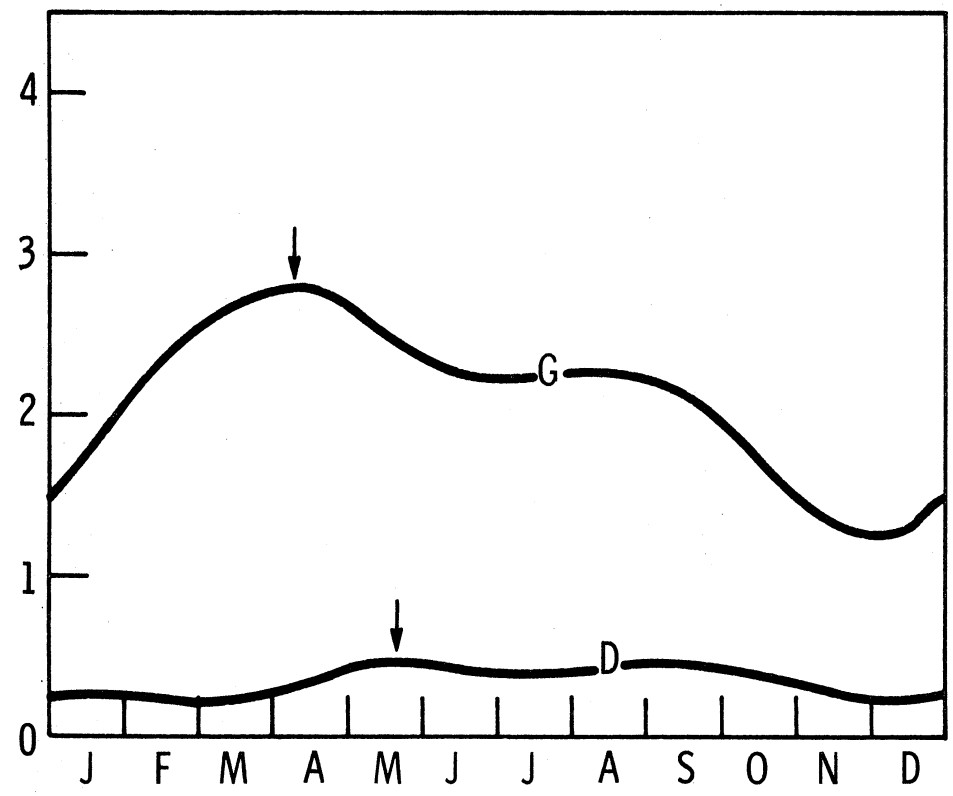

Figure 4.2.11 Same as Figure 4.1.11 but for Southern Hemisphere.

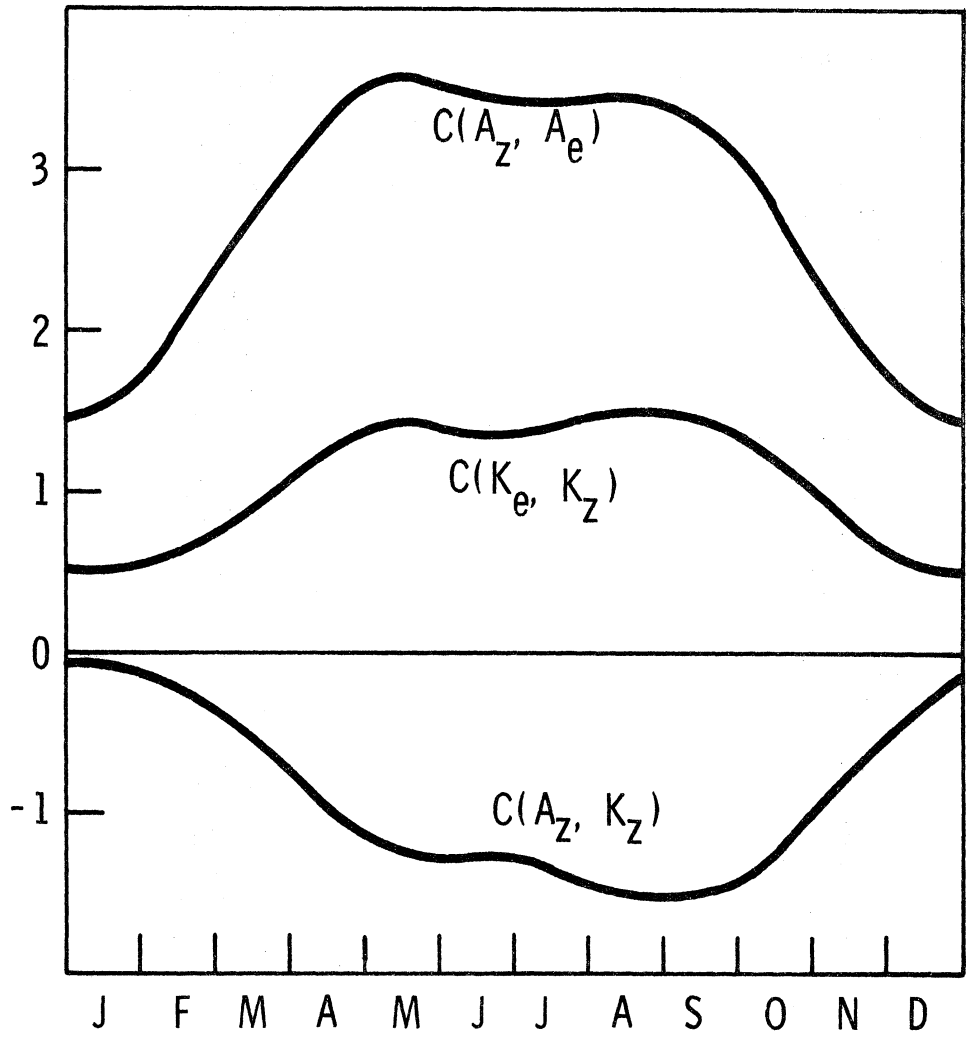

Figure 4.2.12 Same as Figure 4.1.12 but for Southern Hemisphere.

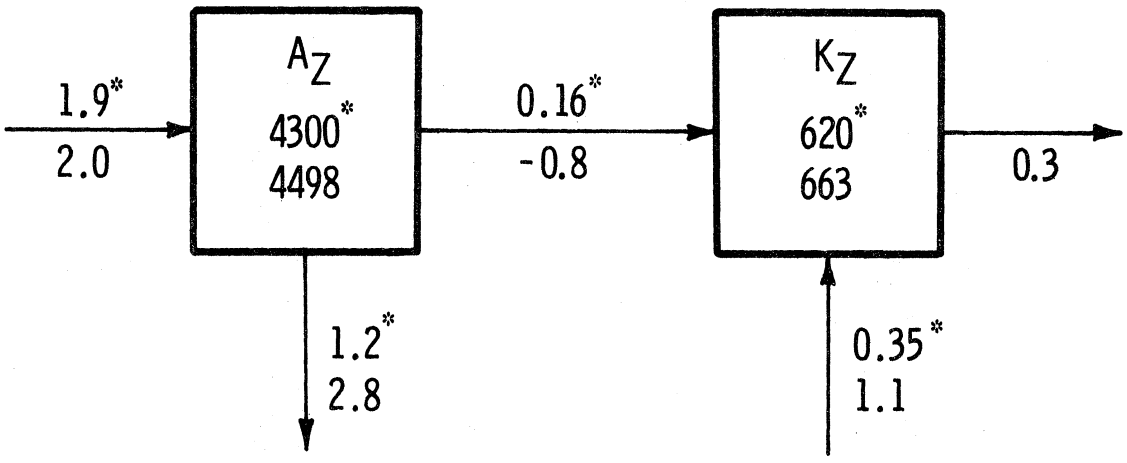

Figure 4.2.13 Same as Figure 4.1.13 but for Southern Hemisphere. Observed values (with asterisk) after Newell et al (1969).

CHAPTER V

SENSITIVITY STUDY

The governing equations of the model contain some parameters introduced by the quasi-geostrophic approximation, others are needed for the representation of sub-grid processes, and finally, exchange coefficients are used for heat and potential vorticity parameterization. These parameters were assigned magnitudes according to average values suggested by observations. The results of the simulation must be considered according to their sensitivity to variations of these mean values. In this chapter we will report results of simulations performed with parameter values changed by reasonable amounts, (Table 5.0.1).

We will be concerned with the quasi-geostrophic constants, f_o and $\bar{\sigma}$, experiments #1 and #2, the sub-grid constants ε and A, experiments # 3 to #6, and the three eddy exchange coefficients, experiments #7 to #15.

5.1 STREAMFUNCTION CONSTANT

The value adopted for f_o was 10^{-4} sec^{-1}, corresponding to Coriolis parameter at 43.3 degrees of latitude. An additional simulation was performed with $f_o = 0.6 \times 10^{-4} sec^{-1}$, a value of f at 23.6 degrees, other factors unchanged.

The variation of f_o introduces modifications in the values of λ^2 and q^2. In the last case the dependence is quadratic and q^2 reduces to about one third of its original value. This implies that the baroclinic effects represented by $q^2\Psi_{Tz}$ in the potential vorticities

TABLE 5.0.1

Exp. #	Parameter in study	Standard value	Value in experiment
1	f_o	10^{-4}	$0.6 \times 10^{-4} sec^{-1}$
2	β	2	$3\ m^4 sec^{-2} t^{-2}$
3	ε	3×10^{-6}	$1.0 \times 10^{-6} sec^{-1}$
4	ε		$9.0 \times 10^{-6} sec^{-1}$
5	A	0.6×10^{-6}	$0.3 \times 10^{-6} sec^{-1}$
6	A		$1.0 \times 10^{-6} sec^{-1}$
7	K_2	(*)	10^o shift south
8	K_2		$2.0 \times 10^6\ m^2 sec^{-1}$
9	K_2		(**)
10	K_1 & K_3	(*)	$K_1 = K_3$ from (*)
11	K_1 & K_3		$K_1 = K_3/3 = 10^6 m^2 sec^{-1}$
12	K_1	(*)	$K_1 = 2.0 \times 10^6 m^2 sec^{-1}$, K_3 from (*)
13	K_1		10^o shift south, K_3 from (*)
14	K_3	(*)	10^o shift south, K_1 from (*)
15	K_3		K_3 from (**), K_1 from (*)

(*): values taken from Table 5.5.1

(**): values taken from Wiin-Nielsen & Sela (1971)

become smaller, although still dominant. As a direct consequence the available potential energy decreases proportionally to f_o^2. This strong dependence indicates that the relatively high value of this energy (by about 20%) must not be of great concern, for a change of only 1% in f_o would give the observed magnitude of the mean zonal available potential energy. Of greater importance is the modification in the meridional gradient of potential vorticity since with the new value for q^2 contributions from the beta and thermal terms become comparable.

As far as the vertical motion is concerned equation (2.1.37) indicates that a decrease of f_o will decrease the importance of the contributions from horizontal advection and local changes of temperature. Consequently the tropical convection increases in magnitude. In January the maximum in trades doubles its value. On the other hand, the high latitude ascent becomes weaker and covers a narrower latitude belt. This improved correlation between the vertical motion and the diabatic heating changes drastically the conversion of energy between zonal available potential and zonal kinetic from -0.8 to +1.1. This corroborates our former statement about a weak Hadley cell being the reason for the negative value of this conversion. A rough guess indicates that a decrease of f_o by 20% would give a value of $C(A_z, K_z)$ about equal to the observed one. However, such a change brings in other undesirable effects.

The use of a smaller f_o produced a decrease of the zonal flow. For instance, the maximum wind in the westerlies diminished by 10 m sec^{-1} at 25 cb and by 13 m sec^{-1} at 75 cb in January. The fraction of the globe covered by easterly winds increased and consequently the transport of momentum became worse. This is an

effect of the weaker thermal forcing (which is proportional to λ^2) and the relation between wind and streamfunction. The kinetic energy decreased to about one half of the standard case. However the dissipation increased, because in the summer months the zonal flow at 75 cb reached larger absolute values (they are mostly negative) than in the winter.

The temperature difference between pole and equator decreased by about 20 degrees in winter and 10 in summer at 50 cb. About the same change occurred at 100 cb. As a consequence the heat transport diminished to about one half.

In conclusion, f_o is an important parameter, and the results are quite sensitive to its value. However, with the present formulation the value assigned seems adequate. Changes in f_o will tend to deteriorate some results while improving others.

5.2 STATIC STABILITY

The second quasi-geostrophic constant is the static stability, $\bar{\sigma}$, for which a value of 2 $m^4 sec^2 t^{-2}$ was chosen. Typical values provided for the months of January and July by Gates (1960) are

Layer (cb)	Jan	July
30-50	3.73	3.66
50-70	2.26	2.20

The value chosen seems thus somewhat low. A simulation was done with $\bar{\sigma}$ = 3 $m^4 sec^2 t^{-2}$, experiment #2. The value of $\bar{\sigma}$ enters linearly in the denominator of the constants λ^2 and q^2. For this reason an increase of 50% in static stability has many of the effects

of a decrease of f_o by 40%. For instance, both increase the geographical domain of easterlies and worsen the simulation of the angular momentum balance. The meridional temperature gradient decreases, but only by a few degrees. The influence of $\bar{\sigma}$ on the different processes that generate vertical motion is the same. Hence, variations in $\bar{\sigma}$ are not so selective as those of f_o. In January the tropical maximum ascent went down by about 30% while the high latitudes ascent diminished by about 40%. Because the temperature changes were restricted mainly to high latitudes there was a higher correlation with the vertical motion and the conversion of energy from zonal available potential to zonal kinetic attained a value of $-.15$ watt/m^2.

Kinetic and available potential energies decreased to 2700 and 350 kj/m^2, respectively, and the same happened to the generation that reached 1.5 watts/m^2.

In general, the sensitivity of the results to this variation was smaller than in the f_o case, although still of considerable magnitude.

5.3 BOUNDARY LAYER FRICTION

The transfer of momentum between the atmosphere and the underlying surface was parameterized in terms of a constant ε. In Section 2.1.d we showed that this factor was proportional to the wind speed near the surface, V_4, to a drag coefficient, c_d, which depends on the roughness of the surface, and other factors which are less variable. Using typical values for V_4 and c_d a value $\varepsilon = 3 \times 10^{-6}$ sec^{-1} was chosen. To study the influence of the uncertain value of ε two additional simulations were done with $\varepsilon = 1 \times 10^{-6}$ sec^{-1} and $\varepsilon = 9 \times 10^{-6}$ sec^{-1}, experiments #3 and #4.

Variations in ε have only slight consequences for the energetics and the thermal field. The most important changes occur in the zonal flow. As an example, changes in the kinetic energy are 6% between simulations using the extreme values of ε. Analogous figures for available potential energy. $C(A_Z, A_E)$ and dissipation are 1%, 12% and 40%. The latter is the most significant change in the energy cycle. The total pole-equator temperature difference varies by 1^{o} K at most.

Changes in the zonal flow are such that with $\varepsilon = 9 \times 10^{-6} sec^{-1}$ a remarkable improvement has been obtained in the angular momentum balance. The flow at 25 cb shows a maximum of 33.4 m/sec^{-1} in January and 11 m/sec^{-1} in July, both at $40^{o}N$. There exist westerlies at 75 cb all year around. In July they occupy the belt between 20 and 50 degrees. At 100 cb there are westerlies between 30 and $70^{o}N$ in January but they disappear in July. The zonal velocity correction necessary for a long term hemispheric balance of angular momentum decreases from 3.4 m/sec^{-1} in the prototype simulation to 1.9 m/sec^{-1} in the case with $\varepsilon = 9 \times 10^{-6} sec^{-1}$.

The effect of an increase in ε on the zonal flow is to decrease the amplitude of the seasonal variations keeping the maxima almost invariable, i.e., it intensifies the summer westerly flow without much change of the winter circulation. From this result, one can infer that in the summer the zonal circulation is frictionally driven while in winter the eddy exchange of momentum overshadows the interaction between the air and the earth surface.

The meridional circulation is increased by a very small amount so that even a difference of one order of magnitude in ε gives

an increase of 4% in the maximum ascent in the equatorial region and about 10% in the middle latitude upward motion.

In conclusion the value of ε hardly effects the results of the simulation with the exception of the zonal flow which improves when ε is increased. The optimum value of ε seems to correspond to a drag coefficient near the upper bound of those recommended in the literature, Cressman (1960).

5.4 INTERNAL FRICTION

The internal friction coefficient A was shown in (2.1.d) to depend on a kinematic viscosity ν, representing the effects of subsynoptic processes, and the temperature T_{2z} squared. The latter fluctuates by about 30% with most of the variance coming from the high latitudes. Estimates of the dynamic viscosity, μ, have been made by Palmen (1955) and Riehl (1951). This information gives A values of 0.6×10^{-6} and 1.3×10^{-6} sec^{-1}, respectively. In the standard simulation we have used the value derived by Palmen.

Two experiments were run, the first with $A = 0.3 \times 10^{-6} sec^{-1}$ and the second with $A = 1.0 \times 10^{-6} sec^{-1}$. In general, changes generated were small and the last case produced results in better agreement with observation. The zonal flow experiences only slight modifications: a decrease in west winds. Temperatures were also changed by small amounts in high latitudes. The temperature difference between pole and equator at 50 cb in January decreased by 6%. The most important variations were in the energy balance. The available potential energy decreased from 4950 to 4400 kj/m^{-2}. The kinetic energy diminished by 160 units and the conversion $C(A_z, K_z)$ was reduced to -0.4 $watts/m^{-2}$.

The value of this parameter does not play a significant role in the outcome of the experiments although it helps to improve some of them to a limited extent.

5.5 EDDY COEFFICIENTS

The model includes three eddy exchange coefficients. One for transport of heat, K_2, and two for transport of potential vorticities, K_1 and K_3. All of them were taken as time independent and assigned values used by Sela and Wiin-Nielsen (1971) which were determined on the basis of a diagnostic study by the same authors (Wiin-Nielsen and Sela, 1971). Since the study was done under quasi-geostrophic conditions values of the coefficients were determined for latitudes between 25^{o} and 80^{o}N. The basic data extended over the whole year 1963. Monthly mean values for each latitude were computed. They represent therefore a rather smoothed distribution. However, the fact that the coefficients represent zonally averaged effects decreases the importance of using monthly mean values. Due to the small size of data sample monthly mean values were averaged and the annual mean used in the simulation. This additional smoothing filters out seasonal changes, and the extent to which they are important is shown in the results of the simulations discussed in Chapter 4. Between the Equator and 25^{o}N of latitude the magnitudes were fixed by subjective extrapolation with no observational evidence to support them. The values used in the simulations are presented in Table 5.5.1.

Since each exchange coefficient is a function of latitude the numerical study of their influence is not straightforward. Based on the results of Wiin-Nielsen and Sela (1971) we will assume that the meridional variation has one maximum in mid-latitudes, and we will

TABLE 5.5.1

EDDY EXCHANGE COEFFICIENTS

Latitude	K_3	K_2	K_1
deg.	10^6 m^2 sec^{-1}		
0	1.3	0.1	0.5
5	1.3	0.1	0.5
10	1.3	0.1	0.5
15	1.3	0.2	0.5
20	1.3	0.4	0.5
25	1.3	0.5	0.5
30	1.3	0.6	0.5
35	1.3	1.3	0.5
40	1.5	2.2	0.4
45	3.5	3.3	0.6
50	6.6	5.0	1.1
55	7.4	6.0	1.8
60	5.8	5.4	2.4
65	4.5	4.3	2.6
70	3.7	3.5	2.7
75	2.9	2.5	2.2
80	2.0	1.3	1.5
85	1.0	0.6	0.7
90	0.0	0.0	0.0

Source: Figure 2 from Sela and Wiin-Nielsen (1971).

try to assess the importance of its magnitude and location. It is important to keep in mind that the transfer coefficient for quasi-conservative quantities is unique (Bretherton, 1966 a) and that the difference we make here between K_2, as a heat transfer coefficient, and those of potential vorticity, K_1 and K_3, is due to the different role they play in the numerical model and to the diagnostic evaluation used to determine their values.

We will start with the heat exchange coefficient and continue with the potential vorticities.

5.5.1 Heat Eddy Exchange Coefficient

The K_2 coefficient is used to evaluate the vertical motion from equation (2.1.37) and in the energy conversions between eddies and the zonal component. It is irrelevant as far as the basic dependent variables are concerned. Because the integral constraints that relate the eddy exchanges of momentum and heat are not satisfied, changes in K_2 do not alter K_1 and K_3.

According to equation (2.1.37) the vertical motion is determined by four contributions: the local change of temperature, the product of the meridional variations of K_2 and temperature, the product of K_2 and the Laplacian of the temperature, and the diabatic heating.

The local change of temperature makes, normally, a very small contribution (less than 0.5×10^{-6} cb sec^{-1}). When the diabatic term reaches a level of 50 ly/day, it contributes about 12×10^{-6}cb/sec. Thus the thermal forcing guarantees ascent in the tropical regions and polar descent, unless K_2 or its gradient happen to be very high. Typical contributions in mid-latitudes for all the terms are:

$$\omega_2 \frac{\bar{\sigma} p_s}{4 f_o} = \frac{\partial \psi_{Tz}}{\partial t} - \nabla K_2 \cdot \nabla \psi_{Tz} - K_2 \nabla^2 \psi_{Tz} - \frac{R}{2 f_o c_p} H_{2z} \qquad (5.5.1)$$

$$0.5 \qquad 8. \qquad 1. \qquad 12.$$

where the figures represent contributions in 10^{-6} cb sec^{-1}.

Three experiments were run changing the values of K_2 as shown in Fig. 5.5.1. In experiment #7, the standard profile of the coefficient was shifted 10 degrees equatorward. In experiment #8 a constant value equal to $2 \times 10^{-6} m^2 sec^{-1}$ was chosen. A profile with smoother variations was chosen for experiment #9 so that the gradient of K_2 was different from the standard case. Actually, profile 9 is taken from Wiin-Nielsen and Sela (1971), Fig. 13. From relation (5.5.1) and the profile of K_2, as determined by these authors, it is apparent that a constant eddy exchange coefficient is not a good representation. The outcome of the experiments can only be considered in terms of vertical motion and energetics since the coefficients for potential vorticity were not modified.

The most important consequence of using a constant K_2, experiment #8 , were the effects in tropical regions where descent replaced upward motion. The cause of this drastic change is the large increase of the third term in (5.5.1) which overcame the diabatic heating contribution. The region covered by the polar front ascent shifted about 10^{o} to the south, narrowed and the maximum ascent reduced to one half. The energetics associated with the vertical motion remained almost invariable indicating a compensation between low and high latitudes effects: the Hadley cell becomes indirect, weak and

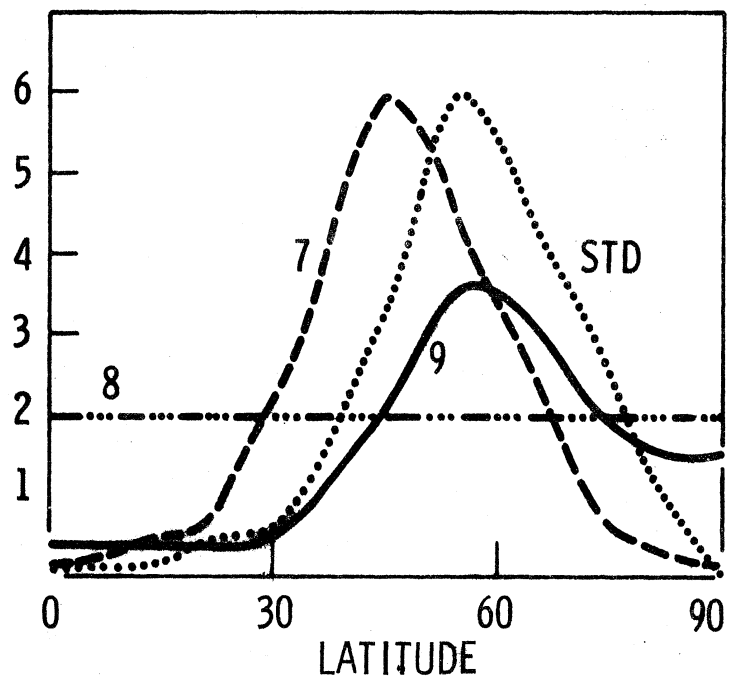

Figure 5.5.1 Profiles of exchange coefficient K_2 in experiments #7, #8 and #9 beside the profile in the standard simulations. Units: 10^6 m^2/sec.

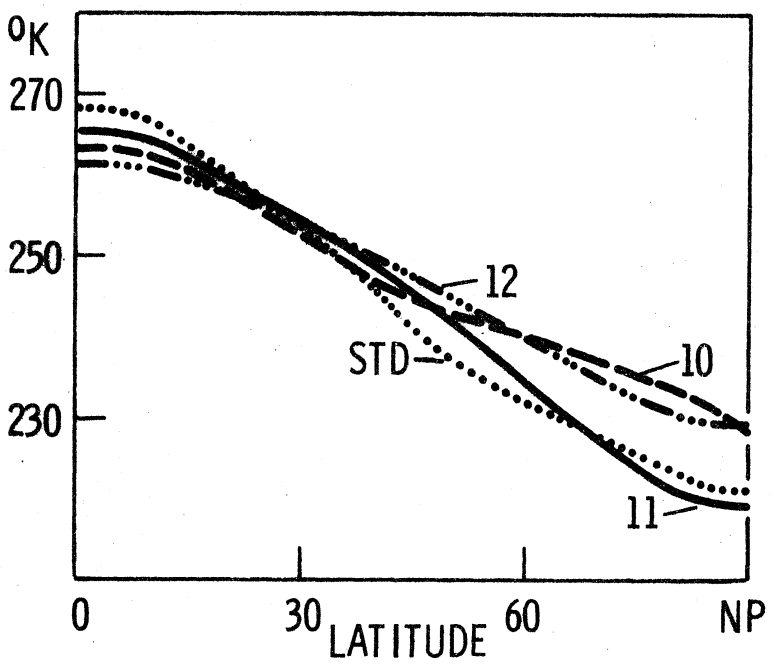

Figure 5.5.2 Temperature profile for January at 50 cb in experiments #10, #11 and #12 beside the profile in the standard simulation. Units : °K .

covers less area, while the polar cell gains intensity and becomes more extense. Conversions expressed in terms of K_2 remain very much the same probably because the value chosen is not far from the global mean.

Experiment #7, with K_2 values shifted towards the equator, showed that the vertical velocity profile has the middle latitude zero determined almost completely by the peak of K_2. This is due to the dominant role of the gradient of K_2 in equation (5.5.1) and suggests, because the observations do not support a large gradient of vertical motion around 50° of latitude, that the maximum of K_2 must be less sharp than used in the simulations. The shifting of the profile towards lower latitudes produces an increase in its mean value. This increase is felt in the energetics and the three conversions showed values notably larger, $C(A_z, K_z) = -2.2$, $C(A_z, A_E) = 4.1$ and $C(K_E, K_z) = 2.6$ watts/m^{-2}.

Experiment #9 used values of K_2 with a lower maximum and gentler variations. It presents also larger values in tropical and polar regions. The results show that this is a more realistic profile for middle latitudes where smoother transition and smaller values for the ascent are obtained. In low latitudes the larger K_2 tend to decrease the ascent by small contributions of the third term in (5.5.1). In high latitudes the diabatic term dominates. Since the mean value of K_2 is smaller in this experiment, the conversions associated with it decrease: $C(A_z, A_E) = 1.8$ watts m^{-2} and $C(K_E, K_z) = 0.3$ watts m^{-2}. Because of the weaker Ferrel cell we also obtain $C(A_z, K_z) = 0.3$ watts m^{-2}.

In conclusion the K_2 shape has strong influences on the vertical motion in middle latitudes and through its mean value

determines the energy conversions from the zonal to the eddy components.

5.5.2 Potential Vorticity Eddy Exchange Coefficients

The fact that potential vorticity is specified at two levels makes the discussion more cumbersome so we shall restrict it to the more outstanding features. K_1 and K_3 will be modified keeping K_2 invariable.

A first step in the study of the diagnostic eddy coefficients for potential vorticity is the evaluation of the importance of their functional dependence on the independent variables pressure and latitude. In this respect our efforts will be guided by some considerations of Green (1970) and the results obtained by Wiin-Nielsen and Sela (1971).

As far as the pressure dependence is concerned equation (2.3.5) is of some help. For the two-level model it originates relations (2.3.10) and (2.3.11) which can be written as

$$\int_{\pi/2}^{\pi/2} \cos^2\varphi \left\{ K_1 \frac{\partial}{a\partial\varphi} (f+\zeta_1) + (K_2-K_1)\, q^2 \frac{\partial \psi_{Tz}}{a\partial\varphi} \right\} d\varphi = 0 \qquad (5.5.2)$$

$$\int_{\pi/2}^{\pi/2} \cos^2\varphi \left\{ K_3 \frac{\partial}{a\partial\varphi} (f+\zeta_3) + (K_3-K_2)\, q^2 \frac{\partial \psi_{Tz}}{a\partial\varphi} \right\} d\varphi = 0 \qquad (5.5.3)$$

Since, except near the equator, $f >> \zeta_i$ for any level, they indicate that the eddy coefficients must, on the mean, decrease with height: $K_3 > K_2 > K_1$. In particular this must happen in the baroclinic

regions where the temperature gradient is large. By the same argument equation (2.3.15) indicates that the annual mean behavior associates westerlies with regions where $K_3 > K_1$. Equation (2.3.3) also suggests an exponential variation with the square value of the pressure wherever the meridional temperature variation is important and fairly constant with height. In terms of exchange efficiency, large values of the coefficients in the lower troposphere have been explained as a consequence of the presence of the critical level (Green, 1970).

The values calculated by Wiin-Nielsen and Sela (1971) are in agreement with these considerations as can be seen from Table 5.5.1. The difference (K_3-K_1) is large between 40 and 70 degrees of latitude.

Experiment #10 shows the consequences of using K_1 and K_3 equal to the diagnostic values for level 3 shown in Table 5.5.1. This modification represents a substantial increase of K_1. Under these conditions equation (5.5.2) cannot be satisfied. The model force the dependent variables trying to decrease the magnitude of the inconsistency. For instance, the meridional temperature gradient is decreased by $14^{o}K$ in January and $6^{o}K$ in July bringing the annual mean of available potential energy down to $2000\ kj/m^2$. The small value of the temperature gradient almost destroys the ascent in mid-latitudes forced by the contribution of the second term in equation (5.5.1). As a consequence, very large values of $C(A_z, K_z)$ are obtained ($1.4\ watts/m^2$). The zonal flow is dominated by easterlies, the trades reaching large magnitudes. This that can be interpreted as an effort to satisfy equations (5.5.2) and (5.5.3) which if added give

$$\int \cos^2\varphi \left\{ (K_1+K_3) \frac{\partial}{a\partial\varphi} (Q_1+Q_3) + (K_3-K_1) \frac{\partial}{a\partial\varphi} (Q_3-Q_1) \right\} d\varphi = 0 \qquad (5.5.4)$$

In this experiment the second term in the brackets vanishes so that $Q_1 + Q_3 = 2(f + \zeta_2)$ has to be negative, particularly in low latitudes, to satisfy the relation. The very large easterlies at 100 cb generate a high boundary layer dissipation (4.2 watts/m^2).

In conclusion, the eddy coefficients must decrease with height especially in mid-latitudes where westerlies are the observed prevailing winds near the surface.

The next experiment was related to the latitudinal dependence of the coefficients. K_1 and K_3 were taken independent of latitude, equal to 10^6 m^2/sec and 3×10^6 m^2/sec, respectively. In winter, the absence of the gradient of the exchange coefficient shifted the zonal wind maximum to 65°N. Likewise, the westerlies maximum moved to 65°N and 70°N at 75 and 100 cb respectively. The trade winds covered a broader latitude belt. In summer, easterlies covered the hemisphere at 100 and 75 cb. Temperatures changed comparatively little. The total pole-equator difference in January was reduced by 4°K at 50 cb. Polar easterlies seem to be related to small values of K_3 since they are not present at any time of the year. The larger average value of K_3, and to a lesser extent of K_1, increased the conversion $C(K_E, K_z)$.

The latitudinal variation of K_1 and K_3 seems thus to be of importance mainly in the zonal flow structure.

The next experiment was done with $K_1 = 2.0 \times 10^6 m^2 sec$ and K_3 as in Table 5.5. The results corroborate that a large value of K_1 generates easterlies, shifting the maximum west wind polewards. The thermal field was modified decreasing the pole-equator contrast by changes in the very low and high latitudes (Fig. 5.5.2).

The last experiment with K_1 was performed with the values shown in Table 5.5 shifted by 10 degrees of latitude equatorwards. Changes in the zonal flow included a larger area covered by easterlies and a weaker maximum (24 m sec^{-1} at 25 cb in January), probably caused by the global increase of K_1. The most important effect, nevertheless, was the displacement of the maximum wind from $45^{o}N$ to $25^{o}N$ at 25 cb and the tendency to generate a secondary maximum around $80^{o}N$. The cause of the second feature is related to the decrease of the gradient of K_1. Due to the decrease of zonal speed, kinetic energy is reduced by 50% and $C(K_E, K_z)$ diminished to 0.37 watts m^{-2}. We conclude that the location of the maximum zonal flow is determined to a large extent by the profile of K_1.

To determine the influence of the location of the maximum of K_3 another experiment was run with K_3 shifted by 10 degrees equatorwards. Its results showed that the influence of the K_3 profile is less drastic: it displaced the jet by 5 degrees only. It also increased the zonal flow maxima by about 14% at 25 cb, 25% at 75 cb and 45% at 100 cb. This differentiated addition gave a substantial improvement in the momentum balance. The thermal field remained almost unchanged, and the energetics showed only small changes.

Finally a last experiment was done with K_3 taken from the results of Wiin-Nielsen and Sela (1971), Fig. 12. This represents a sharper maximum and a lower global value. The only substantial change was in the zonal flow which diminished in intensity and wider areas were covered with easterlies.

5.6 AN IMPROVED CASE

To substantiate the influence of some of the modifications

just discussed an improved case was evaluated. For this case the following modifications were done:

i) The K_3 profile was shifted 15 degrees of latitude towards the equator so that its maximum was located at 40^{o}N.

ii) The K_2 profile was modified to adjust to that reported by Wiin-Nielsen and Sela (1971) and shown in Fig. 5.5.1 as experiment #9.

iii) The boundary layer friction was increased by making $\epsilon = 10^{-5}\,sec^{-1}$.

iv) The three eddy coefficients were modified in the neighborhood of the poles so as to make them approach unity at the pole itself.

The outcome of such an experiment is shown in Fig. 5.6.1 to 5.6.5 for those variables significantly affected by the aforementioned changes.

The thermal field was modified only in the proximities of the pole by the larger coefficients. The temperature at the pole in January increased by 4.5 ^{o}K at 50 cb and 100 cb; in July it increased by about 2^{o}K at both levels.

The zonal flow improved because of the shift of the K_3 profile and the stronger friction. The wind maximum moved to 40^{o}N in better agreement with observations, Fig. 5.6.1 , but still kept its latitude throughout the year. At the same time, the area covered by the easterlies decreased and some westerlies are present in summer in midlatitudes at 75 cb, Fig. 5.6.2. The velocity correction necessary to attain angular momentum balance, globally and over the year, decreased from 3.4 to 0.9 m/sec. The winter intensity of the zonal flow remained very much the same but it became stronger in summer.

The vertical velocity, shown in Fig. 5.6.3, presents modifications due to the change in K_2. The subtropical descent became

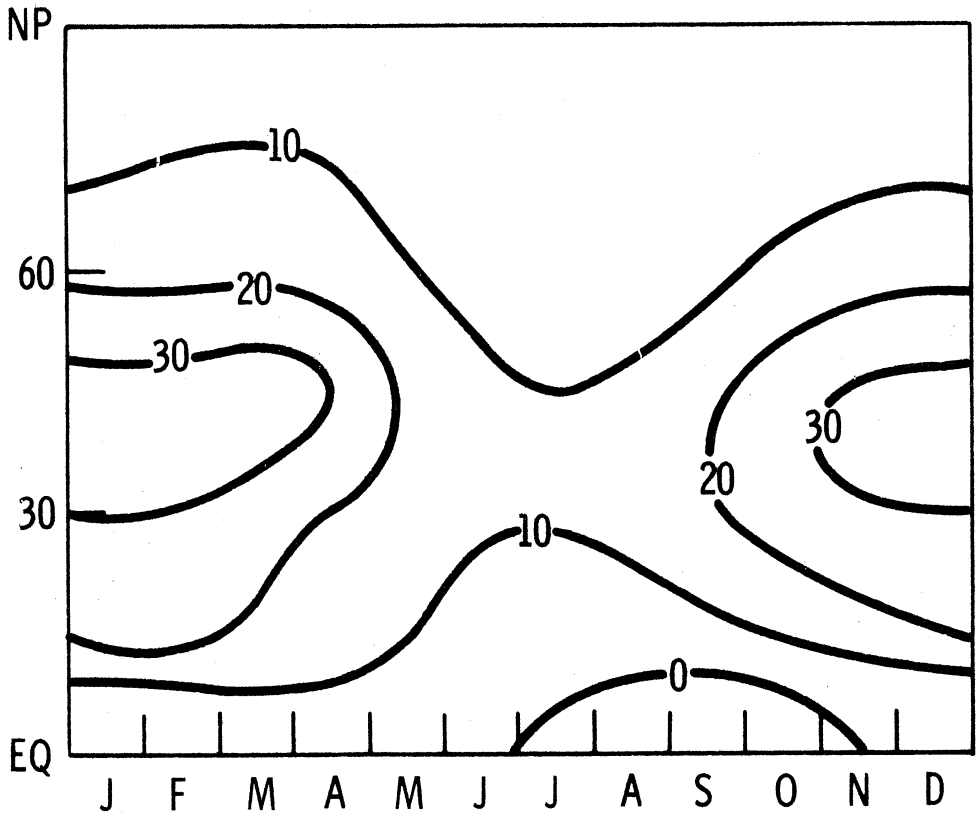

Figure 5.6.1 Same as Figure 4.1.5 for the improved case.

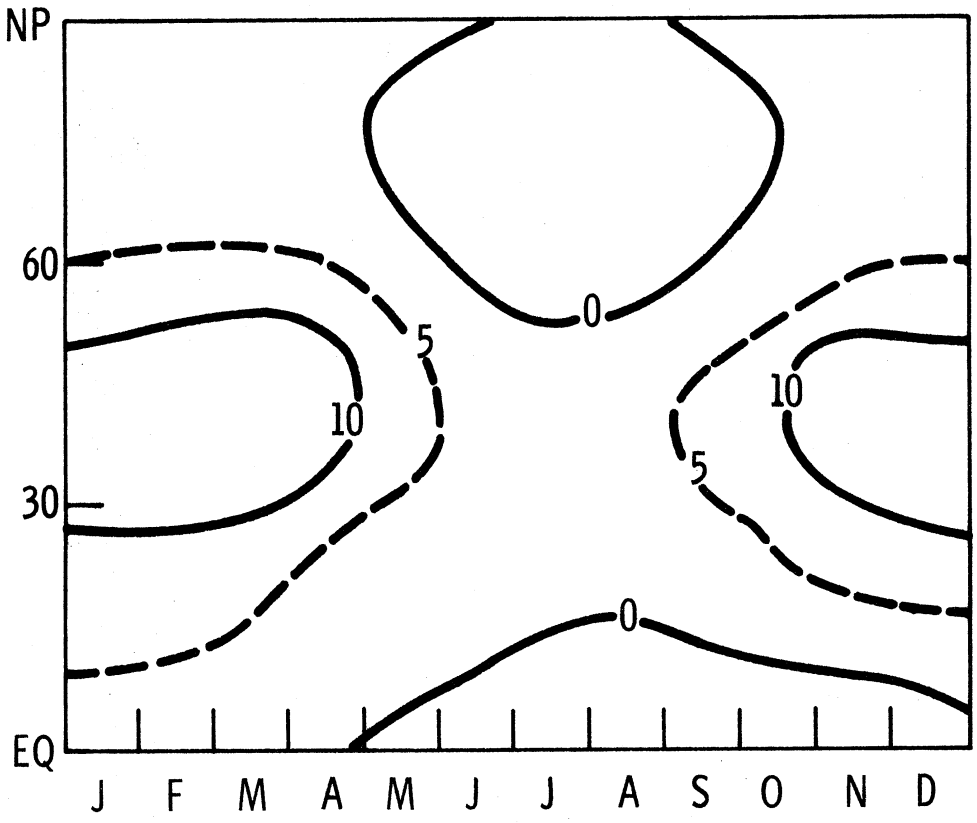

Figure 5.6.2 Same as Figure 4.1.6 for the improved case.

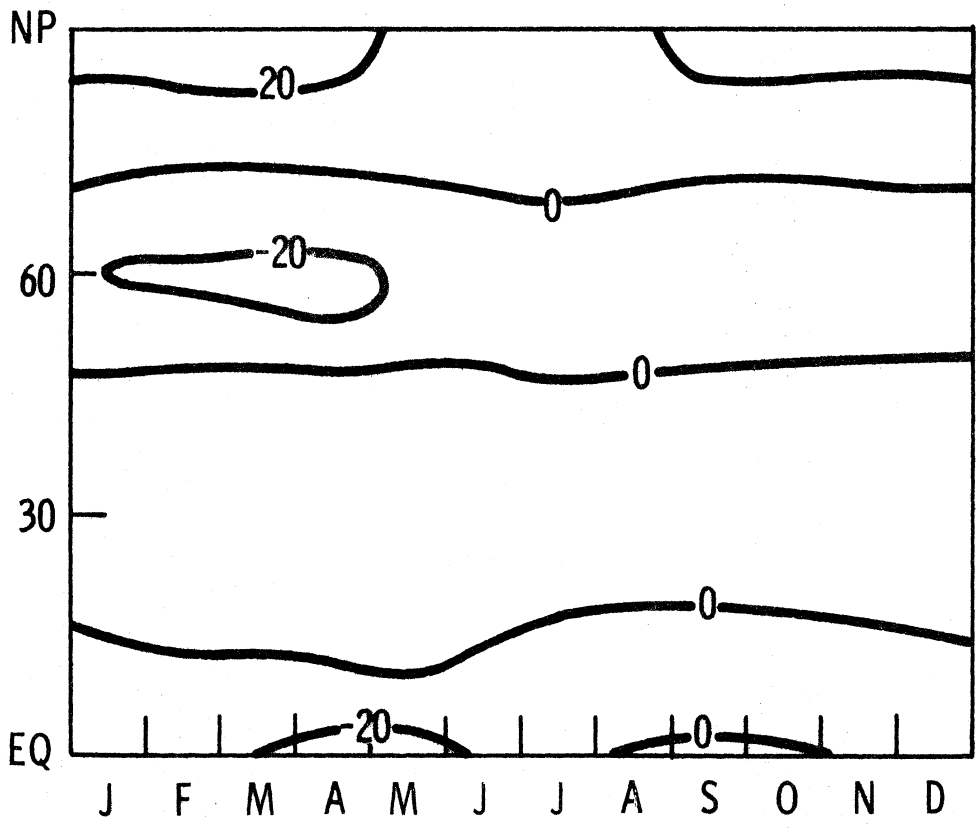

Figure 5.6.3 Same as Figure 4.1.7 for the improved case.

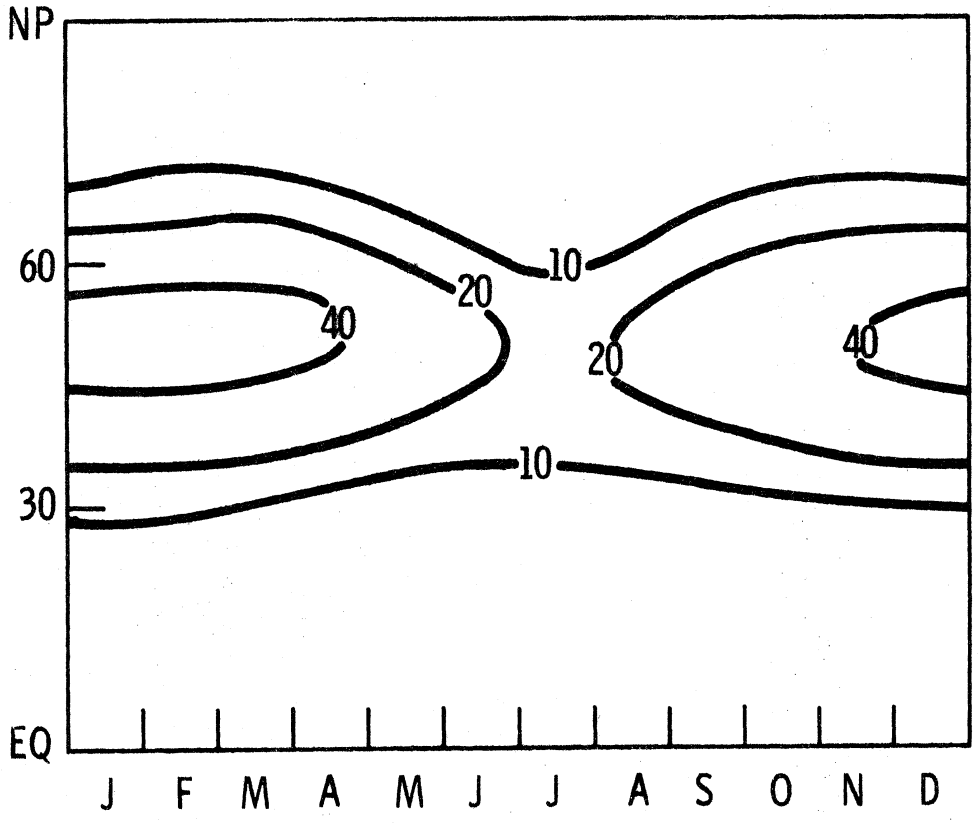

Figure 5.6.4 Same as Figure 4.1.8 for the improved case.

slower, a change not supported by observation. The ascent associated with the polar front narrowed and decreased in intensity improving agreement with observation. The strong meridional gradient around 50^{o}N disappeared. However, the seasonal fluctuation is still too weak. The change in K_2 introduced some modifications in the magnitude of the heat transport but not in its geographical configuration, Fig. 5.6.4.

The momentum transport kept its negative values at all latitudes during summer while it attained very large positive values in winter. After correcting for zero flux at the equator there was a maximum at 30^{o}N of about 83×10^{15} ton m^2/sec^2, for January about 2.7 times the observed annual mean (Lorenz, 1967).

The mean annual energy box diagram, Fig. 5.6.5 shows important differences with that of Fig. 4.1.13 but only some of them can be considered improvements. The low value of $C(A_z, A_E)$ can be explained by the lack of a tropical mean circulation but the large value of $C(A_z, K_z)$ indicates that the subtropical descent became too small.

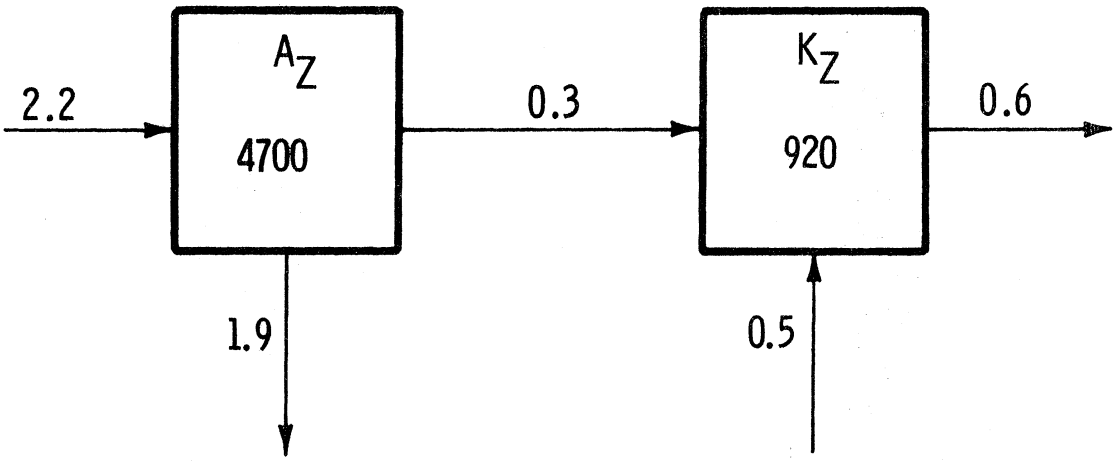

Figure 5.6.5 Same as Figure 4.1.13 for the improved case.

CHAPTER VI

EDDY EXCHANGE PROCESSES

We have seen in Chapters 4 and 5 that the diagnostic coefficients are able to model most of the important features of the axisymmetric circulation. However, the summer conditions in the zonal flow are not well reproduced and the wind maxima do not appear at the right latitude nor oscillate with the season. Some of these features are difficult to simulate in a quasi-geostrophic model because they depend heavily on the tropical circulation. But some improvement can be expected from a more realistic parameterization.

The macroscale transport processes are mean meridional circulations and eddy fluxes. The first process is essentially ageostrophic, and it is excluded from the governing equations of the model, but not from the diagnostic values of the exchange coefficients. The eddy fluxes can be separated into those due to the very long waves and those due to the synoptic scale perturbations. The importance of this division is related to the fact that a parameterization by means of eddy coefficients is not very suitable for the ultra-long waves so that their effects are misrepresented in the modelling. Nevertheless, the diagnostic eddy coefficients include their effects. Had the coefficients been determined as functions of the internal variables of the model the ultralong waves would be in error to a larger extent.

From observational studies it is apparent that all kinds of fluxes have important seasonal variations. Therefore, if the eddy exchange coefficients are representations of the eddy activity it seems natural to expect them to have a strong time dependence. When these

variations are determined by the current state of the simulation a feedback mechanism is included which increases the utility of the model for climate change studies.

In the past, the problem of eddy flux parameterization has been closely linked to results of baroclinic instability studies (Charney, 1959; Green, 1970; Kurihara, 1970; Saltzman and Vernekar, 1971; Stone, 1972 a and b). An exception is Smagorinsky (1964) who estimated the meridional transport of momentum through the lower boundary stress. This technique is useful under steady conditions only. Green (1970), using a mixing length approach, also elaborates on a finite amplitude justification which rests on the importance of the steering level and the validity of Eady's optimum slope for finite displacements. Both features are related to small amplitude studies, but stand a better chance to be correctly extrapolated into the finite amplitude domain than the phase speed and growth rate provided by a linear baroclinic theory.

We will suggest an extension of some results by Green (1970) and Stone (1972 b) which relate the eddy exchange coefficient for quasi-conservative quantities to the most relevant features of the mean zonal field. With this goal in mind we will digress to study the nature of the eddy exchange process and its applicability to the case in which we are interested.

6.1 NATURE OF THE EDDY EXCHANGE

Eddy exchanges are the macroconsequence of the excursions of a population of microelements. Every one of these possesses characteristics related to the environment where its migration started. They are modified, relatively slowly, to those of the new environment.

The idea of exchange coefficients rests on the assumption that a sufficiently stable mean field can be defined. Its macrovariations are due to the action of a large number of small eddies having a short lifetime with respect to the time scale of the changes in the macrofield. In other words, it is assumed that the frequency spectra of the transfer presents a gap. Being more specific, the transfer of mean zonal properties, which vary with a typical time scale of three months, must be performed, in the bulk by the transient waves and to a lesser extent by the stationary ones.

It is important to note that in contrast to the interpretation in the kinetic theory of gases our case is related to quantities that change slowly (quasi-conservative). There is not an exact conservation followed by a catastrophic exchange. For a quasi-conservative quantity one can distinguish between three time scales. First, the very slow variation of the mean zonal field, τ_f . At the other end, the fast displacement takes the microelement from its origin to a substantially different environment in a typical time τ_j . In between is the relaxation time, τ_r , required to smear out the differences between the element and its new surroundings. This is a measure of how conservative the process is. It is crucially important that the first time scale is very long compared with the other two. The displacement time must be shorter than the relaxation time. Hence we require

$$\tau_f >> \tau_r > \tau_j \qquad (6.1.1)$$

If the quantity in question is not conservative the second inequality is not satisfied and we cannot be certain that we are transferring anything at all.

The first requirement is satisfied when dealing with the seasonal variations, and the daily cycle has been smoothed out (then $\tau_f \sim$ 3 months). Even for the very long waves the criterion is fairly well fulfilled. The relaxation time is determined by diabatic and subgrid phenomena which, with the exception of latent heat release, have a time scale of several days. This is somewhat larger than the time required by a typical particle to travel an appreciable fraction of the earth radius. This criterion then is marginally satisfied especially in places where there exists important release of heat by condensation.

6.1.1 Exchange Properties of Eddies

If G represents a quasi-conservative property for isobaric motion, like potential vorticity, over periods of time τ such that $\tau_j < \tau < \tau_f$ it is possible to define a field $G(\lambda, \varphi, p)$ with a zonal mean $G_z(\varphi, p)$ Bretherton (1966 a) has shown that the flux of property G is given by

$$(G'v)_z = -\frac{\partial G_z}{a\partial\varphi}\bigg|_{\varphi=\varphi_0} a^2 \left[\frac{d}{dt}\left(\frac{1}{2}\eta^2\right)\right]_z \qquad (6.1.2)$$

defining the eddy coefficients as

$$K = a^2\left[\frac{d}{dt}\left(\frac{1}{2}\eta^2\right)\right]_z \qquad (6.1.3)$$

where η denotes the south-north displacement of a parcel starting from latitude φ_0 : $\eta = \varphi - \varphi_0$.

Relation (6.1.2) was first found by Taylor (1921) and is valid under the requirement

$$\frac{\left.\frac{\partial^2 G_z}{\partial \varphi^2}\right|_{\varphi=\varphi_0}}{2\left.\frac{\partial G_z}{\partial \varphi}\right|_{\varphi=\varphi_0}} \eta \ll 1 \qquad (6.1.4)$$

If G presents typical variations across distances of the order of the earth radius this inequality gives $\eta \ll$ 13000 km. It includes the cyclonic waves but is marginal with respect the ultra long waves.

Equation (6.1.3) allows a direct computation of the eddy exchange coefficient when some tracer provides knowledge of the meridional displacements η (using results from the GHOST Project, Wooldridge and Reiter (1970) have computed values for the Southern Hemisphere at 200 mb). This equation also points out the universal character of the coefficient for quasi-conservative properties that comply with condition (6.1.4). This relation for K does not depend on the random character of the eddy motion nor its small amplitude and is therefore valid for stationary or finite amplitude disturbances.

The small perturbation theory permits some additional interpretation. Identifying G with the potential vorticity Q, the transport in terms of zonal mean and its deviations is

$$(vQ')_z = -\left.\frac{\partial Q_z}{\partial \varphi}\right|_0 (v\eta)_z$$

Consider the mean zonal flow at an isobaric level

$$\frac{dx}{dt} = U(\varphi)$$

where $dx = a\cos\varphi d\lambda$, and a small perturbation superposed on it

$$\frac{dy}{dt} = v(\lambda,\varphi,t) = v(\varphi)\cos\alpha(x-c_o t)$$

where $dy = a\,d\varphi$. Let us compute the trajectory of a particle that starts at $y(0) = y_o$, $x(o) = 0$. To the lowest order $x = U(\varphi_o)$ and

$$v = \frac{dy}{dt} = v(\varphi_o)\cos\left[\alpha\{U(\varphi_o) - c_o\}t\right] ;$$

hence

$$y = y_o + \frac{v_o}{\alpha(U_o - c_o)}\sin\left[\alpha(U_o - c_o)t\right]$$

where $U_o = U(\varphi_o)$ and $v_o = v(\varphi_o)$. Then

$$a\eta = y - y_o = \frac{v_o}{\alpha(U_o - c_o)}\sin\left[\alpha(U_o - c_o)t\right]$$

Therefore

$$a(v\eta)_z = v_o^2\left[\frac{\sin\left\{2\alpha\frac{U_o - c_o}{U_o}x\right\}}{2\alpha(U_o - c_o)}\right]_z \qquad (6.1.5)$$

In general c_o is a complex eigenvalue that varies with latitude independently of U_o . If c_o is real the zonal mean of the bracket vanishes, since the inner quantity is harmonic in x (or λ). Therefore a neutral wave is unable to support exchange unless $U_o = c_o$. Due to the fact that in most cases this condition will be satisfied locally this mechanism will be operative in narrow latitude zones where

$$a(v\eta)_z = a\left[\frac{d}{dt}\left(\frac{1}{2}\eta^2\right)\right]_z = v_o^2\, t$$

so that a parcel is caught in the wave and taken away from its original latitude with the meridional displacement η increasing monotonically with time.

If c_o is complex the bracket is not harmonic anymore and does not vanish when averaged. An unstable wave always support transfer, but in a more effective way when $c_o = U_o$.

The importance of the critical layer (where the basic flow of velocity equals the phase velocity of the wave) has been stressed by Dickinson (1969) who for an ensemble of statistically stationary, small amplitude, geostrophic waves, in adiabatic reversible flow with no sources of potential vorticity pointed to the critical layer mechanism as the only one capable of forcing a zonal flow by making the eddies transport potential vorticity. In this case the mean value of the rate of particle dispersion can be interpreted in terms of the power spectrum $\Gamma_v(\nu)$ of the meridional eddy motion at the critical frequency, i. e.

$$\left\langle\left[\frac{d}{dt}\left(\frac{1}{2}\eta^2\right)\right]_z\right\rangle = \frac{1}{2a^2}\,\Gamma_v(\nu = \alpha U_o)$$

where the wedge brackets indicate a time mean and

$$\left\langle (v^2)_z \right\rangle = \frac{1}{2\pi}\int_{-\infty}^{\infty} \Gamma_v(\nu)\, d\nu$$

Diabatic effects and other sources of potential vorticity represent additional forcing mechanisms of a zonal flow perturbed by small amplitude, statistically stationary, geostrophic waves.

Finally we still have the finite amplitude waves that in the neutral and unstable cases will support transport processes. Relation (6. 1. 3) indicates that in all likelihood these waves are very effective agents. However, very little is known about them. If we ignore the ultra-long stationary waves and accept that finite amplitude eddies originate from small unstable perturbations, we have at our disposal the results from baroclinic instability theory that at least shed some light on the processes that generates them.

Summarizing we have identified three possible causes for the eddy transfer: a critical layer mechanism, small amplitude unstable waves and finite amplitude waves. It is not easy to asses their relative importance. As a working hypothesis we will assume that baroclinic unstable waves are the responsible agents of transport. Because unstable waves in mature stages tend to present a smaller growth rate than small amplitude waves and because nonlinear effects eventually stop the development, information gained through linear theories has to be used with care. We will only try to determine from baroclinic instability studies the most relevant features of the mean zonal state that favor the generation of waves and its growth.

6. 1. 2 Generation of Eddies: Baroclinic Instability

The fundamental cause for the existence of the large scale eddies is the differential solar heating and its immediate consequence: the meridional temperature gradient. The birth and initial growth of the disturbances embedded in such an environment has been studied extensively. However, in most of the cases the problem has been simplified to such an extent that although qualitative conclusions may still be valid, the magnitude of the results is subject to considerable

error. Very frequently the assumptions include: hydrostatic, quasi-geostrophic, adiabatic and frictionless motion, the beta plane approximation, and a basic flow independent of the meridional coordinate with only small deviations from it permitted. Some of these simplifying hypotheses rest on observations and therefore do not detract from the applicability of the conclusions. Others have been introduced to overcome mathematical difficulties and their implications have to be considered with care. Such is the case with the smallness of deviations, introduced to gain linearity, beta plane approximation and basic flow independence of meridional coordinate, which makes the differential equations separable. The change from the beta plane approximation to spherical geometry has several consequences. First the stabilizing action of the Rossby parameter will change with latitude, but the effect of such a change is probably small because the order of magnitude of β remains invariable and our main concern are the most unstable waves and not the marginal cases. The spherical geometry has little effect on the equations of motion adding only small metric terms, but the differential operators have to be modified. In general we can expect little modification by removing this approximation.

The smallness of deviations from the basic state is the key assumption that relieves the nonlinearity of the mathematical problem. At the same time, it limits the validity of results to those cases where waves have amplitudes so small that they do not modify the basic flow substantially nor do they interact among themselves. The most one can obtain from linear baroclinic theory is an initial growth rate and the identification of those features of the basic flow which are most important for eddy motion generation.

A basic flow independent of the meridional coordinate gives results quantitatively different from those where both vertical and meridional shear are included. Pedlosky (1964 b) has proved that omission of horizontal shear overestimates the growth rate and phase speed of disturbances, but does not change the minimum vertical wind shear necessary for instability. It changes also the spectrum of unstable waves by a shift towards longer waves. The most important difference for our purposes is that when only vertical shear is considered the parameters determining instability are the thermal wind, the β effect and static stability, (see for instance Miles, 1964); when only horizontal shear is included the important feature is the meridional variation of the absolute vorticity (Kuo 1949, Fjørtoft 1951); but if both effects are considered, the meridional gradient of potential vorticity becomes the determining factor (Charney and Stern (1962), Pedlosky 1964 a, Bretherton 1966 a).

The most relevant results for our particular case are those of Pedlosky (1964 a and b) who considers an incompressible two-level model in a beta channel of width 2ℓ. His results have been adapted to our model in Appendix III. He establishes a necessary condition for instability, equation (A. III. 6), and sets an upper bound to the growth rate of the small eddies, equation (A. III. 11), both in terms of the meridional gradients of potential vorticity of the basic flow. He also concludes that eddies that behave like the atmospheric ones, i. e., eddies that converts zonal potential energy into eddy kinetic and then into zonal kinetic energy, occur in a basic flow with no extrema of potential vorticity in the upper level. This result, in the light of previous conclusions, implies a lower level with potential vorticity

gradient of opposite sign to that in the upper level if the necessary condition for instability is to be satisfied. This, in turn, can be interpreted in terms of the thermal wind, which has to be large enough to make such gradient in the lower layer negative.

The upper bound on the growth rate is proportional to the maximum value of the product $u_i \frac{\partial Q_i}{a \partial \varphi}$. Since potential vorticity is very uniform for the kind of geostrophic flow under considerations (Phillips, 1963) this maximum is determined by the sign of the derivative and the wind profile, so that, with some accuracy, we can state that $u_1 \frac{\partial Q_1}{a \partial \varphi}$ evaluated near the jet stream will determine the growth rate.

6.2 RECENT MODELS OF THE HEAT TRANSPORT

Lately two parameterizations of the heat transport have been published by Green (1970) and Stone (1972 b). The first used perturbation solutions to obtain a normalized vertical profile of the exchange coefficient. The magnitude of the coefficient was obtained for the vertically integrated value by assuming that one half of the typical zonal available potential energy is converted into eddy kinetic energy, that the meridional and zonal eddy kinetic energies are equal, and that the correlation between the eddy meridional velocity and the eddy entropy when normalized to the product of the root mean square value of these two quantities is constant. He obtains a relation

$$\langle K \rangle \left\langle \frac{\partial \theta}{\partial y} \right\rangle \propto \left(\frac{1}{\theta} \frac{\partial \theta}{\partial z} \right)_s^{-\frac{1}{2}} (\Delta\theta)^2 \qquad (6.2.1)$$

where the wedge brackets represents a zonal-time-pressure mean, the subscript s a standard value and $\Delta\theta$ the typical tropospheric difference of potential temperature θ across the baroclinic region.

Stone (1972 b) used Eady's (1949) model in his analysis. This model assumes a Boussinesq, adiabatic, inviscid and hydrostatic fluid located between two horizontal planes rotating with an angular speed f/2. For the perturbation analysis a basic state consisting of a zonal flow with constant vertical shear and no horizontal variations is considered. Stone (1972 b) expands the dependent variables in powers of a common amplitude and then considers the first and second order solutions which are necessary to evaluate the eddy fluxes. The amplitude of these fluxes cannot be determined from the linearized theory where it is assumed to be small but increasing exponentially with time. To assign a magnitude it is assumed that the basic state can be taken as the mean state of the real atmosphere, thus making identical the constant Richardson number of the Eady's model with that obtained from mean values of the temperature field in the meridional plane. The next assumption is that the perturbations attain the same vertically integrated amplitude as the basic flow. This condition determines the amplitudes and provides, for a large Richardson number, the relation:

$$\overline{v\theta} \propto f^{-2} \left(\frac{1}{\theta} \left\langle \frac{\partial \theta}{\partial z} \right\rangle \right)^{1/2} \left(\left\langle \frac{\partial \theta}{\partial y} \right\rangle \right)^2 \qquad (6.2.2)$$

where the wedge brackets represent now the mean value on the meridional plane and the bar a time-zonal mean.

Equations (6. 2. 1) and (6. 2. 2) agree in the linear dependence of the eddy coefficient on the meridional gradient of temperature but differ with respect to the static stability. Because the static stability shows very small seasonal changes it is difficult to decide which dependence is better. Using a relation similar to (6. 2. 2) for the vertical transfer of heat Stone (1973 b) has concluded that assuming a constant value for the static stability is not a bad approximation when studying climatic changes. Therefore, the difference between (6. 2. 1) and (6. 2. 2) is of little consequence.

6.3 A PARAMETERIZATION FOR MOMENTUM TRANSPORT

In previous sections we have presented some arguments and results which suggest a way to parameterize the meridional eddy flux of momentum in an indirect fashion.

The first conclusion is that it is easier to model the eddy transfer of a quantity the more conservative it is. In spite of the fact that this is a direct consequence of the nature of the mechanism of transfer it is only in Green's (1970) paper that the use of potential vorticity is indicated as a way to parameterize the momentum transport.

A second idea derived from Bretherton's (1966 a) formulae for the eddy coefficient, is that any conservative quantity provides the same information if it satisfies the relation (6. 1. 4). This restriction indicates that some difficulty can be found in the representation of the ultra-long waves.

A third and very suggestive piece of information comes from the baroclinic instability theory: the decisive parameter, when both vertical and horizontal shear are included in the basic state, is the meridional gradient of potential vorticity. Thus the necessary condition

for instability is a generalization of the criteria for barotropic and baroclinic instabilities, see Appendix III.

Finally we have the results of Green (1970) and Stone (1972 b) for the heat flux. A conclusion can be drawn from them due to the universal character of the eddy coefficient. Because the transfer coefficient is the same for any quasi-conservative quantity the heat transport formula obtained by the aforementioned authors provide an estimate for the transfer coefficient of potential vorticity by cyclonic waves, and can be used in the parameterizations of momentum transport. Their results also suggest a more general parameterization. The eddy coefficient expressions (6. 2. 1) and (6. 2. 2) show that the main dependence is on the thermal wind in terms of which the stability criterion for baroclinic waves is expressed. Following the generalizations obtained by Pedlosky (1964 a) for the instability criterion it seems natural to think that the result of Stone (1972 b), who ignored the effect of variations of the Coriolis parameter, can be extended to make the eddy coefficient proportional to the meridional gradient of potential vorticity. Such a refinement may not be important in winter when most of the contribution to the gradient come from baroclinic effects but should become important in summer as the barotropic effects get at least as important as the baroclinic.

Let us then postulate as a more suitable parameterization for the potential vorticity exchange coefficients an expression like

$$K(\varphi, t) = f(\varphi, t) \int_{\varphi_1}^{\varphi_2} \alpha \left| \frac{\partial Q_z}{\partial \varphi} \right| \, d\varphi \qquad (6.3.1)$$

where the interval (φ_1 , φ_2) encompasses the bulk of the baroclinic region, f (φ) is a shape factor and α a proportionality constant to be fixed by numerical experimentation or from observational studies.

The shape factor f(φ) was introduced because the evidence provided by Sela and Wiin-Nielsen (1971) indicates that the maximum of the exchange coefficients is much sharper than those of the mean zonal variables. This selectivity has been attributed to the critical layer mechanism (Green, 1970). Within the baroclinic region f (φ) is normalized to integrate to one, but corrections to the coefficients are applied in the tropical regions, where potential vorticities are not conservative quantities, and the very high latitudes, where the zonal mean losses statistical meaning.

Considering the two-level model we are going to define one exchange coefficient for each level:

$$K_i(\varphi, t) = f(\varphi, t) \int_{\varphi_1}^{\varphi_2} \alpha_i \left| \frac{\partial Q_{iz}(\varphi, t)}{\partial \varphi} \right| d\varphi \qquad i = 1, 3 \qquad (6.3.2)$$

The exchange coefficient K_2 will be expressed as a weighted mean of K_1 and K_3:

$$K_2(\varphi, t) = f(\varphi, t) \int_{\varphi_2}^{\varphi_1} \left\{ 0.3\, \alpha_1 \left| \frac{\partial Q_{iz}}{\partial \varphi} \right| + 0.7\, \alpha_3 \left| \frac{\partial Q_{3z}}{\partial \varphi} \right| \right\} d\varphi$$

The bias towards level 3 is justified by the evaluations of Wiin-Nielsen and Sela (loc. cit.) and by the vertical asymmetry due to the location of the steering level (Green, 1970).

The shape factor $f(\varphi)$ is taken at every time step from a Beta distribution, $\beta(x_i/n, r)$, where the parameter n was fixed according to the observed profiles of K_1 and K_3, and r is evaluated from the first moment of the distribution of $\alpha_1 \left| \partial Q_{1z}/\partial \varphi \right|$ with respect to the pole and considering contributions from 30 to 90 degrees of latitude. This last feature allows for changes in the location of the maximum. The independent variable in the Beta distribution is defined by $x_i = \frac{i - 6}{13}$ so that $0 \leq x_i \leq 1$.

In the tropical regions, where we have no quasi-conservative quantity evaluated from the model, we used constant values for the exchange coefficients very much like those of Table 5.5.1. In high latitudes a linearly decreasing profile was used. A detailed description of these modification as well as numerical values for all constants is included in Appendix IV.

In summary, the time dependent coefficients change in magnitude according to the mean gradient of potential vorticity in the baroclinic region and the geographical location of their maxima varies to a lesser extent because of the determination of the parameter r at each time step. This parameterization was introduced in the model described in Chapter 2 and a two year simulation was run for the Northern Hemisphere.

6.4 RESULTS OF A NONLINEAR SIMULATION

The annual variation of the exchange coefficients is depicted in Fig. 6.4.1. The profiles shown are instantaneous values corresponding to the 15^{th} day of each month. It is seen that the seasonal variation of the three coefficients is quite important reaching very low values in summertime. In particular K_3 becomes so small that

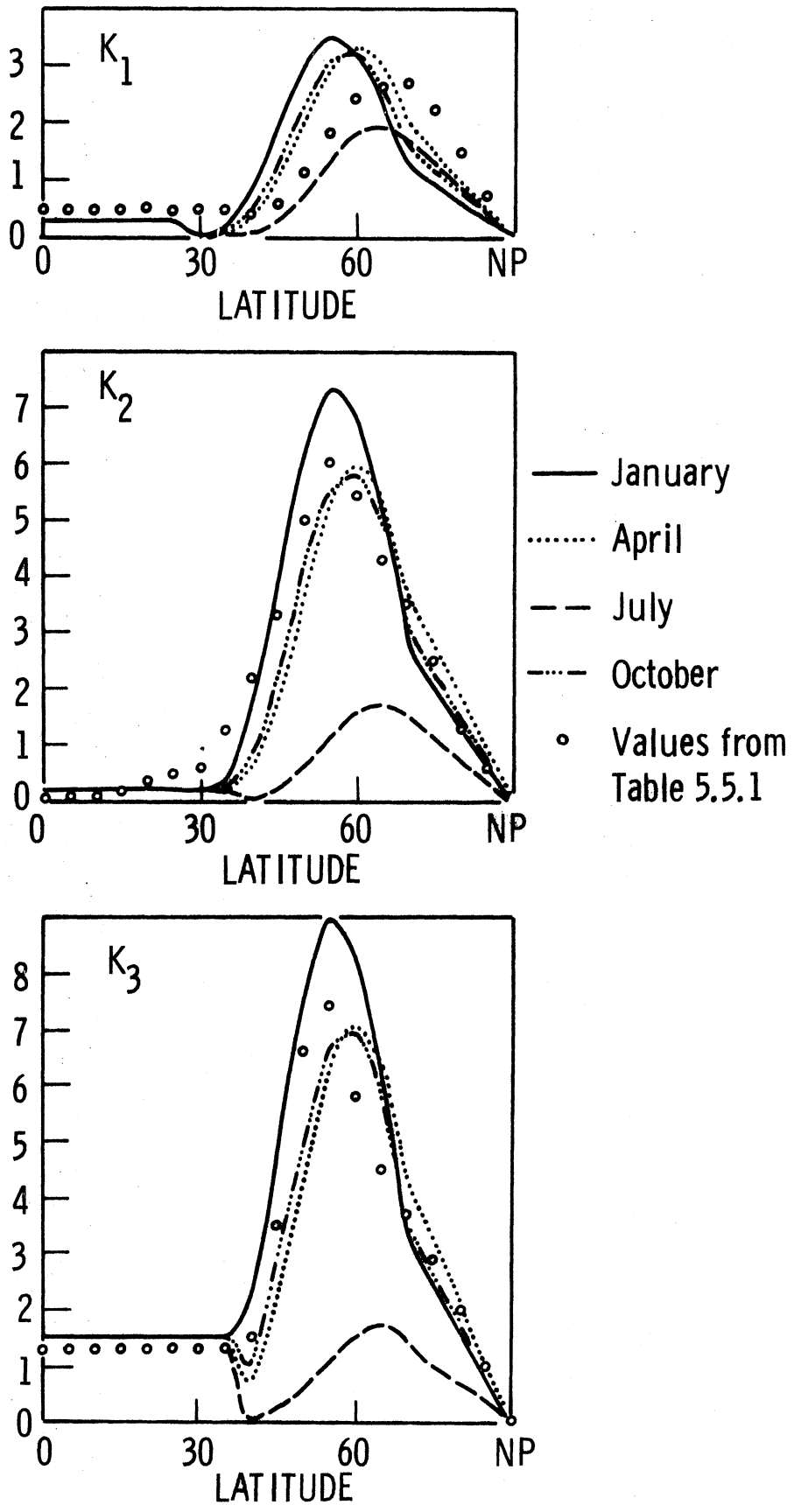

Figure 6.4.1 Seasonal variations of eddy coefficients at 25 cb, K_1, 50 cb, K_2, and 75 cb, K_3, in the nonlinear simulation of the Northern hemisphere. Units : 10^6 m^2/sec.

a substantial discontinuity is produced in the transition from the tropical fixed values. Even more important, the normal size sequence is altered and $K_3 < K_2 < K_1$ for a short period of time (the month of July). On the other hand the peak of the distribution shows a seasonal change of location: a ten-degrees migration poleward in summer. It is evident from the graphs that the very low values have a short lifetime and that during more than six months the peak is quite high . Comparing with the diagnostic values shown in Table (5. 5. 1) these are very similar to winter magnitudes for K_2 and K_3 but for K_1 the maximum is shifted polewards by about 10 degrees and the magnitudes are about an annual mean value.

The thermal field, Figs. (6. 4. 2) and (6. 4. 3), shows little change with respect to that obtained using time independent exchange coefficients at 50 cb. The seasonal amplitude in high latitudes is smaller and there is a concentration of baroclinicity in winter between 20 and 45 degrees of latitude. The latitudinal gradients for the extreme months, Figs. (6. 4. 4) and (6. 4. 5) show some improvement at both levels with a better simulation in summer and near the surface level.

The zonal flow at 25 cb is shown in Fig. (6. 4. 6) which represents a substantial improvement over that obtained with the diagnostic coefficients. In January the maximum zonal wind is now correctly located (at 30^{o}N) and its magnitude is slightly overestimated. There is also a five degree migration of the maximum towards higher latitudes in summer which is reasonable for a model in which the tropical circulation is underestimated. In winter a secondary maximum appeared near 75^{o}N which is not present in tropospheric observations of the Northern Hemisphere. In summer maxima is correctly estimated in magnitude.

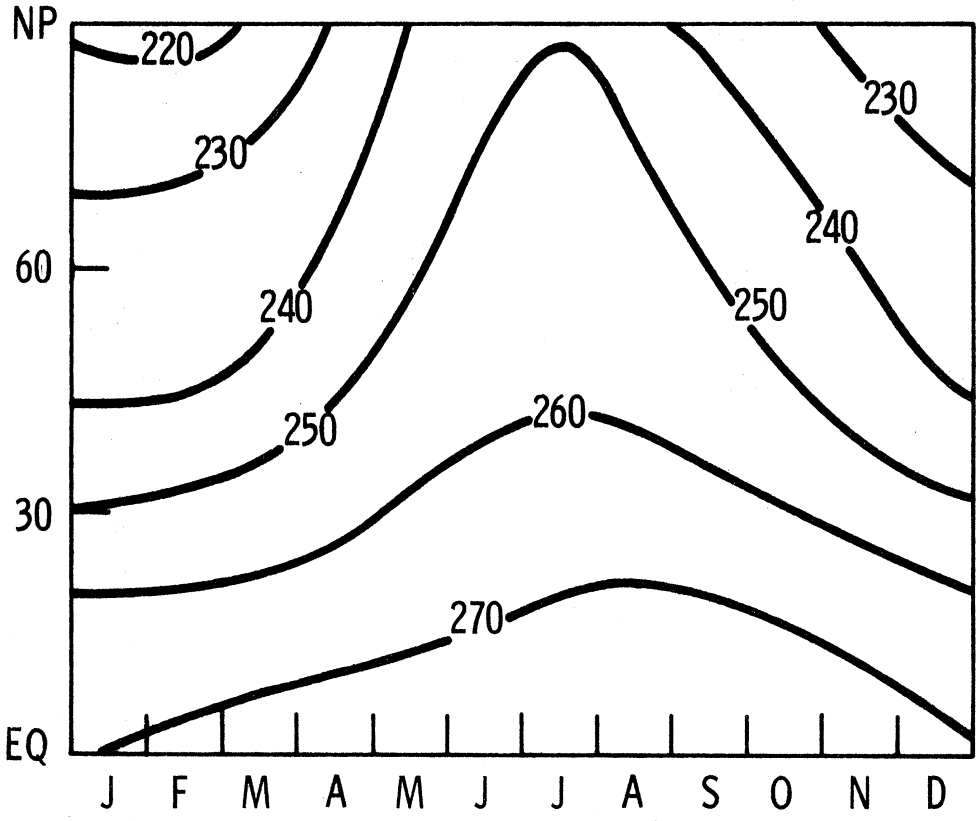

Figure 6.4.2 Same as Figure 4.1.1 for nonlinear simulation.

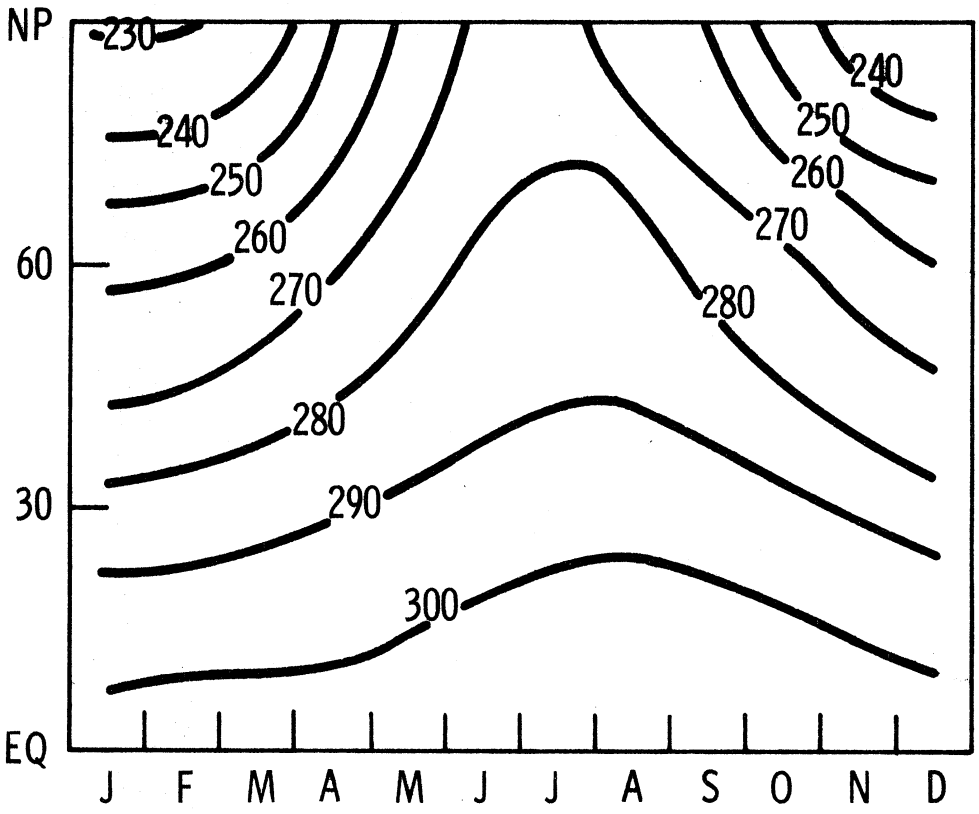

Figure 6.4.3 Same as Figure 4.1.2 for nonlinear simulation.

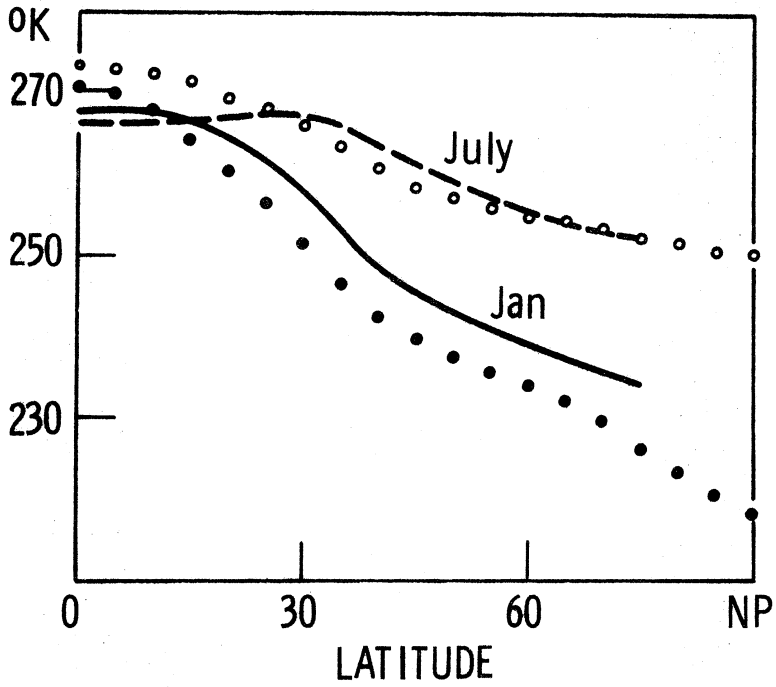

Figure 6.4.4 Same as Figure 4.1.3 for nonlinear simulation.

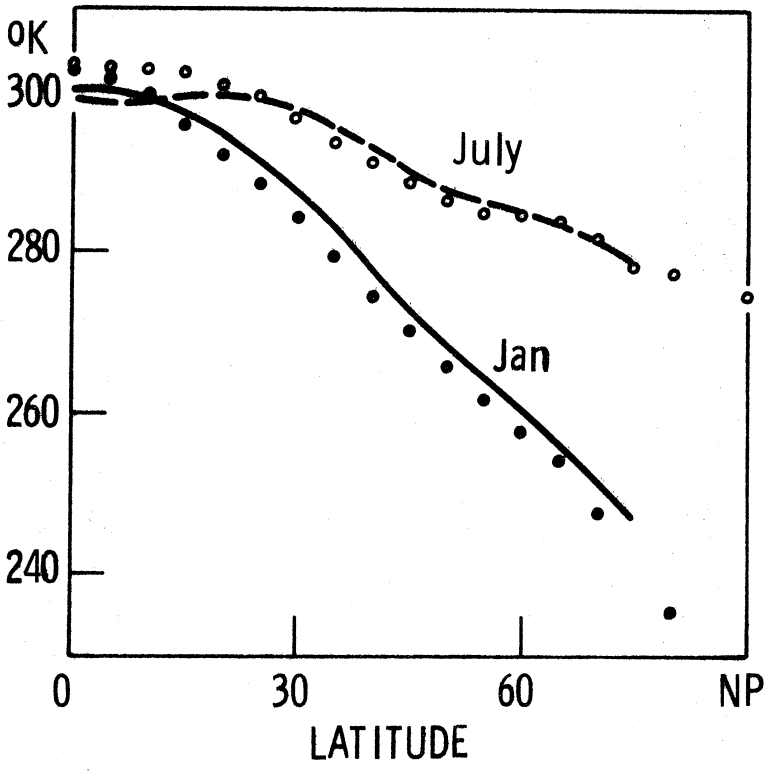

Figure 6.4.5 Same as Figure 4.1.4 for nonlinear simulation.

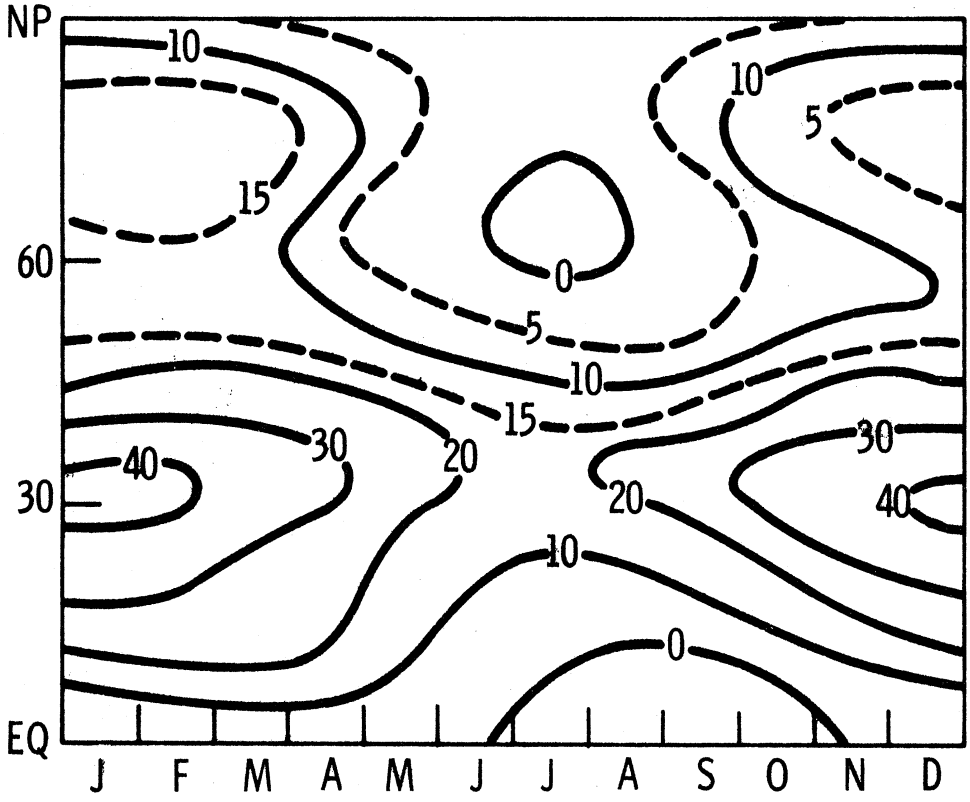

Figure 6.4.6 Same as Figure 4.1.5 for nonlinear simulation. Velocity correction 1.2 m/sec.

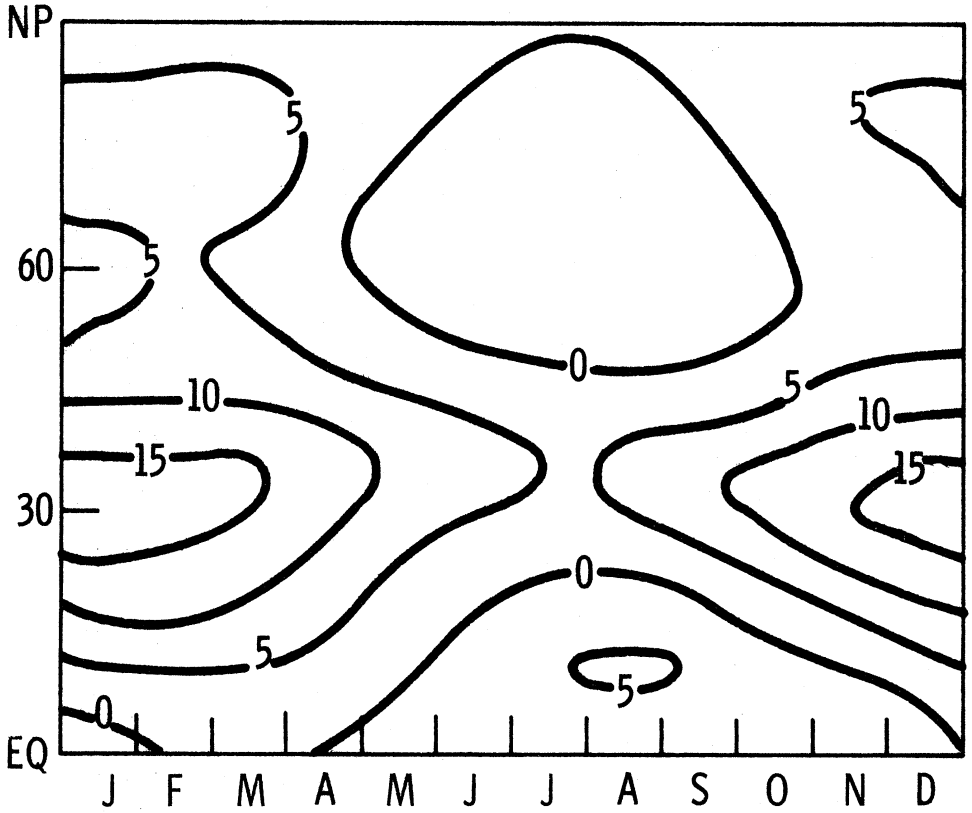

Figure 6.4.7 Same as Figure 4.1.6 for nonlinear simulation. Velocity correction 1.2 m/sec.

The flow at 75 cb, Fig. (6. 4. 7), appears too high in winter but in summer is correctly simulated. There has been improvement also in the momentum balance since there are some westerlies in July between 20^{o}N and 50^{o}N.

The field of vertical motion, Fig. (6. 4. 8), is now subject to stronger seasonal changes of intensity and structure. The three cell scheme is well defined in the winter time. In summer there are also three cells but the polar front ascent has been replaced by a narrow region about 45^{o} with weak vertical motion. In the transition months there exist three regions of ascent although the important ones are still those associated with the polar front and the tropical convection. This irregular behaviour of the vertical motion is present in the observations reported by Oort and Rasmusson (1971).

The heat transport shown in Fig. (6. 4. 9) presents strong seasonal fluctuations mainly due to a lower value in the summer months, although the winter maximum is also smaller than in the linear simulations. Considering the transient eddies transport only, the winter and summer maximum are about twice the observed values, indicating that the value of K_2 is too large, but that seasonal fluctuations in magnitude are simulated fairly well. A comparison with results obtained using diagnostic values of the exchange coefficients is not straight forward because they include the effects of the ultra-long quasi-stationary waves, while the time dependent formulation might not include their effects.

The angular momentum transport shows the effects of the global imbalance, although there is improvement. For instance the zonal velocity correction necessary to attain a zero transfer of angular

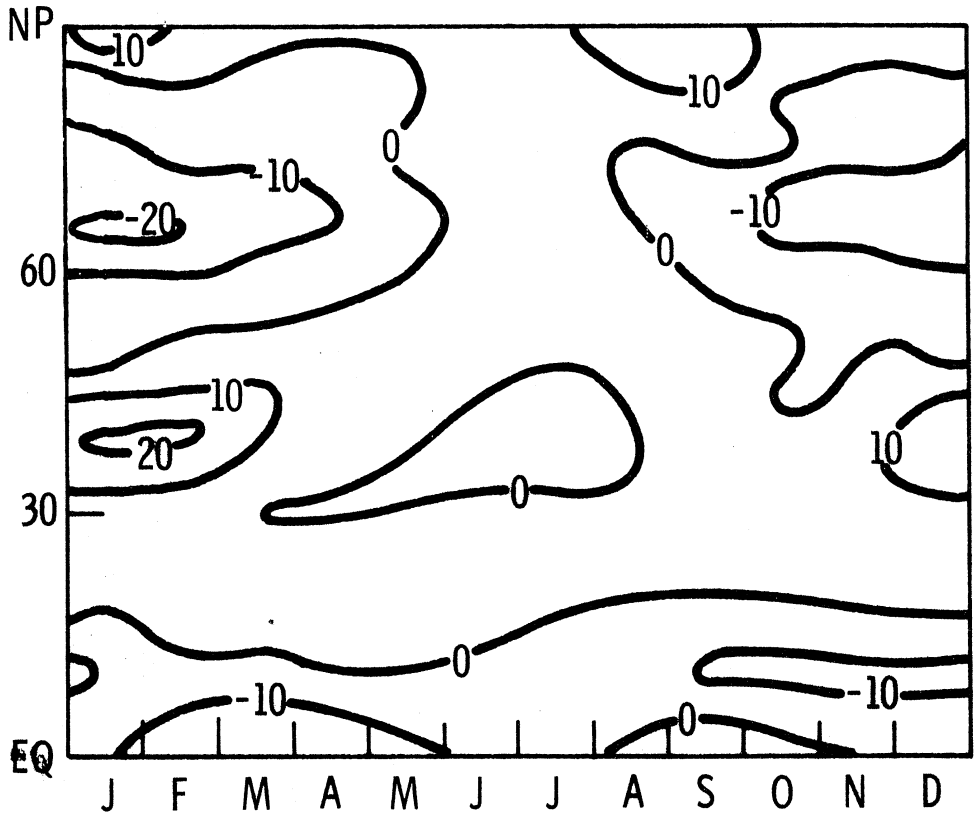

Figure 6.4.8 Same as Figure 4.1.7 for nonlinear simulation.

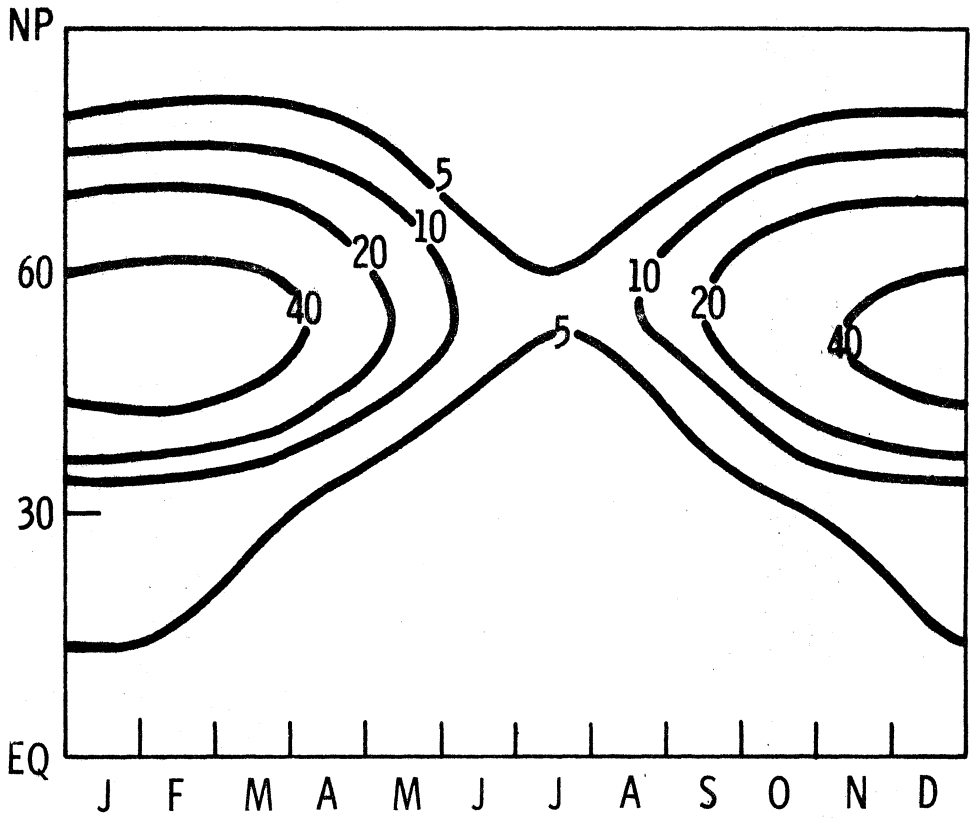

Figure 6.4.9 Same as Figure 4.1.8 for nonlinear simulation.

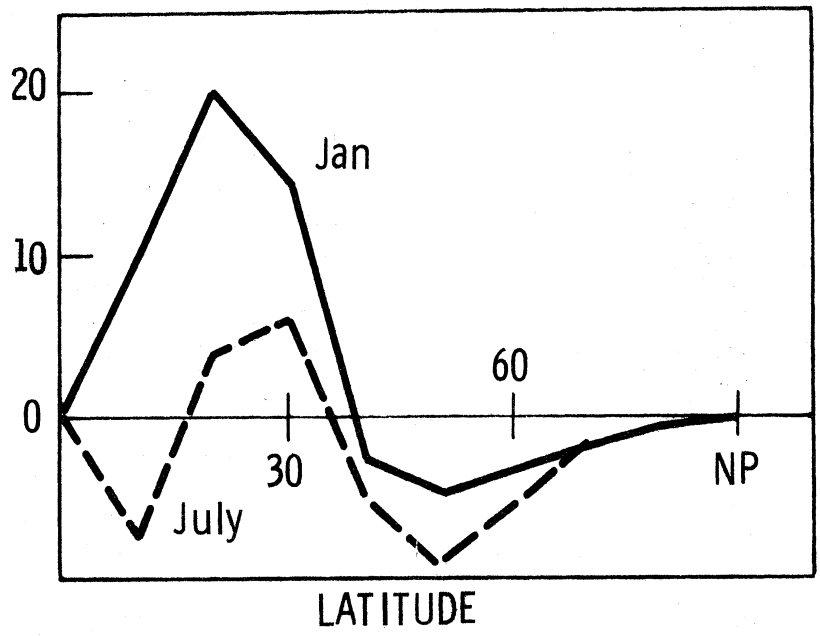

Figure 6.4.10 Same as Figure 4.2.9 for non linear simulation.

momentum between the earth and the atmosphere is 1.2 m/sec. Fig. (6.4.10) shows schematically the variations of the poleward angular momentum transport, corrected for zero crossequator flux, for the months of January and July.

The energetic evolution of the model is presented in Figs. (6.4.11) to (6.4.13). The seasonal fluctuations of zonal available potential and kinetic energies is only slightly different from their counterparts of the linear model. The time lag between generation and dissipation is about 24 days and their time evolution is again very similar to former results.

The conversions show some change. First $C(A_z, A_E)$ which is proportional to the heat transport presents values which are about one half of the corresponding results of the linear simulation. The difference between the observed value of 3 watts/m^2 and the simulation is due to the absence of a mean meridional circulation and the exclusion of very long waves to some extent. The conversion between the eddy and zonal kinetic energies shows a small positive value except in the fall when a barotropic behaviour of the eddies dominates. The small value of $C(K_E, K_z)$ can be blamed on the misrepresentation of the ultra-long waves which make up for a large fraction of the momentum transport in winter (Wiin-Nielsen et. al., 1963). The conversion between the two zonal energies is small and almost invariable throughout the year. The large positive value obtained is due to the vertical velocity field which in summer gives a large correlation with temperature.

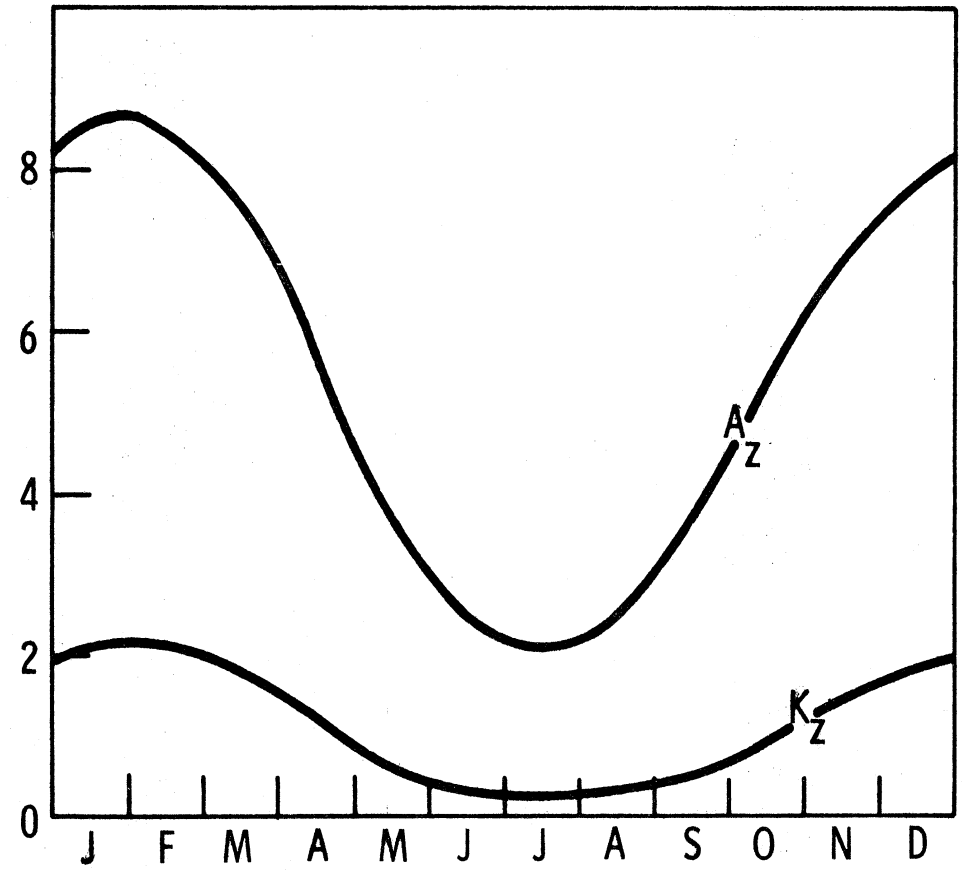

Figure 6.4.11 Same as Figure 4.1.10 for nonlinear simulation.

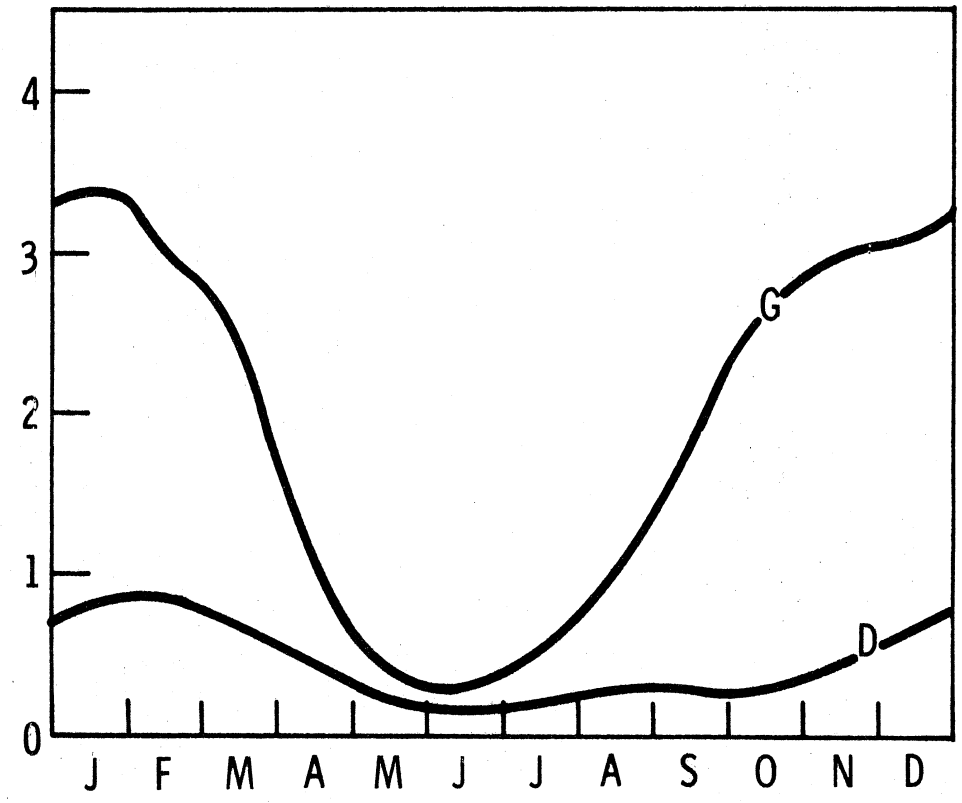

Figure 6.4.12 Same as Figure 4.1.11 for nonlinear simulation.

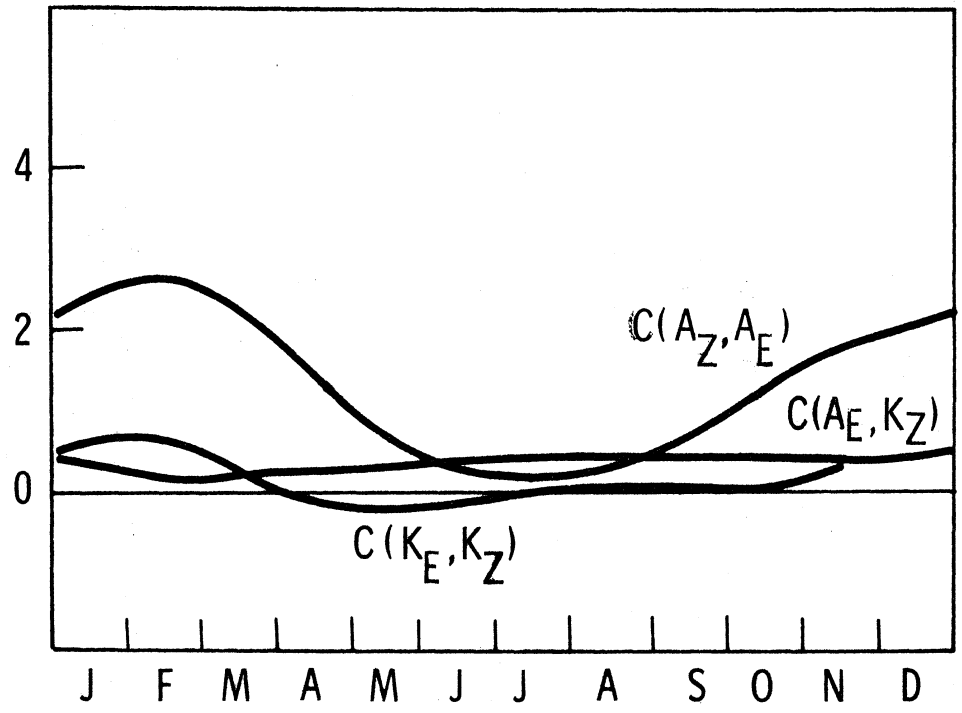

Figure 6.4.13 Same as Figure 4.1.12 for nonlinear simulation.

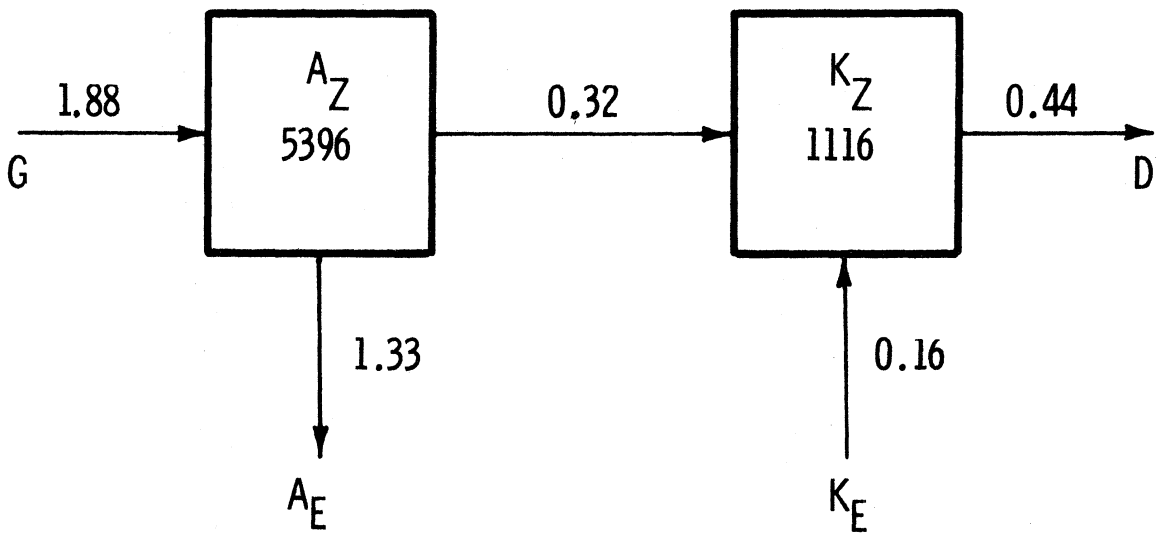

Figure 6.4.14 Same as Figure 4.1.13 for nonlinear simulation.

CHAPTER VII

CONCLUSIONS

This attempt to simulate the axisymmetric part of the general circulation of the atmosphere is based on a hemispheric two-level quasi-geostrophic model. The eddy fluxes have been parameterized in terms of quasiconservative quantities only,through a diagnostic and a time dependent formulation.

The model itself, very simple and inexpensive to operate, has several shortcomings which hamper the validation by comparison with observations. Among these the most important is due to the quasi-geostrophic character of the governing equations. Because of this feature the tropical regime is poorly represented. By the same reason the insertion of an artificial boundary at the equator is not important.

When fluxes are parameterized in terms of diagnostic coefficients the transports by the very long waves is present in the eddy coefficients. This is not a complete representation of their effects, but a partial one. When the time dependent formulation of the coefficients is used, the influence of the ultra long waves is excluded to a larger extent.

The parameterizations of the eddy fluxes of heat and potential vorticities, both considered as quasiconservative quantities in terms of unique exchange coefficients,determine their vertical variation through the global constraints of the angular momentum transport. Therefore, the exchange coefficients at the three active levels of the model are not independent of each other. Because of the

misrepresentation of the tropical mechanisms of transport, which cover about one half of the earth, it is safer to ignore the integral constraints for the sake of those latitudes properly represented in the model. An additional fact that detracts from the use of these integral constraints is the nonconservative character of the thermal streamfunction. This feature of the thermal streamfunction led us to avoid a formulation of K_2 in terms of its meridional gradient in the time dependent coefficients case.

The model is very sensitive with respect to the streamfunction constant f_o and the boundary layer friction coefficient ε. Some of the results, like the zonal available potential energy, has to be considered within somewhat large uncertainties compatible with the model. Increasing the empirical coefficient of skin friction ε allows an improvement of the zonal flow in summertime. Hence, some defects, like polar easterlies extending too far away from the pole, are features that can be corrected by an increase of ε. This is an inference which is substantiated by the improvement of the zonal flow for the Southern Hemisphere case.

The results of the study have to be considered within the frame that the restrictions and flexibilities just mentioned are able to define.

The first conclusion that can be drawn is that many of the unrealistic features obtained in former studies can be relieved by the use of a more complete heating function. In particular, we must include the release of latent heat which determines to a large extent the meridional variations of the thermal forcing. This modification produced a much more realistic temperature field and quantities

associated with it are improved correspondingly. As a consequence, the approach of casting the governing equations in terms of quasi-conservative quantities and through them parameterizing the eddy flux of nonconservative quantities, such as momentum, seems to be quite successful. Through the use of diagnostic time independent eddy coefficients it is possible to reproduce the observed thermal and flow fields and most of their seasonal evolutions. In some aspects the energetics of the hemispheric atmosphere is simulated quite well in the annual mean as well as in the seasonal variations.

A second conclusion relates to the variation of the eddy exchange coefficients in space. A characteristic feature of the results by Wiin-Nielsen and Sela (1971) is the sharp maximum of the exchange coefficients between latitudes 50 and 70. Such a peak appears also in the results of Clapp (1970) for the heat transport by cyclonic eddies. The omission of the latitude dependence in the mixing coefficients results in a zonal flow where the maximum wind moves to high latitudes (70^{o} N). This omission is unreasonable. Baroclinicity and cyclonic activity are characteristically concentrated in midlatitudes. The pressure dependence of the eddy exchange coefficients is also of primary importance as theory and observation show. Therefore, we must conclude that the use of austauch coefficients constant in time and space is not suitable for our purposes.

The time dependent formulation of the eddy coefficients introduced produces somewhat stronger seasonal fluctuations which in most of the cases are supported by observations. However the implicit exclusion of the ultra long waves makes it difficult to verify the results. This approach restores the nonlinearity of the

model and for that reason itself it is an improvement for climate simulation purposes. We feel that although the postulated parameterization is far from being an ideal one, it represents a promising improvement.

The results presented here cannot be taken as a conclusive proof, but show that the mechanism introduced does work in the right sense in the seasonal fluctuations and is able to reproduce observed features otherwise excluded.

In the experiments reported here, the thermal field behaved in a comparatively stable way with respect to the field of zonal motion. The energetic cycle is very stable. This is probably a result of their being integrated quantities, but not only the annual mean values share this stability. The phase relations of the annual cycle also appeared to change little from one experiment to the other.

Finally, we would like to suggest some avenues that, in our judgement, are worth further exploration. In relation to the thermal forcing, there has been an appreciable modification of the derived values of the surface albedo in low latitudes during the last few years. It seems desirable to modify the thermal forcing so as to include this new information. However, this is not a straightforward change because other fluxes may have to be altered at the same and/or other latitudes. The Southern Hemisphere seems to be worth additional efforts directed toward an improvement of the heating function.

As far as the model is concerned, the most important limitation is in its quasi-geostrophic nature. Hence, an obvious suggestion is the use of a model based on the primitive equations.

In such a case, the model can be made global and the eddy fluxes expressed in terms of quasi-conservative quantities such as potential vorticity.

Retaining a quasi-geostrophic formulation there is one modification that can produce improvement. Because the vertical divergence of radiative fluxes reaches higher values in the lower troposphere and condensation processes are also concentrated there, and because the heat transport is biased towards the same levels, it seems natural to modify the vertical structure of the model as to specify temperature at levels 1 and 3 as is made with vorticities. This kind of model suggested by Lorenz (1957) allows in addition changes in static stability and avoids the necessity of using a constant f_o. Therefore, the equator can be crossed without a discontinuity in the zonal flow. However, no significant improvement in the low latitudes can be expected as long as quasi-geostrophy is present.

APPENDIX I

FINITE DIFFERENCES EQUATIONS

A.I.1 Prognostic Equations

Potential vorticities are obtained from two equations of the form

$$\frac{\partial Q_i}{\partial t} = \frac{1}{a^2 \cos\varphi} \frac{\partial}{\partial \varphi} \left(K_i \cos\varphi \frac{\partial Q_i}{\partial \varphi} \right) + S_i \qquad i=1, 3 \qquad \text{(A.I.1.1)}$$

These relations can be considered as two separate parabolic partial differential equations with source terms that couple them:

$$S_1 = - \lambda^2 H_{2z} - 2A \zeta_{Tz}$$

$$S_3 = \lambda^2 H_{2z} + 2A \zeta_{Tz} - \varepsilon \left(\frac{3}{2} \zeta_{3z} - \frac{1}{2} \zeta_{1z} \right) \qquad \text{(A.I.1.2)}$$

We will deal then with the general form (A.I.1.1) omitting the subscript until it becomes necessary.

Boundary conditions for the solution of (A.I.1.1) have already been determined in Section 2.2. The initial condition for our experiments will be a simple state, say

$$Q_{iz} = f + \delta q^2 \psi_{Tz}$$

where ψ_{Tz} is independent of latitude. This initial condition and non vanishing values for K_i imply a state such that there is no mean relative motion, but well developed cyclonic random action still exists.

It is certainly contradictory in itself because cyclonic activity derives its energy from meridional temperature differences and this in term implies a vertical wind shear on a rotating earth.

However, we will not be concerned with the spin up problem and will concentrate the attention on the phenomena of the steady regime that will show little trace of the initial condition from which they evolved. From a mathematical point of view the initial condition can be arbitrary.

Given boundary conditions at $\varphi = 0$ and $\varphi = \frac{\pi}{2}$ (for the NH) and an initial condition the problem stated by (A. I. 1. 1) has a unique solution, Richtmyer and Morton (1957).

The stability of the computation is insured by the use of the Crank-Nicholson scheme. The source terms (A.I. 1.2) however, contains a part that cannot be expressed in terms of the corresponding potential vorticity Q and the scheme cannot be maintained for these terms. They will be used as of the last time step computed, hence they lag the diffusion term in (A. I. 1.1) by half time step (6 hours). This must be of minor importance since the typical time scale we are concerned with is of the order of three months and source mechanisms have a characteristic period considerably larger than the time step used.

With a time step Δt equal to 12 h. and a latitude grid length $\Delta\varphi$ of 5 degrees, using a superscript n for the time level and a subscript m for the grid point, with $m=1$ for the equator and $m=19$ for the pole, we can write the difference form corresponding to (A. I. 1. 1):

$$\frac{Q_m^{n+1} - Q_m^n}{\Delta t} = \frac{1}{2a^2(\Delta\varphi)^2}\left[K_{m+\frac{1}{2}}\frac{\cos\varphi_{m+\frac{1}{2}}}{\cos\varphi_m}\left(Q_{m+1}^{n+1} + Q_{m+1}^n\right) - 2K_m\left(Q_m^{n+1} + Q_m^n\right) + K_{m-\frac{1}{2}}\frac{\cos\varphi_{m-\frac{1}{2}}}{\cos\varphi_m}\left(Q_{m-1}^{n+1} + Q_{m-1}^n\right)\right] + S_m^n \qquad \text{(A. I. 1. 3)}$$

for $1 < m < 19$ and $n \geq 0$. Rearranging

$$Q_{m+1}^{n+1}\left[\frac{-\Delta t}{2(a\Delta\varphi)^2}K_{m+\frac{1}{2}}\frac{\cos\varphi_{m+\frac{1}{2}}}{\cos\varphi_m}\right] + Q_m^{n+1}\left[1 + \frac{\Delta t}{(a\Delta\varphi)^2}K_m\right] +$$

$$+ Q_{m-1}^{n+1}\left[\frac{-\Delta t}{2(a\Delta\varphi)^2}K_{m-\frac{1}{2}}\frac{\cos\varphi_{m-\frac{1}{2}}}{\cos\varphi_m}\right] = Q_{m+1}^{n}\left[\frac{\Delta t}{2(a\Delta\varphi)^2}K_{m+\frac{1}{2}}\frac{\cos\varphi_{m+\frac{1}{2}}}{\cos\varphi_m}\right] +$$

$$+ Q_m^n\left[\frac{-\Delta t}{(a\Delta\varphi)^2}K_m\right] + Q_{m-1}^n\left[\frac{\Delta t}{2(a\Delta\varphi)^2}K_{m-\frac{1}{2}}\frac{\cos\varphi_{m-\frac{1}{2}}}{\cos\varphi_m}\right] + S_m^n \qquad \text{(A.I.1.4)}$$

Define

$$C_m^{\pm} = \frac{\Delta t}{2(a\Delta\varphi)^2}K_{m\pm\frac{1}{2}}\frac{\cos\varphi_{m\pm\frac{1}{2}}}{\cos\varphi_m}$$

$$2C_m = C_m^+ + C_m^- \qquad \text{(A.I.1.5)}$$

Equation (A.I.1.4) can now be written as

$$-C_m^+ Q_{m+1}^{n+1} + (1 + 2C_m) Q_m^{n+1} - C_m^- Q_{m-1}^{n+1} = B_m^n \qquad \text{(A.I.1.6)}$$

where

$$B_m^n = S_m^n + C_m^+ Q_{m+1}^n + (1 - 2C_m) Q_m^n + C_m^- Q_{m-1}^n$$

and $m = 2, 3, \ldots, 18$ and $n > 0$.

The limit form of equation (A.I.1.1) at the pole were (2.2.12) and (2.2.13) from where it is apparent that we have to provide a one-sided finite difference form for the first and second derivatives of

potential vorticity. It is in this process that the boundary condition (2.2.23) imposed at the end of Section 2.2 is useful.

At this point we note that all numerical schemes adopted thus far, have truncation errors of second order. The first and second derivatives have been approximated by central differences and for quadrature the trapezoidal rule has been used. To be consistent we must require the same order forms for the boundary equations. Note also that equation (A.I. 1.6) has a tridiagonal matrix which can be easily decomposed into an upper and a strictly lower triangular matrix. We could satisfy the truncation order requirement without imposing zero values of first and third derivative of Q, but the matrix of the system (A.I.1.6) would not be tridiagonal anymore. We chose to satisfy the second order truncation error, keep a tridiagonal matrix and impose (2.2.23). With $\partial Q/\partial\varphi = \partial^3 Q/\partial\varphi^3 = 0$ we can approximate

$$\frac{\partial^2 Q}{\partial\varphi^2} = \frac{2}{(\Delta\varphi)^2} \left(Q_{18} - Q_{19} \right) + O\left[(\Delta\varphi)^2\right]$$

and the finite difference equation for the pole becomes

$$\frac{Q_{19}^{n+1} - Q_{19}^{n}}{\Delta t} = \frac{2}{(a\Delta\varphi)^2} K_{19} \left(Q_{18}^{n} + Q_{18}^{n+1} - Q_{19}^{n} - Q_{19}^{n+1} \right) + S_{19}^{n}$$

or

$$\frac{-2\Delta t}{(a\Delta\varphi)^2} Q_{18}^{n+1} K_{19} + \left(1 + \frac{2\Delta t}{(a\Delta\varphi)^2} K_{19} \right) Q_{19}^{n+1} =$$

(A.I. 1.7)

$$\frac{2\Delta t}{(a\Delta\varphi)^2} Q_{18}^{n} K_{19} + \left(1 - \frac{2\Delta t}{(a\Delta\varphi)^2} \right) Q_{19}^{n} + S_{19}^{n} .$$

So if we define

$$C_{19} = \frac{\Delta t}{(a\Delta\varphi)^2} K_{19}$$

$$B_{19}^n = S_{19}^n + (1 - 2C_{19}) Q_{19}^n + 2C_{19} Q_{18}^n$$

We can write (A.I.1.7) as

$$(1 + 2C_{19}) Q_{19}^{n+1} - 2C_{19} Q_{18}^{n+1} = B_{19}^n .$$

(A.I.1.8)

Likewise for the equator (2.2.20) and (2.2.21) give for

n = 1, with

$$C_1 = \frac{\Delta t}{2(a\Delta\varphi)^2} K_1$$

$$B_1^n = S_1^n + (1 - 2C_1) Q_1^n + 2C_1 Q_2^n$$

the equation

$$(1 + 2C_1) Q_1^{n+1} - 2C_1 Q_2^{n+1} = B_1^n .$$

(A.I.1.9)

We can write a matrix relation for the equation (A.I.1.1.)

$$A \vec{x} = \vec{b}$$

where the transposes $\vec{x}^T$ and $\vec{b}^T$ of $\vec{x}$ and $\vec{b}$ respectively are

$$\vec{x}^T = \left[Q_1^{n+1}, Q_2^{n+1}, \ldots, Q_{19}^{n+1}\right] \qquad \vec{b}^T = \left[B_1^n, B_2^n, \ldots, B_{19}^n\right]$$

and the matrix A is

$$\begin{bmatrix} 1+2C_1 & -2C_1 & & & & & \\ -C_2^- & 1+2C_2 & -C_2^+ & & & & \\ & -C_3^- & 1+2C_3 & -C_3^+ & & & \\ & & \cdots & \cdots & \cdots & & \\ & & & \cdots & \cdots & \cdots & \\ & & & & -C_{18}^- & 1+2C_{18} & -C_{18}^+ \\ & & & & & -2C_{19} & 1+2C_{19} \end{bmatrix} = A$$

Considering (A.I. 1.5) we can see that this matrix is strictly diagonal dominant and therefore nonsingular.

A.I.2 Helmholtz Equation for Thermal Streamfunction Ψ_T.

The equation for Ψ_T is (2.2.26), valid for all inner grid points, which in finite difference form becomes

$$\frac{\cos\varphi_{m-\frac{1}{2}}}{(a\Delta\varphi)^2\cos\varphi_m}\Psi^n_{T,\,m-1} - \left[\frac{2}{(a\Delta\varphi)^2} + q^2\right]\Psi^n_{T,\,m} + \frac{\cos\varphi_{m+\frac{1}{2}}}{(a\Delta\varphi)^2\cos\varphi_m}\Psi^n_{T,\,m+1} = \frac{1}{2}\left(Q^n_{1,\,m} - Q^n_{3,\,m}\right) \qquad \text{(A.I.2.1)}$$

where $n \geq 0$, $m = 2, 3, \ldots, 18$.

The limit form of the equation at the pole is (A.I.2.10) and its finite difference form is

$$-\left[\frac{4}{(a\Delta\varphi)^2} + q^2\right]\psi^n_{T,19} + \frac{4}{(a\Delta\varphi)^2}\psi^n_{T,18} = \frac{1}{2}\left(Q^n_{1,19} - Q^n_{3,19}\right) \qquad \text{(A.I.2.2)}$$

For the equator we had equation (2.2.19).

Since we know that the boundary condition $\partial\psi_T/\partial\varphi = 0$ chooses an even ψ_T with respect to the equator we can write

$$\left.\frac{\partial^2\psi_T}{\partial\varphi^2}\right|_1 = \frac{2}{(\Delta\varphi)^2}\left(\psi_{T,2} - \psi_{T,1}\right) + O\left[(\Delta\varphi)^2\right]$$

and the finite difference form of (2.2.19) is

$$-\left[\frac{2}{(a\Delta\varphi)^2} + q^2\right]\psi^n_{T,1} + \frac{2}{(a\Delta\varphi)^2}\psi^n_{T,2} = \frac{1}{2}\left(Q^n_{1,1} - Q^n_{3,1}\right) \qquad \text{(A.I.2.3)}$$

In matrix form

$$A\,\vec{x} = \vec{b}$$

where

$$\vec{x}^T = \left[\psi^n_{T,1}, \psi^n_{T,2}, \ldots, \psi^n_{T,19}\right]$$

$$\vec{b}^T = \left[\frac{1}{2}(Q^n_{1,1} - Q^n_{3,1}), \frac{1}{2}(Q^n_{1,2} - Q^n_{3,2}), \ldots, \frac{1}{2}(Q^n_{1,19} - Q^n_{3,19})\right]$$

and if we now define

$$D^{\pm}_m = \frac{1}{(a\Delta\varphi)^2}\,\frac{\cos\varphi_{m\pm1/2}}{\cos\varphi_m}$$

$$D = (a\Delta\varphi)^{-2}$$

$$D_m = D^+_m + D^-_m$$

We can write

$$\begin{bmatrix} -(2D+q^2) & 2D & & & & & \\ D_2^- & -(2D_2+q^2) & D_2^+ & & & & \\ & D_3^- & -(2D_3+q^2) & D_3^+ & & & \\ & & \cdots & \cdots & \cdots & & \\ & & & \cdots & \cdots & \cdots & \\ & & & D_{18}^- & -(2D_{18}-q^2) & D_{18}^+ & \\ & & & & & -(4D+q^2) & \end{bmatrix} = A$$

The strict diagonal dominance of the tridiagonal matrix is evident, hence its inverse exists.

APPENDIX II

SPLINE INTERPOLATION

The divided differences of a function f(x), k times differentiable in $[a, b]$, given at a set of discrete points x_i, distinct or not, can be defined as

$$f[x_i, x_{i+1}, \ldots, x_{i+k}] = \begin{cases} f(x_i) & k = 0 \\ \dfrac{f[x_{i+1}, \ldots, x_{i+k}] - f[x_i, \ldots, x_{i+k-1}]}{x_{i+k} - x_i} & k>0 \ , \ x_i < x_{i+k} \\ \dfrac{f^{(k)}(x_i)}{k!} & k>0 \ , \ x_i = x_{i+1} = \ldots = x_{i+k} \end{cases} \tag{A.II.1}$$

Then

$$p_k(x) = \sum_{j=0}^{k} \left\{ f[x_i, \ldots, x_{i+j}] \prod_{r=0}^{j-1} (x - x_{i+r}) \right\}$$

is the unique polynomial of degree less or equal to k which interpolates f(x) at x_i, $x_{i+1}, \ldots, x_{i+k}$.

The spline scheme interpolates a function f(x), given at N+1 points x_i, i=1, 2, . . . , (N+1), by a cubic piecewise polynomial $g_\pi(x)=P_i(x)$, where $P_i(x)$ is a cubic polynomial such that

$$\left.\begin{aligned} P_i(x_i) &= f(x_i) \\ P_i(x_{i+1}) &= f(x_{i+1}) \end{aligned}\right\} \quad i = 1, 2, \ldots, N$$

The other two conditions needed to fully determine $P_i(x)$ will be chosen as to make $P_i(x)$ agree with f(x) not only in value, but also in slope at x_i and x_{i+1}. Therefore, $g_\pi(x)$ is continuous and differentiable.

Using the divided differences (A. II. 1) we can write

$$P_i(x) = f(x_i) + f\left[x_i, x_i\right](x-x_i) + f\left[x_i, x_i, x_{i+1}\right](x-x_i)^2 +$$
$$+ f\left[x_i, x_i, x_{i+1}, x_{i+1}\right](x-x_i)^2(x-x_{i+1})$$

which using the identity

$$x-x_{i+1} = (x-x_i) + (x_i-x_{i+1})$$

can be transformed into

$$P_i(x) = c_{1,i} + c_{2,i}(x-x_i) + c_{3,i}(x-x_i)^2 + c_{4,i}(x-x_i)^3 \qquad \text{(A. II. 2)}$$

where

$$c_{1,i} = f(x_i) = f_i$$

$$c_{2,i} = f'(x_i) = s_i$$

$$c_{3,i} = (\Delta y_i)^{-1}\left\{3f\left[x_i, x_{i+1}\right] - 2s_i - s_{i+1}\right\}$$

$$c_{4,i} = (\Delta y_i)^{-2}\left\{-2f\left[x_i, x_{i+1}\right] + s_i + s_{i+1}\right\}$$

$$\Delta y_i = y_{i+1} - y_i \qquad \text{(A. II. 3)}$$

These $c_{j,i}$ are such that $g_\pi(x)$ defined by

$$g_\pi(x) = P_i(x) \qquad \text{if} \qquad x \in \left[x_i, x_{i+1}\right]$$
$$= \sum_{j=1}^{4} c_{j,i}(x-x_i)^{j-1} \qquad i = 1, 2, \ldots, N$$

satisifies

$$\left.\begin{aligned} g_\pi(x_j) &= f_j \\ g'_\pi(x_j) &= s_j \end{aligned}\right\} \qquad j = 1, 2, \ldots, (N+1)$$

So if we know x_i, f_i and s_i for $i=1, 2, \ldots, (N+1)$ we can find $g_\pi(x)$, which is called the cubic Hermite interpolant. However, normally we have no information on the derivatives s_i, and we must choose some method to estimate them. In the spline scheme we determine them so that $g_\pi(x)$ is twice differentiable, i.e.,

$$P''_{i+1}(x_i) = P''_i(x_i) \qquad i= 2, 3, \ldots, N$$

Using (A.II.2) this condition gives

$$\Delta y_i\, s_{i-1} + 2(\Delta y_i - \Delta y_{i-1})\, s_i + \Delta y_{i-1} s_{i+1} =$$

$$3\left\{\frac{\Delta f_{i-1}}{\Delta y_{i-1}}\, y_i + \frac{\Delta f_i}{\Delta y_i}\, y_{i-1}\right\} \qquad i=2, 3, \ldots, N \qquad \text{(A.II.4)}$$

These are N-1 relations among N+1 unknowns s_i, $i=1, 2, \ldots, (N+1)$. If we pick the end points derivatives, s_1 and s_{N+1}, we can in principle determine $s_2, s_3, \ldots, s_N$ by (A.II.4).

With x_i, f_i, and s_i known the relations (A.II.3) serve to evaluate $c_{j,i}$ and (A.II.2) to obtain interpolated values. Note that (A.II.2) is a picewise cubic polynomial continuous and twice differentiable at the data points.

APPENDIX III

INSTABILITY OF A TWO LEVEL MODEL

A. III. 1 Basic Relations

In this appendix we will consider the stability of a zonal current which varies with latitude and pressure, so that a perturbation can grow at expense of the zonal available potential or the zonal kinetic energy. This will be done specifically for the two-level standard model, which we are using, and in terms of potential vorticities whenever possible. This analysis follows Pedolsky's (1964a) presentation.

The governing equations of the standard two level quasi-geostrophic model for an adiabatic and frictionless flow can be written in terms of the potential vorticities (equations (2. 1. 16) and (2. 1. 17)).

$$\left(\frac{\partial}{\partial t} - \frac{\partial \psi_i}{\partial y}\frac{\partial}{\partial x} + \frac{\partial \psi_i}{\partial x}\frac{\partial}{\partial y}\right)\left[\frac{\partial^2 \psi_i}{\partial x^2} + \frac{\partial^2 \psi_i}{\partial y^2} + f + \frac{q^2}{2}\delta(\psi_3 - \psi_1)\right] = 0 \qquad \text{(A. III. 1. 1)}$$

where $\delta = \begin{cases} 1 \\ -1 \end{cases}$ when $i = \begin{cases} 1 \\ 3 \end{cases}$

For simplicity we will work in a beta channel of width $2l$. Suppose we have a steady basic state which satisfies equation (A. III. 1. 1), is independent of x and varies with y and the level of the model, say,

$$u_i = \begin{cases} U_1(y) & i = 1 \\ U_3(y) & i = 3 \end{cases}$$

Let us introduce a perturbation to this basic flow

$$\Phi_i = \begin{cases} \Phi_1 & i = 1 \\ \Phi_3 & i = 3 \end{cases}$$

The perturbation equation is

$$\left(\frac{\partial}{\partial t} + U_i \frac{\partial}{\partial x}\right)\left[\frac{\partial^2 \Phi_i}{\partial x^2} + \frac{\partial^2 \Phi_i}{\partial y^2} + \frac{q^2}{2}\delta\left(\Phi_3 - \Phi_1\right)\right] +$$

$$+ \frac{\partial \Phi_i}{\partial x}\frac{\partial}{\partial y}\left[-\frac{\partial U_i}{\partial y} + f + \frac{q^2}{2}\delta\int\left(U_3 - U_1\right)dy\right] = 0 \qquad i=1, 3$$

Since the coefficients of perturbation quantities are independent of x and t we can assume that the perturbation is harmonic in x and t with wavenumber α :

$$\Phi_i = \mathrm{Re}\left\{\phi_i(y)\, e^{i\alpha(x-ct)}\right\} \qquad \text{(A.III.1.2)}$$

Substitution of (A.III.1.2) into the perturbation equation gives

$$(U_i - c)\left(\phi_i'' - \alpha^2 \phi_i\right) + \phi_i\left(\beta - U_i'' + \frac{q^2}{2}\delta\left(U_1 - U_3\right) + \right.$$

$$\left. + \frac{q^2}{2}\left(U_i - c\right)\delta\left(\phi_3 - \phi_1\right)\right) = 0 \qquad \text{(A.III.1.3)}$$

where $\beta = \dfrac{df}{dy}$.

Noting that the basic flow potential vorticities are

$$Q_i = -U_i'' + f + \frac{q^2}{2}\delta\left(\phi_3 - \phi_1\right)$$

we can write (A.III.1.3)

$$(U_i - c)\left(\phi_i'' - \alpha^2 \phi_i\right) + \phi_i \frac{\partial Q_i}{\partial y} = (U_i - c)\frac{q^2}{2}\delta\left(\phi_1 - \phi_3\right) \qquad \text{(A.III.1.4)}$$

At the boundaries of the channel, $y=\pm 1$, the perturbation meridional velocity must vanish for all x, hence $\phi_i = 0$.

Since both the governing equation (A. III. 1. 4) and the boundary conditions are homogeneous, solutions will exist for certain values of $c=c_r+ic_i$.

A. III. 2 Necessary Conditions for Instability

Assume a growing disturbance ($c_i \neq 0$), so that division by (U_i-c) is permissible. Then multiply the first equation of (A. III. 1. 4) by $2\phi_1^*/ q^2(U_1-c)$, where asterisk denotes a complex conjugate quantity, and the second by $2\phi_3^*/ q^2(U_3-c)$, and the two equations are integrate from $y=1$ to $y=-1$. Using integration by parts and the boundary conditions one gets

$$\int dy \left\{ \sum_{i=1,3} \left[\frac{|\phi_i|^2}{U_i-c} \frac{\partial Q_i}{\partial y} \right] \right\} = \int dy \left\{ \sum \left(|\phi_i'|^2 + \alpha^2 |\phi_i|^2 \right) + \frac{q^2}{2} |\phi_1 - \phi_3|^2 \right\} \qquad \text{(A. III. 2. 1)}$$

The imaginary part of this relation provides

$$\int dy \left\{ \sum_{i=1,3} \left(\frac{|\phi_i|^2}{|U_i - c|^2} \frac{\partial Q_i}{\partial y} \right) \right\} = 0 \qquad \text{(A. III. 2. 2)}$$

showing that a necessary condition for instability is that the potential vorticity gradients cannot have the same sign everywhere. Because

$$\frac{\partial Q_i}{\partial y} = -U_i'' + \beta + \frac{q^2}{2} \delta (U_1 - U_3) \qquad i = 1, 3 \qquad \text{(A. III. 2. 3)}$$

this statement indicates that β is a stabilizing factor, the thermal wind $U_T = \frac{1}{2}(U_1 - U_3)$ is a destabilizing influence, and the static stability included in the denominator of q^2 tend to make the flow stable.

If we identify the basic flow with the zonal mean wind, observations show that its relative vorticity is unimportant compared with the other terms in the right hand side of (A. III. 2. 3), we have approximately

$$\frac{\partial Q_i}{\partial y} = \beta + \delta q^2 U_T \qquad \text{(A. III. 2. 4)}$$

and a necessary condition for instability is

$$U_T > \frac{\beta}{q^2}$$

a well known relation deduced by Phillips (1954), for a basic flow independent of y, by the solution of the eigenvalue problem.

In the barotropic case ($U_T = 0$) the necessary condition for instability is the same, but in terms of absolute vorticity. For a continuously stratified fluid Pedolsky (loc. cit.) has shown that the condition reduces to the well known result of Kuo (1949) and Fjørtoft (1951).

The real part of (A. III. 2. 1) gives, using (A. III. 2. 2)

$$\int dy \left\{ \sum_{i=1,3} \left(\frac{|\phi_i|^2}{|U_i - c|^2} U_i \frac{\partial Q_i}{\partial y} \right) \right\} =$$

$$\int dy \left\{ \sum_{i=1,3} \left(|\phi_i'|^2 + \alpha |\phi_i|^2 \right) + \frac{q^2}{2} |\phi_i - \phi_3|^2 \right\} > 0 \qquad \text{(A. III. 2. 5)}$$

Hence the product of the zonal flow and the meridional gradient of potential vorticity must be somewhere positive in unstable flows.

A. III. 3 Growth Rate and Upper Bound

Relation (A. III. 2. 5) allows the determination of an upper bound to the growth rate of the perturbation. Considering that

$$\left| U_j - c \right|^2 \geq c_i^2 \qquad j = 1, 3$$

and that if g(y) is a well behaved function that vanishes at y=± 1

$$\int \left| g' \right|^2 dy \geq \frac{\pi^2}{4l^2} \int \left| g \right|^2 dy \qquad \text{(A. III. 3. 1)}$$

we can deduce from (A. III. 2. 5)

$$c_i^2 \leq \frac{1}{\alpha^2 + \frac{\pi^2}{4l^2}} \max_{i=1,3} \left(U_i \frac{\partial Q_i}{\partial y} \right) \qquad \text{(A. III. 3. 2)}$$

A. III. 4 A Semicircle Theorem

Starting from Equation (A. III. 1. 3) and following Pedlosky (loc. cit.) one can find that the results of this author are unchanged for our model, since the terms which could make a difference are lost in the simplification of the inequalities. The results are

$$U_{min} - \frac{\beta}{2\left(\alpha^2 + \frac{\pi^2}{4l^2}\right)} \leq c_r \leq U_{max} \qquad \text{(A. III. 4. 1)}$$

and

$$\left(c_r - \frac{U_{max}+U_{min}}{2} \right)^2 + c_i^2 \leq \left(\frac{U_{max}-U_{min}}{2} \right)^2 + \frac{\beta}{\alpha^2 + \frac{\pi^2}{4l^2}} \frac{U_{max}-U_{min}}{2} \qquad \text{(A. III. 4. 2)}$$

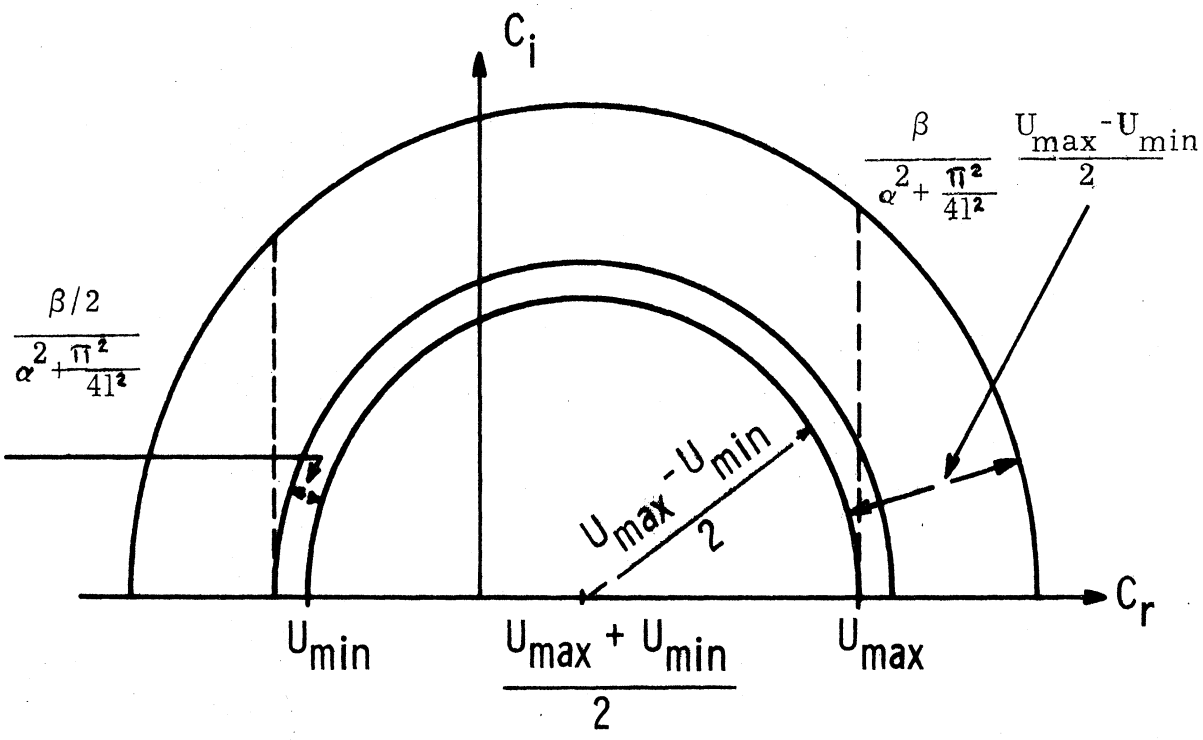

Remembering that U_{max} and U_{min} can be at the same level or not we see that instability can be due to the vertical or horizontal shear. To make the flow stable it is necessary to have both zero.

The beta influence results in unstable waves moving slower than the minimum basic wind, but U_{max} is still an upper bound to the phase speed.

A. III. 5 Short Wave Cut-off

The short wavelength cut-off of the unstable waves can also be expressed in terms of the potential vorticity gradient (Pedlosky, 1964a; Bretherton, 1966b).

APPENDIX IV

TIME DEPENDENT COEFFICIENTS

Expressing the latitude φ in degrees the expressions adopted for the three eddy exchange coefficients are

$$K_1 = f(\varphi, t) \int_{30}^{85} \alpha_1 \left| \frac{\partial Q_{1z}}{\partial \varphi} \right| \quad d$$

$$K_3 = f(\varphi, t) \int_{30}^{85} \alpha_3 \left| \frac{\partial Q_{3z}}{\partial \varphi} \right| \quad d\varphi$$

$$K_2 = f(\varphi, t) \int_{30}^{85} \left(0.3\, \alpha_1 \left| \frac{\partial Q_{1z}}{\partial \varphi} \right| + 0.7\, \alpha_3 \left| \frac{\partial Q_{3z}}{\partial \varphi} \right| \right) d\varphi$$

The constants α_1 and α_3 were fixed by a combination of numerical experiments and the information provided by the diagnostic study of Wiin-Nielsen and Sela (1971). The values used in the nonlinear simulation reported in Chapter 6 were $\alpha_1 = 0.25 \times 10^{17}$ m^2 and $\alpha_3 = 2.5 \times 10^{17}$ m^2. The shape factor $f(\varphi)$ at a given time, was taken from a Beta distribution $\beta(x/r, n)$. The parameter n was taken as time independent and its value was determined by adjusting Beta distributions to the diagnostic profiles determined by the aforementioned authors. Since the variations of n for different levels differed slightly a mean value of n=12 was taken. The adjustment was made considering only the values from 30 degrees to the pole and using the mean and variance of the distribution with respect to the pole. Then for the distribution

$$f(x) = \beta(x/r, n) = \frac{x^{r-1} (1-x)^{n-r-1}}{\beta(r, n-r)} \qquad \text{for} \quad \begin{matrix} 0 \leq x \leq 1 \\ n > r > 0 \end{matrix}$$

where $x = (90 - \varphi)/60$ and

$$\beta(r, n-r) = \int_0^1 x^{r-1} (1-x)^{n-r-1} \, dx$$

the mean and the variance are respectively

$$\mu_1 = \frac{r}{n} \qquad \text{and} \qquad \mu_2 = \frac{n-r}{n(n+1)} .$$

The magnitude of r was obtained at every time step from an evaluation of μ_1 for the integrand of K_2:

$$r = n \frac{\sum_{i=6}^{18} \left\{ \left(0.3\, \alpha_1 \left| \frac{\partial Q_{1z}}{\partial \varphi} \right|_i + 0.7\, \alpha_3 \left| \frac{\partial Q_{3z}}{\partial \varphi} \right|_i \right) \left(\frac{19-i}{13} \right) \right\}}{\sum_{i=6}^{18} \left\{ 0.3\, \alpha_1 \left| \frac{\partial Q_{1z}}{\partial \varphi} \right|_i + 0.7\, \alpha_3 \left| \frac{\partial Q_{3z}}{\partial \varphi} \right|_i \right\}}$$

Therefore

$$\int_0^{90} f(\varphi) \, d\varphi = 1$$

Inthe tropical regions the eddy exchange coefficients were modified in the following way:

$$\text{for } \begin{cases} 0 \leq \varphi \leq 25 \\ 1 \leq i \leq 6 \end{cases} \qquad K_{j,i} = K'_{j,i} \qquad j=1, 2, 3$$

$$\text{for } \begin{cases} 25 \leq \varphi \leq 35 \\ 6 < i \leq 8 \end{cases} \qquad K_{1,i} = K_{1,i} \qquad K_{j,i} = \max \begin{cases} K'_{j,i} \\ K_{j,i} \end{cases} \quad j=2, 3$$

In the high latitudes the coefficients were modified as follows:

$$\text{for } \begin{cases} 70 < \varphi \leq 90 \\ 15 < i \leq 19 \end{cases} \qquad K_{j,i} = K''_{j,i} \qquad j = 1, 2, 3$$

where

$$K'_{j,i} = \begin{cases} 0.3 \times 10^6 \ m^2 sec^{-1} & j=1 \\ 0.2 \times 10^6 \ m^2 sec^{-1} & j=2 \\ 1.5 \times 10^6 \ m^2 sec^{-1} & j=3 \end{cases}$$

$$K''_{j,i} = K_{j,15} \frac{(90-\varphi)}{20} \qquad j= 1, 2, 3$$

and $K_{j,i} = K_j(\varphi_i)$.

REFERENCES

Bretherton, F. P., 1966a: Critical Layer Instability in Baroclinic Flows, Quart. J. Roy. Meteor. Soc., Vol. 92, 325-334.

Bretherton, F. P., 1966b: Baroclinic Instability and the Short Wavelength Cut-off in Terms of Potential Vorticity, Quart. J. Roy. Meteor. Soc., Vol. 92, 393-403.

Bryan, K., 1969: Climate and the Ocean Circulation: the Ocean Model, Mon. Wea. Rev., Vol. 97, 806-827.

Clapp, P., 1970: Parameterization of Macroscale Transient Heat Transport for Use in a Mean-Motion Model of the General Circulation, J. Appl. Meteor., Vol. 9, 554-563.

Cressman, G. P., 1960: Improved Terrain Effects on Barotropic Forecasts, Mon. Wea. Rev., Vol. 88, 2-12 and 327-342.

Charney, J., 1959: On the General Circulation of the Atmosphere, Rossby Memorial Volume: The Atmosphere and the Sea in Motion, Rockefeller and Oxford University Presses, New York, 178-193.

Charney, J., 1960: Integration of the Primitive and Balance Equations, Proc. of the Int'l. Symp. on Numerical Weather Prediction, 7-13 November 1960, Tokyo, 131-152, (published March 1962).

Charney, J. and M. E. Stern, 1962: On the Stability of Internal Baroclinic Jets in a Rotating Atmosphere, J. Atmos. Sci., Vol. 19, 159-172.

Charney, J., 1971: Geostropic Turbulence, J. Atmos. Sci., Vol. 28, 1087-1095.

Davies, P., 1963: An Analysis of the Atmospheric Heat Budget, J. Atmos. Sci., Vol. 20, 5-22.

REFERENCES (continued)

Dickinson, R. E., 1969: Theory of Planetary Wave Zonal Flow Interaction, J. Atmos. Sci., Vol. 26, 73-81.

Eady, E. T., 1949: Long Waves and Cyclone Waves, Tellus, Vol. 1, 33-52.

Fjortoft, R., 1951: Stability Properties of Large-Scale Atmospheric Disturbances, Compendium of Meteorology, Amer. Meteor. Soc., Boston, 454-463.

Green, J. S. A., 1970: Transfer Properties of the Large-Scale Eddies and the General Circulation of the Atmosphere, Quart. J. Roy. Meteor. Soc., Vol. 96, 157-185.

Jenne, R., H. Van Loon, J. J. Taljaard, and H. L. Crutcher, 1968: Zonal Means of Climatological Analysis of the Southern Hemisphere, Notos, Vol. 17, 35-52.

Krueger, A. F., J. S. Winston and D. A. Haines, 1965: Computations of Atmospheric Energy and its Transformation for the Northern Hemisphere for a Recent Five Year Period, Mon. Wea. Rev., Vol. 93, 227-238.

Kuo, H., 1949: Dynamic Instability of Two-Dimensional Non-Divergent Flow in a Barotropic Atmosphere, J. Meteor., Vol. 6, 105-122.

Kurihara, Y., 1970: A Statistical-Dynamical Model of the General Circulation of the Atmosphere, J. Atmos. Sci., Vol. 27, 847-870.

Laikhtman, D. L., et al., 1970: Problems in Dynamic Meteorology, World Meteorological Organization, WMO- N 261. TP. 146, Geneva, Switzerland, Edited by A. Wiin-Nielsen, 245, Appendix 15.

REFERENCES (continued)

List, R., 1951: Smithsonian Meteorological Tables, Smithsonian Misc. Tables, Vol. 114, Washington.

London, J., 1957: A Study of the Atmospheric Heat Balance, Report: New York University, Dept. of Meteor. and Ocean., College of Engineering.

London, J. and T. Sasamori, 1971: Radiative Energy Budget of the Atmosphere, Space Res., XI, 639-649.

Lorenz, E. N., 1955: Available Potential Energy and the Maintenance of the General Criculation, Tellus, VII, 157-167.

Lorenz, E. N., 1960: Energy and Numerical Weather Prediction, Tellus, XII, 364-373.

Lorenz, E. N., 1967: The Nature and Theory of the General Circulation of the Atmosphere, WMO, Geneva, 161 pp.

Manabe, S., 1969: The Atmospheric Circulation and the Hydrology of the Earth's Surface, Mon. Wea. Rev., Vol. 97, 739-774.

Miles, J. W., 1964: Baroclinic Instability of the Zonal Wind, Rev. of Geophy., Vol. 2, 155-176.

Möller, F., 1951: Vierteljahrsten des Niederschlags fur die ganze Erde, Petersmanns Geograph. Mitt., Vol. 95, 1-7.

Neumann, G. and W. J. Pierson, Jr., 1966: Principles of Physical Oceanography, Prentice-Hall, Inc., Englewood Cliffs, New Jersey, 545 pp., Table 14.3, pg. 437.

Newell, R. E., et al., 1969: The Energy Balance of the Global Atmosphere, The Global Circulation of the Atmosphere, Edited by G. A. Corby, Pub. by Roy. Meteor. Soc., London, Joint Conf. held 25-29 Aug. 1969 at the Roy. Soc. London.

REFERENCES (continued)

Newton, C. W., 1972: Southern Hemisphere General Circulation in Relation to Global Energy and Momentum Balance Requirements, Met. Monographs, Vol. 13, Amer. Meteor . Soc., Boston, 215-240.

Oort, A., 1964: On Estimates of the Atmospheric Energy Cycle, Mon. Wea. Rev., Vol. 92, 483-493.

Oort, A. and E. M. Rasmusson, 1971: Atmospheric Circulation Statistics, NOAA Professional Paper 5, U. S. Dept. of Commerce, Nat. Ocean. and Atmos. Admin., Rockville, Md., 323 pp.

Palmen, E., 1955: On the Meridional Circulation in Low Latitudes of the Northern Hemisphere in Winter and the Associated Meridional and Vertical Flux of Angular Momentum, Soc. Scient. Fennica., Comm. Phys. Math., Vol. 17, 1-33.

Palmen, E. and W. Newton, 1969: Atmospheric Circulation Systems, Academic Press, New York, 603 pp.

Pedlosky, J., 1964a: The Stability of Currents in the Atmosphere and the Ocean: Part I, J. Atmos. Sci., Vol. 21, 201-219.

Pedlosky, J., 1964b: The Stability of Currents in the Atmosphere and the Ocean: Part II, J. Atmos. Sci., Vol. 21, 342-353.

Phillips, N. A., 1956: The General Circulation of the Atmosphere: A Numerical Experiment, Quart. J. Roy. Meteor. Soc., Vol. 82, 123-164.

Phillips, N. A., 1963: Geostrophic Motion, Rev. of Geophy., Vol. 1, 123-176.

REFERENCES (continued)

Richtmyer, R. D. and K. W. Morton, 1957: Difference Methods for Initial Value Problems, 2nd Edition, Interscience Publishers, New York, 405 pp.

Riehl, H., 1951: The North-East Trade of the Pacific Ocean, Quart. J. Roy. Meteor. Soc., Vol. 77, 598-626.

Saltzman, B., 1967: On the Theory of the Mean Temperature of Earth Surface, Tellus, Vol. XIX, 219-229.

Saltzman, B., 1968: Steady State Solutions for the Axially Symmetric Climate Variables, Pure Appl. Geophys., Vol. 69, 237-259.

Saltzman, B. and A. Vernekar, 1971: An Equilibrium Solution for the Axially Symmetric Component of the Earth's Macroclimate, J. Geophys. Res., Vol. 76, 1498-1524.

Sasamori, T., J. London and D. V. Hoyt, 1972: Radiation Budget of the Southern Hemisphere, Meteor. Mon., Vol. 13, N 35, Meteorology of the Southern Hemisphere, Edited by C. W. Newton, Published by the American Meteor. Soc., Boston.

Sela, J. and A. Wiin-Nielsen, 1971: Simulation of the Atmospheric Annual Energy Cycle, Mon. Wea. Rev., Vol. 99, 460-468.

Sellers, W. S., 1965: Physical Climatology, The University of Chicago Press, Chicago, 272 pp.

Smagorinsky, J., 1963: General Circulation Experiments with the Primitive Equations: I the Basic Experiment, Mon. Wea. Rev., Vol. 91, 99-164.

Smagorinsky, J., 1964: Some Aspects of the General Circulation, Quart. J. Roy. Meteor. Soc., Vol. 90, 1-14.

REFERENCES (continued)

SMIC, 1971: Inadvertent Climate Modification, Report of the Study of Man's Impact on Climate, The MIT Press, Cambridge, Mass., 308 pp.

Stone, P. H., 1972a: A Simplified Radiative-Dynamical Model for the Stability of Rotating Atmospheres, J. Atmos. Sci., Vol. 29, 405-418.

Stone, P. H., 1972b: On Non-Geostrophic Baroclinic Stability: Part III, The Momentum and Heat Transports, J. Atmos. Sci., Vol. 29, 419-426.

Stone, P. H., 1973: The Effect of Large Scale Eddies on Climatic Change, J. Atmos. Sci., Vol. 30, 521-529.

Taylor, G. I., 1921: Diffusion by Continuous Movements, Proc. Lond. Math. Soc., Vol. 20, 196-212.

Van Loon, H., 1972: Wind in the Southern Hemisphere, Meteor. Mon., Vol. 13, Ed. by C. L. Newton, American Meteor. Soc., Boston.

Vonder Haar, T. H. and V. E. Suomi, 1971: Measurements of the Earth's Radiation Budget from Satellites During a Five-Year Period, Part I: Extended Time and Space Means, J. Atmos. Sci., Vol. 28, 305-314.

Vonder-Haar, T. and A. Oort, 1973: New Estimate of Annual Poleward Energy Transport by Northern Hemisphere Oceans, J. Phys. Ocean, Vol. 3, 169-172.

Wiin-Nielsen, A., J. A. Brown and M. Drake, 1963: On Atmospheric Energy Conversion Between the Zonal Flow and the Eddies, Tellus, Vol. 15, 261-279.

REFERENCES (concluded)

Wiin-Nielsen, A., 1967: On the Annual Variation and Spectral Distribution of Atmospheric Energy, Tellus, Vol. XIX, 540-559.

Wiin-Nielsen, A., 1969: On Atmospheric Response to Large Scale Seasonal Forcing, Proc. of the WMO/IUGG Symp. on Numerical Wea. Prediction, Tokyo, Japan, Nov. 20-Dec. 4, 1968, Japan Meteor. Agency, Tokyo, IV-21-IV-27.

Wiin-Nielsen, A., 1970: A Theoretical Study of the Annual Variation of the Atmospheric Energy, Tellus, Vol. 22, 1-16.

Wiin-Nielsen, A. and J. Sela, 1971: On the Transport of Quasi-Geostrophic Potential Vorticity, Mon. Wea. Rev., June, Vol. 99, 447-459.

Wooldridge, G. and Reiter, E., 1970: Large Scale Atmospheric Circulation Characteristics as Evident from GHOST Balloon Data, J. Atmos. Sci., Vol. 27, 183-194.